Distribution Agreement

In presenting this thesis or dissertation as a partial fulfillment of the requirements for an advanced degree from Emory University, I hereby grant to Emory University and its agents the non-exclusive license to archive, make accessible, and display my thesis or dissertation in whole or in part in all forms of media, now or hereafter known, including display on the world wide web. I understand that I may select some access restrictions as part of the online submission of this thesis or dissertation. I retain all ownership rights to the copyright of the thesis or dissertation. I also retain the right to use in future works (such as articles or books) all or part of this thesis or dissertation.

Signature:

Michael DiCandia   11/28/2022
Name   Date

1

Title   Investigation of the factors that regulate sporulation initiation in Clostridioides difficile

Author   Michael DiCandia

Degree   Doctor of Philosophy

Program   Biological and Biomedical Sciences

Genetics and Molecular Biology

Approved by the Committee

Shonna McBride

Advisor

Marcin Grabowicz

Committee Member

Charles Moran

Committee Member

Phil Rather

Committee Member

Yih-Ling Tzeng

Committee Member

Accepted by the Laney Graduate School

Kimberly Jacob Arriola, PhD, MPH

Dean, James T. Laney School of Graduate Studies

Investigation of the factors that regulate sporulation initiation in
Clostridioides difficile

By

By Michael A. DiCandia
B.S., Gettysburg College, 2015

Advisor: Shonna M. McBride, Ph.D.

An abstract of
A dissertation submitted to the Faculty of the
James T. Laney School of Graduate Studies of Emory University
In partial fulfillment of the requirements for the degree of
Doctor of Philosophy

Graduate Division of Biological and Biomedical Science
Genetics and Molecular Biology

2022

Abstract

Investigation of the factors that regulate sporulation initiation in
Clostridioides difficile

By Michael A DiCandia

     Clostridioides difficile is an anaerobic, Gram-positive pathogen that is responsible for *C. difficile* infection (CDI). To spread to new hosts, *C. difficile* must form metabolically-dormant spores. Spo0A is the conserved, master regulator of sporulation in all spore-forming bacteria and must be activated by phosphorylation at a conserved aspartate residue for sporulation to initiate. Though the regulatory proteins that control Spo0A in *Bacillus* species have been identified, the direct regulators of Spo0A in *C. difficile* are incompletely defined. To gain insight into the molecular mechanisms that govern sporulation initiation in *C. difficile*, we performed site-directed mutagenesis of Spo0A and examined the effects on sporulation. As Spo0A shares high sequence similarity between *Bacillus subtilis* and *C. difficile*, we chose to mutate conserved Spo0A residues that are functionally important for interaction with sporulation regulatory proteins in *B. subtilis*. Our data demonstrate that mutation of conserved Spo0A residues significantly impacts sporulation frequency, suggesting that these sites are likewise important for sporulation in *C. difficile*. Additionally, we sought to define the Spo0A interactome to identify direct Spo0A regulators. In our co-immunoprecipitation experiments, we identified a putative *C. difficile* ortholog to the *Bacillus* protein, Spo0E as a Spo0A interacting partner. In *Bacillus*, Spo0A is directly dephosphorylated by Spo0E to inhibit sporulation. However, functional evidence for Spo0E function in *C. difficile* and other spore-forming anaerobes is lacking. To determine Spo0E function in *C. difficile*, we created a *spo0E* mutant. Mutation of *spo0E* resulted in increased sporulation, demonstrating Spo0E represses sporulation in *C. difficile*. Unexpectedly, the *spo0E* mutant exhibited increased toxin production and motility, providing the first known evidence that Spo0E is involved in physiological processes independent of Spo0A. Accordingly, the *spo0E* mutant had increased virulence and earlier toxin production *in vivo*, demonstrating that Spo0E regulates *C. difficile* pathogenesis. We found that Spo0E repressed motility in *B. subtilis*, indicating that Spo0E has conserved functionality outside of sporulation. Lastly, we found that putative Spo0E orthologs are broadly conserved, including in non-sporulating bacteria and Archaea, further demonstrating that Spo0E is not simply a repressor of sporulation. Altogether, our findings further our understanding of the factors and mechanisms that impact sporulation initiation and pathogenesis in *C. difficile*.

Investigation of the factors that regulate sporulation initiation in
Clostridioides difficile

By

By Michael A. DiCandia
B.S., Gettysburg College, 2015

Advisor: Shonna M. McBride, Ph.D.

A dissertation submitted to the Faculty of the
James T. Laney School of Graduate Studies of Emory University
In partial fulfillment of the requirements for the degree of
Doctor of Philosophy

Graduate Division of Biological and Biomedical Science
Genetics and Molecular Biology

2022

Acknowledgments

First I would like to thank my advisor, Shonna. She has taught me how to formulate hypotheses and interpret data in a biologically relevant and meaningful way. Further, she has allowed me to pursue my own intellectual curiosities while allowing me to learn and grow from my mistakes. The lessons I learned from her mentorship will undoubtedly influence my future scientific and personal endeavors.

I would also like to thank the members of the McBride Lab for their unwavering support and for truly fostering a kind, intellectual, and wholesome workspace environment. I am forever grateful for the wonderful friendships we have formed over the years.

I am grateful for encouragement from my parents. I could not have completed this extensive and trying journey without their moral support.

Meredith has been a steadfast source of happiness for me. I cannot fathom completing this degree without her. I'd also like to acknowledge my bowtie-sporting Corgi, Kevin, for helping to relieve the stresses of graduate school.

To the rest of my committee, mentors, friends, and colleagues: I sincerely thank you for helping to make my graduate school experience wholly enjoyable. I have learned valuable lessons and advice that will guide me for the rest of my life. I am grateful that I can reflect so fondly on all of those who have been a source of support throughout the pursuit of this doctorate.

Table of Contents

Abstract

Acknowledgments

Table of Contents

List of Tables and Figures

List of Tables and Figures

Chapter 2

Table 1: Sporulation frequencies of *C. difficile* Spo0A site-directed mutants

Table 2: Spo0A site-directed mutant morphology and growth phenotypes

Table 3: Bacterial strains and plasmids

Table 4: Oligonucleotides

Table S1: Luminescence outputs from split-luciferase assay

Table S2: Cloning and vector construction details

Figure 1: Evolutionary divergent strategies for Spo0A activation

Figure 2: Conservation of the Spo0A receiver domains in *B. subtilis* and *C. difficile*

Figure 3: Mutagenesis of conserved Spo0A residues results in both increased and decreased *C. difficile* sporulation frequency

Figure 4: The conserved aspartate residue of *C. difficile* Spo0A is phosphorylated

Figure 5: Residues necessary for Spo0A dimerization in other Firmicutes are functionally conserved in *C. difficile*

Figure S1: Predicted Spo0A structure and domain architecture

Figure S2: Alignment of receiver domain residues of *B. subtilis* Spo0A and Spo0F, and *C. difficile* Spo0A

Figure S3: Stability of Spo0A mutant alleles

Figure S4: Predicted wildtype and site-directed mutant Spo0A structures

Figure S5: Spo0A divergence in Firmicutes

Chapter 3

Table 1: Prominent factors identified in protein pulldowns in *C. difficile*

Table S1: Filtered proteins identified in Spo0E pulldown

Table S2: Filtered proteins identified in Spo0A pulldown

Table S3: Bacterial strains and plasmids

Table S4: Oligonucleotides

Table S5: Cloning and vector construction details

Figure 1: Spo0E represses sporulation, toxin, and motility in *C. difficile*

Figure 2: Disruption of *spo0E* increases morbidity and early production of toxins during infection

Figure 3: Spo0E repression of motility is conserved

Figure 4: Spo0E-like proteins are conserved and widespread

Figure S1: Construction and confirmation of the *spo0E* mutant

Figure S2: *spo0E* phenotypes are complemented with reintroduction of *spo0E*

Figure S3: Proteins that co-purify with Spo0E

Figure S4: Model of Spo0E influence on sporulation initiation in *C. difficile*

Chapter 1: Introduction

I: *Clostridioides difficile*

    a. *Clostridioides difficile* is a prominent nosocomial pathogen

Clostridioides difficile is a leading hospital acquired pathogen in the United States and causative agent of *C. difficile* infection (CDI). CDI was associated with more than 29,000 deaths, over 450,000 cases, and billions of dollars in increased healthcare costs according to the Centers for Disease Control and Prevention (CDC) (1–3). In addition to widespread hospital acquisition, CDI is also frequently recurrent, with an estimated 20% of patients experiencing recurrent infections (2). As a result, CDI poses a significant burden on both the economy and the healthcare system in the United States.

CDI is a highly contagious gastrointestinal disease, with the most common symptom associated with CDI being diarrhea (4). Recently, a more virulent *C. difficile* strain (B1/NAP1/027) has emerged that is less responsive to treatment, and this has been associated with an increase of CDI cases (5–7). Additionally, the number of CDI-associated hospital discharges doubled in the United States between 2001 and 2005, further highlighting the increasing burden of CDI (8).

    b. Risk factors for CDI

The majority of hospital acquired *C. difficile* infections occur in the elderly over the age of 65, immunocompromised individuals, or patients currently or recently under the treatment of antibiotics (1,2,9,10). The mortality rate for CDI patients 80 years old or older is 13%, and mortality in at-risk patients is 6% within 3 months of acquiring CDI (11). Additional risk factors are associated with healthcare facilities, such as duration of stay and a prior room occupant having CDI (12,13). In fact, it is estimated that 70% of CDI cases are hospital-acquired (1).

The most common risk factor for susceptibility to CDI is antibiotic usage. Every class of antibiotics with the exception of tetracyclines are associated with increased risk for later

developing CDI (14,15). After antibiotic treatment, patients remain susceptible to developing

CDI for up to three months (16). Alarmingly, 15% of hospitalized patients administered

antibiotics will develop CDI, and 21% of hospitalized patients are colonized with *C. difficile*,

demonstrating the devastating potential antibiotic treatment in hospital settings has for

facilitating acquisition of CDI (17).

Antibiotic usage disrupts the gut microbiome, rendering a patient to become susceptible

to developing CDI (18). In healthy individuals, *C. difficile* competes poorly against the normal gut

microbiome for nutrients, such as amino acids. Additionally, the healthy gut microbiome

provides protection against developing CDI, since *C. difficile* cannot effectively obtain the

nutrients required for colonization (19). However, antibiotic treatment dramatically decreases the

diversity of the gut microbiome, particularly against intestinal species that can directly inhibit *C.

difficile* colonization (19,20). With the loss of species complexity in the gut microbiome following

antibiotic treatment, *C. difficile* has less competition for nutrients and can therefore proliferate

and ultimately cause CDI as it traverses through the colon. Further, the disruption of the gut

microbiome following antibiotic use will also drastically alter the composition of the metabolic by-

products that are normally produced by commensal species (19,21,22). The altered metabolic

landscape of the gut provides a variety of changes that help facilitate *C. difficile* colonization and

ultimately CDI. For example, loss of species that produce fatty acids in the gut results in a

dampened immune response, and loss of species that metabolize primary bile acids helps

facilitate *C. difficile* colonization, as primary bile acids induce germination of *C. difficile* spores

(23,24). Through the loss of competition for nutrients in combination with an altered gut

metabolic profile, antibiotic treatment can provide a gut environment that highly favors *C. difficile*

outgrowth and colonization.

c. Dissemination of CDI

C. difficile is a Gram-positive, anaerobic spore-forming bacterium. As a strict anaerobe,

C. difficile must form hardy, metabolically dormant spores in order to survive in the environment and spread from host to host. The ability to sporulate allows *C. difficile* to persist in the environment and remain inert until a susceptible host comes in physical contact with hosts or fomites contaminated with *C. difficile* spores (25–27). Since *C. difficile* spores are inherently resistant to alcohol-based sanitizers and most cleaning products, and can easily spread between patients or from healthcare providers to patients, the hospital setting provides ample opportunity for highly susceptible individuals already seeking medical care to also become exposed to *C. difficile*.

Once ingested following acquisition from a contaminated source, *C. difficile* spores germinate in the small intestine in the presence of bile salts (28–31). As *C. difficile* then moves from the small intestine to the colon, actively growing *C. difficile* cells release the toxins TcdA and TcdB (32,33). Once released, TcdA and TcdB will glucosylate Rho GTPases that serve to maintain the integrity of the actin cytoskeleton of intestinal epithelial cells (32,34). Following intoxication and subsequent disruption of tight junctions, epithelial cells become rounded and ultimately die through apoptosis or necrosis. The loss of epithelial cell tight junctions facilitates symptoms of CDI and can result in severe diarrhea, pseudomembranous colitis, or toxic megacolon (32,34–36). Additionally, the toxins induce secretion of cytokines to damaged epithelial cells, such as IL-1, IL-6, and IL-8 that may further increase cell permeability and exacerbate diarrheal symptoms (37). The release of immune factors that cause inflammation can also damage gut tissue, further damaging the host (33,37,38). Ultimately, *C. difficile* cells initiate sporulation in the colon and are eventually shed to the environment in the host's feces to continue the cycle of disease through the spread of spores (39).

C. difficile forms recalcitrant spores that are difficult to eliminate from the environment. In addition to facilitating persistence in the environment, spores are a useful vehicle for transmission, particularly in healthcare settings that house susceptible patients, including those

suffering from CDI that shed spores into the environment. For example, spores can be spread to new hosts through contaminated clothing, medical devices, and by healthcare workers (13,40–42). While preventative measures such as the use of protective clothing and gloves can help mitigate the risk of spreading *C. Difficile* spores, a study in 2015 estimated that 46% of cases of nosocomially-acquired CDI occurred after removal of protective clothing, further highlighting hospital settings as a significant risk factor for CDI development (43).

II. Endospore formation

a. Sporulation is a survival mechanism

Sporulation is a unique survival strategy that facilitates resistance to environmental stressors, such as heat exposure, limited nutrient availability, exposure to antimicrobial agents, and desiccation. The formation of a spore is an incredibly complex developmental process that requires fine-tuned checkpoints and regulation. During sporulation, the bacterial cell transitions from an actively growing state to complete metabolic dormancy, and can be reanimated upon the return of favorable environmental conditions that include the required germinant. Sporulation is thus a means of survival and is not a method of replication since one cell becomes one spore (44). Incredibly, there have been numerous examples of reanimating spores after millions of years of dormancy, demonstrating the extreme hardiness and survivability of forming a spore (45,46). The precise mechanisms and events that lead to sporulation will be discussed in greater detail.

b. Mechanism of endospore formation

Spore formation is characterized by specialized asymmetric cell division that involves lysis of the original cell (mother cell) and release of a mature spore (47). The complete process of sporulation is carried out through seven stages denoted by roman numerals, with the initiation of sporulation occurring at stage 0, while the cell is still actively growing (47–49). Briefly, as the

cell decides to initiate sporulation, genomic DNA rearranges to form the axial filament, defining stage I of sporulation (50). During stage II, asymmetric cell division begins between the mother cell and developing prespore, with genomes segregating to the poles of the mother cell and prespore (51). The mother cell then engulfs the prespore to form the forespore at stage III, and peptidoglycan is then added to the forespore to create an inner cell wall layer and an outer cortex at stage IV (52,53). Spore coat proteins are then added to the developing forespore at stage V, and further maturation of the forespore occurs at stage VI (50). At stage VII, the mature spore lyses from the mother cell and is released. The spore's core is dehydrated between stages III – VII, which allows the spore to survive extreme environmental insults until the spore is stimulated to germinate (50,54).

Spore formation is restricted to the members of the Firmicutes (recently renamed Bacillota) and are defined as Gram-positive bacteria with low G+C content (55). While not all Firmicutes form spores, many members encode the genes required for all stages of sporulation, including notable pathogens such as *Clostridium botulinum*, *Clostridium perfringens*, *Paeniclostridium sordellii*, *Bacillus anthracis*, *Bacillus cereus*, and *C. difficile*. In particular, two classes of Firmicutes that will be further detailed here are the anaerobic Clostridia, and the aerobic or facultative aerobic Bacilli.

III. Key regulators of sporulation initiation

    a. Spo0A, the master regulator of sporulation

Spo0A is the master transcriptional regulator of sporulation, and is conserved in all endospore-forming bacteria (56,57). Spo0A is a response regulator (transcription factor) that has a receiver domain, which facilitates sensory inputs from regulatory proteins, and a DNA-binding domain that regulates transcription (58,59). In *B. subtilis*, Spo0A was shown to directly and indirectly control expression of over 500 genes that are needed for sporulation and post-

exponential growth processes (58). Spo0A must be activated through phosphorylation at a conserved aspartate residue in order to bind to DNA to regulate gene expression (56,60). This mechanism of activation by phosphorylation at a functional aspartate residue is highly conserved and commonly used by bacteria to regulate signal transduction. Specifically, two-component systems consist of signal transduction via phosphorylation between sensor kinases and response regulator transcription factors in response to environmental stimuli (59,61,62). As a response regulator, Spo0A activation through phosphorylation is absolutely required for sporulation to occur and Spo0A activation cannot be bypassed. As sporulation is energetically costly to the cell, Spo0A activation is tightly regulated to prevent inappropriate initiation of sporulation (63–67). In fact, the decision to undergo sporulation was ultimately shown to be an all-or-nothing decision in *B. subtilis*, demonstrating that sporulation initiation is a highly controlled cell fate (68).

All spore-forming members of the Firmicutes encode Spo0A (58). Interestingly, despite being more closely related to *Bacillus*, Firmicutes such as *Listeria* do not possess Spo0A orthologs or sporulation machinery, while some of the more distantly related Firmicutes to Bacilli such as the Clostridia do retain Spo0A (58). This disparity, and the fact that Bacilli and Clostridia have been on separate evolutionary paths since at least the Great Oxygenation Event roughly 2.4 billion years ago, may explain the major differences in Spo0A regulation between Bacilli and Clostridia (69). These key differences and their implications are further discussed.

b. Sporulation initiation in the Bacilli

The ability to sporulate is critical for bacterial survival in environments that do not support growth. Early experiments seeking to characterize regulation of sporulation were largely performed in *B. subtilis*, which became a model for spore formation (63,64,70,70,71). As a result, almost all of the molecular mechanisms known about regulation of sporulation initiation are known from *Bacillus*. In *B. subtilis* and other Bacilli, a multicomponent, expanded two-

component system known as the phosphorelay mediates the flow of phosphate to Spo0A to regulate sporulation initiation (72). In the phosphorelay, the sporulation histidine kinases KinA, KinB, KinC, KinD, and KinE are orphan histidine kinases that directly phosphorylate at a conserved aspartate on the intermediary response regulator, Spo0F (61,64,73–75). Next, Spo0F phosphorylates the phosphotransfer protein Spo0B at a conserved histidine, and activated Spo0B in turn phosphorylates Spo0A at a conserved aspartate. Following activation via Spo0B, phosphorylated Spo0A can then bind DNA to initiate sporulation (58,64,72). This constitutes the phosphorelay, in which kinases and phosphotransfer proteins become phosphorylated at a specific histidine residue, and transfer phosphate to a conserved aspartate of response regulators. Interestingly, Spo0F does not contain a DNA-binding domain, but instead is a single domain response regulator that functions solely to transfer phosphate between KinA-E and Spo0B (64,76,77). The multi-component nature of the phosphorelay provides multiple checkpoints to regulate the transfer of phosphate to Spo0A and entry into sporulation.

There are several mechanisms to prevent Spo0A activation so that sporulation is not prematurely initiated. The Rap family of phosphatases regulate signal transduction in Gram-positive bacteria in response to cell density. For example, *B. subtilis* encodes 11 Rap proteins on the chromosome and maintains an additional 5 Rap proteins on plasmids (78). Rap proteins have an N-terminal effector domain and C-terminal tetratricopeptide repeats (TPR) that facilitate protein-protein interactions (79–83). Specific members of *B. subtilis* Rap phosphatases, including RapA, RapB, RapE, RapH, and RapJ, use their effector domain to directly dephosphorylate Spo0F to prevent phosphotransfer with Spo0B (79–81,84–86). The remaining Rap proteins regulate gene expression by binding DNA through their DNA-binding domain (87–89). Rap activity is further regulated by interaction with quorum sensing signals known as Phr peptides (78,86–88). Phr peptides interact with the Rap C-terminal TPR domain (79,81,90). Phr

binding then inhibits Rap function (78). The complexity of the Rap-Phr system and its influence on the phosphorelay through interactions with Spo0F further demonstrates the tight regulation of Spo0A activation.

In addition to preventing inappropriate sporulation through dephosphorylating Spo0F by Rap proteins, negative regulation of the phosphorelay is also facilitated by Spo0E. The Spo0E family of proteins are small (45 -100 amino acids) aspartyl-phosphate phosphatases that directly dephosphorylate Spo0A to negatively control sporulation (91–94). *B. subtilis* encodes Spo0E and two additional paralogs, YisI and YnzD, that directly repress Spo0A activity (94). Interestingly, in *B. subtilis,* Spo0E appears to be the main Spo0A phosphatase, as *yisI* and *ynzD* single mutants do not impact sporulation, and their repressive effect on sporulation can only be observed in a *yisI ynzD* double mutant background (94). The 3D structural characteristic of Spo0E and Spo0E-like proteins is a simple two strings of α-helices, separated by a short loop (95). Residues in α2 have been identified that are important for Spo0E function, though it remains unclear if residues that comprise α1 are important for function (96). Further, Spo0E and Spo0E-like proteins contain a signature Spo0E motif of five amino acids (SQELD) in the α2-helix, with the serine and aspartate residues being invariant across identified Spo0E orthologs (93,97,98). In particular, the conserved aspartate in the Spo0E motif was found to be functionally important for phosphatase activity upon Spo0A (96). However, functional studies on Spo0E have been largely restricted to *B. subtilis* and *B. anthracis*, potentially limiting interpretation of the functional role of the Spo0E family of proteins (93,95–97,99).

c. Sporulation initiation in the Clostridia

Regulation of Clostridial sporulation initiation is less defined compared to *Bacillus.* Despite the critical role sporulation has in the physiology and pathogenesis in notable Clostridial pathogens like *C. perfringens*, *C. botulinum*, *P. sordellii*, and *C. difficile*, comparatively fewer studies have been performed to investigate the regulation of sporulation in the Clostridia than in

Bacilli. Many components of the *Bacillus* phosphorelay, such as Spo0F or Spo0B, are not encoded in Clostridial genomes, despite the conservation of Spo0A function for sporulation (56,58,98,100–105). While the regulatory pathways that control sporulation initiation have been well characterized in Bacilli, the precise molecular mechanisms of sporulation initiation remain incompletely defined in many Clostridia, including *C. difficile* (56,63–67,72,91,100–104,106).

In some Clostridial species, Spo0A was shown to directly interact with sensor histidine kinases to control Spo0A activity in a manner more similar to the classical two-component system, and by-passing the Spo0F or Spo0B intermediates (101–104). However, in all cases described, only kinases have been identified as Clostridial Spo0A binding partners. Considering the complexity of control of Spo0A activity identified in *Bacillus,* it is tempting to speculate that there are additional mechanisms of Clostridial Spo0A regulation, including for *C. difficile*.

Despite lacking clear orthologs to the phosphorelay proteins Spo0F and Spo0B, *C. difficile* does encode three orphan histidine kinases, PtpA, PtpB, and PtpC, that resemble the *Bacillus* sporulation kinases that activate the phosphorelay. However, unlike in *Bacillus*, these kinases negatively regulate sporulation initiation (100). Although the sporulation kinases PtpA, PtpB, and PtpC do not appear to activate sporulation in *C. difficile*, Spo0A must be phosphorylated for efficient sporulation to occur, suggesting that an unknown mechanism for Spo0A activation exists (56).

RstA was identified as a positive regulator of *C. difficile* sporulation, though the molecular mechanism by which RstA promotes sporulation was not understood (106). Further, RstA directly represses expression of genes required for toxin and motility, demonstrating that RstA has a marked influence over multiple, different mechanisms of *C. difficile* pathogenesis (106,107). RstA belongs to the RRNPP family of proteins, as are the Rap phosphatases in Bacilli. But, unlike the Raps, RstA is comprised of an N-terminal DNA-binding domain, a Spo0F-like TPR domain, and a C-terminal TPR domain (78,106). RstA does not appear to possess the

Rap phosphatase domain, and there is no evidence that RstA is involved in phosphotransfer reactions. Thus, RstA is not a direct ortholog of the Rap phosphatases, and must influence sporulation through a different mechanism than the *Bacillus* Rap proteins. Understanding the role of RstA in facilitating sporulation initiation is thus critical for furthering our understanding of this crucial facet of *C. difficile* physiology.

While obvious orthologs to the Rap phosphatases have not been identified in *C. difficile*, through genomic comparisons we have identified a putative ortholog (*CD630_32710*) to the *Bacillus* protein, Spo0E. To our knowledge, there are no studies describing Spo0E function in the Clostridia. A pan-genome study described putative Spo0E-like orthologs in both aerobic and anaerobic spore-formers, providing the first description of Spo0E-like proteins present in anaerobic spore-formers, but no functional follow-up studies were performed to probe Spo0E function outside of *Bacillus* (97). As previously mentioned, characterization of Spo0E in *Bacillus* identified a signature motif that is characteristic of Spo0E-like proteins (93,97,98). Though well-conserved in *Bacillus*, this motif is considerably more variable in the Clostridia (SKKID in *C. difficile*). Despite this, the predicted 3D structure of the *C. difficile* Spo0E ortholog highly resembles the known crystal structure of *B. anthracis* Spo0E, and the Spo0E motif is predicted to be located in α2, just as in *Bacillus* Spo0E, suggesting that Spo0E may also be a regulator of *C. difficile* sporulation (108).

IV. Toxin production facilitates CDI

a. TcdA and TcdB facilitate symptomatic CDI

As described in Section I, the toxins TcdA and TcdB are the main virulence factors that cause the symptoms of CDI (35). Depending on the *C. difficile* strain causing infection, and individual circumstances such as risk factors and microbiome composition, those colonized with *C. difficile* may experience a range of severity of CDI symptoms. CDI symptoms can vary

considerably, from asymptomatic carriage to ultimately death (18,25,109). However, symptom severity is ultimately mediated by toxin production (18).

The toxins *tcdA* and *tcdB* are encoded within a 19.6 kb region on the chromosome known as the Pathogenicity Locus (PaLoc) (35). Also encoded in the PaLoc are the accessory factors *tcdC*, *tcdR*, and *tcdE*. TcdR is a sigma factor that positively regulates expression of the PaLoc locus, while TcdC is an anti-sigma factor that inhibits TcdR activity (110,111). The role of TcdE is less understood, but it is predicted to act as a holin that facilitates the release of TcdA and TcdB from *C. difficile* (112–115). Further, it was shown that the production of TcdB alone is sufficient to cause severe disease, and that production of TcdA alone caused attenuated virulence, implicating TcdB as the primary driver of CDI disease progression (116).

Multiple factors can directly or indirectly influence sporulation, toxin production, and motility in C. *difficile*. RstA is an interesting example of a regulator of sporulation, toxin, and motility, in which the positive regulation of sporulation was not fully understood. As previously mentioned, RstA is a DNA-binding protein that directly represses toxin and motility gene expression in *C. difficile* (106,107). Putative RstA orthologs are encoded in other pathogenic Clostridia, raising the possibility that RstA may exert conserved and widespread regulation of toxin and sporulation in other Clostridial pathogens. It is therefore important to better understand the molecular mechanisms by which RstA contributes to facilitating *C. difficile* pathogenesis through regulating sporulation and toxin production.

b. CDT is binary toxin that mediates severe CDI

The binary toxin CDT is found in some *C. difficile* strains, including the epidemic B1/NAP1/027 strain, and is associated with increased severity of infection (117,118). Similar to TcdA and TcdB, CDT causes actin destabilization of the gut epithelial cytoskeleton (117,118). However, the mechanism of actin depolymerization differs from TcdA and TcdB, as CDT causes ADP-ribosylation of actin, resulting in protrusion of epithelial cells that facilitates *C. difficile*

colonization (119). Additionally, CDT induces inflammation of gut epithelial cells through Toll

Like Receptor 2 (TLR2) signaling, further enhancing *C. difficile* virulence (118). CDT intoxication

thus represents an additional mechanism that *C. difficile* employs to cause symptoms of CDI

and further spread spores to the environment.

V. Specific Aims

Because sporulation and toxin production are critical to *C. difficile* pathogenesis,

understanding the precise regulation of these processes could lead to rational therapeutic

intervention and drug design. Understanding the regions of Spo0A that are important for

function could allow for targeted inactivation of Spo0A activity. Critically, relatively little is known

about Spo0A regulation in *C. difficile* despite the central role Spo0A has in regulating a

fundamental aspect of *C. difficile* pathogenesis. By identifying the regulatory factors that act

upon Spo0A to modulate its activity, we can better understand how *C. difficile* is regulating

sporulation and toxin production in the host. To increase our understanding of sporulation

initiation in *C. difficile*, the goal of my thesis was to define molecular mechanisms that govern

Spo0A activity in *C. difficile*. Here, I investigated the regulation of *C. difficile* sporulation initiation

through the following specific aims:

1. Identify Spo0A residues that are important for sporulation initiation in *C. difficile*.
2. Characterize Spo0A binding partners that regulate pathogenesis in *C. difficile*.

1. Lessa FC, Mu Y, Bamberg WM, Beldavs ZG, Dumyati GK, Dunn JR, et al. Burden of Clostridium difficile infection in the United States. N Engl J Med. 2015;372(9):825–34.

2. McDonald LC, Gerding DN, Johnson S, Bakken JS, Carroll KC, Coffin SE, et al. Clinical Practice Guidelines for Clostridium difficile Infection in Adults and Children: 2017 Update by the Infectious Diseases Society of America (IDSA) and Society for Healthcare Epidemiology of America (SHEA). Clin Infect Dis. 2018 Mar 19;66(7):e1–48.

3. Vonberg RP, Reichardt C, Behnke M, Schwab F, Zindler S, Gastmeier P. Costs of nosocomial Clostridium difficile-associated diarrhoea. J Hosp Infect. 2008 Sep;70(1):15–20.

4. Burdon DW, Brown JD, Youngs DJ, Arabi Y, Shinagawa N, Alexander-Williams J, et al. Antibiotic susceptibility of Clostridium difficile. J Antimicrob Chemother. 1979 May;5(3):307–10.

5. Pepin J, Valiquette L, Alary ME, Villemure P, Pelletier A, Forget K, et al. Clostridium difficile-associated diarrhea in a region of Quebec from 1991 to 2003: a changing pattern of disease severity. CMAJ. 2004 Aug 31;171(5):466–72.

6. Pepin J, Saheb N, Coulombe MA, Alary ME, Corriveau MP, Authier S, et al. Emergence of fluoroquinolones as the predominant risk factor for Clostridium difficile-associated diarrhea: a cohort study during an epidemic in Quebec. Clin Infect Dis. 2005 Nov 1;41(9):1254–60.

7. Pepin J, Alary ME, Valiquette L, Raiche E, Ruel J, Fulop K, et al. Increasing risk of relapse after treatment of Clostridium difficile colitis in Quebec, Canada. Clin Infect Dis. 2005 Jun 1;40(11):1591–7.

8. Bagdasarian N, Rao K, Malani PN. Diagnosis and Treatment of *Clostridium difficile* in Adults: A Systematic Review. JAMA. 2015 Jan 27;313(4):398.

9. Dubberke ER, Butler AM, Reske KA, Agniel D, Olsen MA, D'Angelo G, et al. Attributable Outcomes of Endemic *Clostridium difficile* –associated Disease in Nonsurgical Patients. Emerg Infect Dis. 2008 Jul;14(7):1031–8.

10. Sammons JS, Localio R, Xiao R, Coffin SE, Zaoutis T. Clostridium difficile Infection Is Associated With Increased Risk of Death and Prolonged Hospitalization in Children. Clin Infect Dis. 2013 Jul 1;57(1):1–8.

11. Karas JA, Enoch DA, Aliyu SH. A review of mortality due to Clostridium difficile infection. J Infect. 2010 Jul;61(1):1–8.

12. Shaughnessy MK, Micielli RL, DePestel DD, Arndt J, Strachan CL, Welch KB, et al. Evaluation of Hospital Room Assignment and Acquisition of *Clostridium difficile* Infection. Infect Control Hosp Epidemiol. 2011 Mar;32(3):201–6.

13. Jullian-Desayes I, Landelle C, Mallaret MR, Brun-Buisson C, Barbut F. Clostridium difficile contamination of health care workers' hands and its potential contribution to the spread of infection: Review of the literature. Am J Infect Control. 2017 Jan;45(1):51–8.

14. Slimings C, Riley TV. Antibiotics and hospital-acquired Clostridium difficile infection: update of systematic review and meta-analysis. J Antimicrob Chemother. 2014 Apr;69(4):881–91.

15. Baines SD, Saxton K, Freeman J, Wilcox MH. Tigecycline does not induce proliferation or cytotoxin production by epidemic Clostridium difficile strains in a human gut model. J Antimicrob Chemother. 2006 Sep 6;58(5):1062–5.

16. Hensgens MPM, Goorhuis A, Dekkers OM, Kuijper EJ. Time interval of increased risk for Clostridium difficile infection after exposure to antibiotics. J Antimicrob Chemother. 2012 Mar;67(3):742–8.

17. McFarland LV. Epidemiology, Risk Factors and Treatments for Antibiotic-Associated Diarrhea. Dig Dis. 1998;16(5):292–307.

18. Pothoulakis C. Pathogenesis of Clostridium difficile-associated diarrhoea: Eur J Gastroenterol Hepatol. 1996 Nov;8(11):1041–7.

19. Keeney KM, Yurist-Doutsch S, Arrieta MC, Finlay BB. Effects of Antibiotics on Human Microbiota and Subsequent Disease. Annu Rev Microbiol. 2014 Sep 8;68(1):217–35.

20. Theriot CM, Koenigsknecht MJ, Carlson PE, Hatton GE, Nelson AM, Li B, et al. Antibiotic-induced shifts in the mouse gut microbiome and metabolome increase susceptibility to Clostridium difficile infection. Nat Commun. 2014;5:3114.

21. Rolfe RD, Helebian S, Finegold SM. Bacterial Interference Between Clostridium difficile and Normal Fecal Flora. J Infect Dis. 1981 Mar 1;143(3):470–5.

22. Drissi F, Buffet S, Raoult D, Merhej V. Common occurrence of antibacterial agents in human intestinal microbiota. Front Microbiol [Internet]. 2015 May 7 [cited 2022 Oct 30];6. Available from: http://www.frontiersin.org/Evolutionary_and_Genomic_Microbiology/10.3389/fmicb.2015.00441/abstract

23. Buffie CG, Bucci V, Stein RR, McKenney PT, Ling L, Gobourne A, et al. Precision microbiome reconstitution restores bile acid mediated resistance to Clostridium difficile. Nature. 2015 Jan 8;517(7533):205–8.

24. Sorg JA, Sonenshein AL. Bile salts and glycine as cogerminants for Clostridium difficile spores. J Bacteriol. 2008 Apr;190(7):2505–12.

25. McFarland LV, Mulligan ME, Kwok RY, Stamm WE. Nosocomial acquisition of Clostridium difficile infection. N Engl J Med. 1989 Jan 26;320(4):204–10.

26. Johnson S, Clabots CR, Linn FV, Olson MM, Peterson LR, Gerding DN. Nosocomial Clostridium difficile colonisation and disease. Lancet. 1990 Jul 14;336(8707):97–100.

27. Savage AM, Alford RH. Nosocomial Spread of *Clostridium Difficile*. Infect Control. 1983 Feb;4(1):31–3.

28. Paredes-Sabja D, Bond C, Carman RJ, Setlow P, Sarker MR. Germination of spores of Clostridium difficile strains, including isolates from a hospital outbreak of Clostridium difficile-associated disease (CDAD). Microbiology. 2008 Aug;154(Pt 8):2241–50.

29. Burns DA, Heap JT, Minton NP. SleC is essential for germination of Clostridium difficile spores in nutrient-rich medium supplemented with the bile salt taurocholate. J Bacteriol. 2010 Feb;192(3):657–64.

30. Giel JL, Sorg JA, Sonenshein AL, Zhu J. Metabolism of bile salts in mice influences spore germination in Clostridium difficile. PLoS One. 2010;5(1):e8740.

31. Francis MB, Allen CA, Shrestha R, Sorg JA. Bile acid recognition by the Clostridium difficile germinant receptor, CspC, is important for establishing infection. PLoS Pathog. 2013 May;9(5):e1003356.

32. Chumbler NM, Farrow MA, Lapierre LA, Franklin JL, Lacy DB. Clostridium difficile Toxins TcdA and TcdB Cause Colonic Tissue Damage by Distinct Mechanisms. Infect Immun. 2016 Oct;84(10):2871–7.

33. Di Bella S, Ascenzi P, Siarakas S, Petrosillo N, di Masi A. Clostridium difficile Toxins A and B: Insights into Pathogenic Properties and Extraintestinal Effects. Toxins. 2016 May 3;8(5):134.

34. Pruitt RN, Lacy DB. Toward a structural understanding of Clostridium difficile toxins A and B. Front Cell Infect Microbiol [Internet]. 2012 [cited 2022 Oct 26];2. Available from: http://journal.frontiersin.org/article/10.3389/fcimb.2012.00028/abstract

35. Kuehne SA, Cartman ST, Heap JT, Kelly ML, Cockayne A, Minton NP. The role of toxin A and toxin B in *Clostridium difficile* infection. Nature. 2010 Oct 7;467(7316):711–3.

36. Brito GA, Fujii J, Carneiro-Filho BA, Lima AA, Obrig T, Guerrant RL. Mechanism of Clostridium difficile toxin A–induced apoptosis in T84 cells. J Infect Dis. 2002;186(10):1438–47.

37. Savidge TC, Pan W hua, Newman P, O'Brien M, Anton PM, Pothoulakis C. Clostridium difficile toxin B is an inflammatory enterotoxin in human intestine. Gastroenterology. 2003;125(2):413–20.

38. Jafari NV, Kuehne SA, Bryant CE, Elawad M, Wren BW, Minton NP, et al. Clostridium difficile Modulates Host Innate Immunity via Toxin-Independent and Dependent Mechanism(s). Lenz LL, editor. PLoS ONE. 2013 Jul 29;8(7):e69846.

39. Abt MC, McKenney PT, Pamer EG. Clostridium difficile colitis: pathogenesis and host defence. Nat Rev Microbiol. 2016 Oct;14(10):609–20.

40. Mitchell BG, Dancer SJ, Anderson M, Dehn E. Risk of organism acquisition from prior room occupants: a systematic review and meta-analysis. J Hosp Infect. 2015 Nov;91(3):211–7.

41. Brooks S, Khan A, Stoica D, Griffith J, Friedeman L, Mukherji R, et al. Reduction in Vancomycin-Resistant Enterococcus and Clostridium difficile Infections following Change to Tympanic Thermometers. Infect Control Hosp Epidemiol. 1998 May;19(5):333–6.

42. Landelle C, Verachten M, Legrand P, Girou E, Barbut F, Buisson CB. Contamination of Healthcare Workers' Hands with *Clostridium difficile* Spores after Caring for Patients with *C. difficile* Infection. Infect Control Hosp Epidemiol. 2014 Jan;35(1):10–5.

43. Tomas ME, Kundrapu S, Thota P, Sunkesula VCK, Cadnum JL, Mana TSC, et al. Contamination of Health Care Personnel During Removal of Personal Protective Equipment. JAMA Intern Med. 2015 Dec 1;175(12):1904.

44. Beskrovnaya P, Sexton DL, Golmohammadzadeh M, Hashimi A, Tocheva EI. Structural, Metabolic and Evolutionary Comparison of Bacterial Endospore and Exospore Formation. Front Microbiol. 2021 Mar 9;12:630573.

45. Cano R, Borucki M. Revival and identification of bacterial spores in 25- to 40-million-year-old Dominican amber. Science. 1995 May 19;268(5213):1060–4.

46. Vreeland RH, Rosenzweig WD, Powers DW. Isolation of a 250 million-year-old halotolerant bacterium from a primary salt crystal. Nature. 2000 Oct;407(6806):897–900.

47. Young IE, Fitz-James PC. Chemical and Morphological Studies of Bacterial Spore Formation. J Biophys Biochem Cytol. 1959 Dec 1;6(3):467–82.

48. Murrell WG. The Biochemistry of the Bacterial Endospore. In: Advances in Microbial Physiology [Internet]. Elsevier; 1967 [cited 2022 Oct 24]. p. 133–251. Available from: https://linkinghub.elsevier.com/retrieve/pii/S0065291108602520

49. Hoch JA. Genetics of Bacterial Sporulation. In: Advances in Genetics [Internet]. Elsevier; 1976 [cited 2021 Sep 8]. p. 69–98. Available from: https://linkinghub.elsevier.com/retrieve/pii/S006526600860437X

50. Buchanan CE, Henriques AO, Piggot PJ. Chapter 8 Cell wall changes during bacterial endospore formation. In: New Comprehensive Biochemistry [Internet]. Elsevier; 1994 [cited 2022 Oct 24]. p. 167–86. Available from: https://linkinghub.elsevier.com/retrieve/pii/S0167730608604111

51. Setlow B, Magill N, Febbroriello P, Nakhimovsky L, Koppel DE, Setlow P. Condensation of the forespore nucleoid early in sporulation of Bacillus species. J Bacteriol. 1991 Oct;173(19):6270–8.

52. Higgins ML, Piggot PJ. Septal membrane fusion ? a pivotal event in bacterial spore formation? Mol Microbiol. 1992 Sep;6(18):2565–71.

53. Tipper DJ, Linnett PE. Distribution of peptidoglycan synthetase activities between sporangia and forespores in sporulating cells of Bacillus sphaericus. J Bacteriol. 1976 Apr;126(1):213–21.

54. Ulanowski Z, Ludlow IK, Waites WM. Water content and size of spore components determined by laser diffractometry. FEMS Microbiol Lett. 1987 Feb;40(2–3):229–32.

55. Galperin MY. Genome Diversity of Spore-Forming *Firmicutes*. Driks A, Eichenberger P, editors. Microbiol Spectr. 2013 Dec 13;1(2):1.2.09.

56. DiCandia MA, Edwards AN, Jones JB, Swaim GL, Mills BD, McBride SM. Identification of functional Spo0A residues critical for sporulation in *Clostridioides difficile* [Internet]. Microbiology; 2022 Feb [cited 2022 Feb 9]. Available from: http://biorxiv.org/lookup/doi/10.1101/2022.02.07.479450

57. Rosenbusch KE, Bakker D, Kuijper EJ, Smits WK. *C. difficile* 630Delta*erm* Spo0A regulates sporulation, but does not contribute to toxin production, by direct high-affinity binding to target DNA. PLoS One. 2012;7(10):e48608.

58. Molle V, Fujita M, Jensen ST, Eichenberger P, González-Pastor JE, Liu JS, et al. The Spo0A regulon of Bacillus subtilis. Mol Microbiol. 2003;50(5):1683–701.

59. Perego M, Hoch JA. Two-Component Systems, Phosphorelays, and Regulation of Their Activities by Phosphatases. In: Sonenshein AL, Hoch JA, Losick R, editors. Bacillus subtilis and Its Closest Relatives [Internet]. Washington, DC, USA: ASM Press; 2014 [cited 2022 Oct 28]. p. 473–81. Available from: http://doi.wiley.com/10.1128/9781555817992.ch33

60. Strauch MA, Hoch JA. Signal transduction in Bacillus subtilis sporulation. Curr Opin Genet Dev. 1993 Apr;3(2):203–12.

61. Hoch JA. Two-component and phosphorelay signal transduction. Curr Opin Microbiol. 2000 Apr;3(2):165–70.

62. Laub MT, Goulian M. Specificity in Two-Component Signal Transduction Pathways. Annu Rev Genet. 2007 Dec;41(1):121–45.

63. Ferrari FA, Trach K, LeCoq D, Spence J, Ferrari E, Hoch JA. Characterization of the *spo0A* locus and its deduced product. Proc Natl Acad Sci U A. 1985 May;82(9):2647–51.

64. Perego M, Cole SP, Burbulys D, Trach K, Hoch JA. Characterization of the gene for a protein kinase which phosphorylates the sporulation-regulatory proteins Spo0A and Spo0F of *Bacillus subtilis*. J Bacteriol. 1989 Nov;171(11):6187–96.

65. Perego M, Spiegelman GB, Hoch JA. Structure of the gene for the transition state regulator, abrB: regulator synthesis is controlled by the spo0A sporulation gene in Bacillus subtilis. Mol Microbiol. 1988 Nov;2(6):689–99.

66. Burbulys D, Trach KA, Hoch JA. Initiation of sporulation in *B. subtilis* is controlled by a multicomponent phosphorelay. Cell. 1991 Feb 8;64(3):545–52.

67. Strauch MA, Wu JJ, Jonas RH, Hoch JA. A positive feedback loop controls transcription of the spoOF gene, a component of the sporulation phosphorelay in Bacillus subtilis. Mol Microbiol. 1993 Mar;7(6):967–74.

68. Kuchina A, Espinar L, Garcia-Ojalvo J, Suel GM. Reversible and noisy progression towards a commitment point enables adaptable and reliable cellular decision-making. PLoS Comput Biol. 2011 Nov;7(11):e1002273.

69. Stephenson K, Lewis RJ. Molecular insights into the initiation of sporulation in Gram-positive bacteria: new technologies for an old phenomenon. FEMS Microbiol Rev. 2005 Apr;29(2):281–301.

70. Baldus JM, Green BD, Youngman P, Moran CP. Phosphorylation of Bacillus subtilis transcription factor Spo0A stimulates transcription from the spoIIG promoter by enhancing binding to weak 0A boxes. J Bacteriol. 1994 Jan;176(2):296–306.

71. Bird TH, Grimsley JK, Hoch JA, Spiegelman GB. Phosphorylation of Spo0A activates its stimulation of in vitro transcription from the Bacillus subtilis spoIIG operon. Mol Microbiol. 1993 Aug;9(4):741–9.

72. Trach K, Burbulys D, Strauch M, Wu JJ, Dhillon N, Jonas R, et al. Control of the initiation of sporulation in *Bacillus subtilis* by a phosphorelay. Res Microbiol. 1991 Oct;142(7–8):815–23.

73. LeDeaux JR, Yu N, Grossman AD. Different roles for KinA, KinB, and KinC in the initiation of sporulation in Bacillus subtilis. J Bacteriol. 1995 Feb;177(3):861–3.

74. LeDeaux JR, Grossman AD. Isolation and characterization of kinC, a gene that encodes a sensor kinase homologous to the sporulation sensor kinases KinA and KinB in Bacillus subtilis. J Bacteriol. 1995 Jan;177(1):166–75.

75. Jiang M, Shao W, Perego M, Hoch JA. Multiple histidine kinases regulate entry into stationary phase and sporulation in Bacillus subtilis. Mol Microbiol. 2000 Nov;38(3):535–42.

76. Jiang M, Tzeng YL, Feher VA, Perego M, Hoch JA. Alanine mutants of the Spo0F response regulator modifying specificity for sensor kinases in sporulation initiation. Mol Microbiol. 1999 Jul;33(2):389–95.

77. Tzeng YL, Hoch JA. Molecular recognition in signal transduction: the interaction surfaces of the Spo0F response regulator with its cognate phosphorelay proteins revealed by alanine scanning mutagenesis. J Mol Biol. 1997 Sep 19;272(2):200–12.

78. Gallego del Sol F, Marina A. Structural basis of Rap phosphatase inhibition by Phr peptides. PLoS Biol. 2013;11(3):e1001511.

79. Baker MD, Neiditch MB. Structural Basis of Response Regulator Inhibition by a Bacterial Anti-Activator Protein. Stock A, editor. PLoS Biol. 2011 Dec 27;9(12):e1001226.

80. Parashar V, Jeffrey PD, Neiditch MB. Conformational change-induced repeat domain expansion regulates Rap phosphatase quorum-sensing signal receptors. PLoS Biol. 2013;11(3):e1001512.

81. Parashar V, Mirouze N, Dubnau DA, Neiditch MB. Structural basis of response regulator dephosphorylation by Rap phosphatases. PLoS Biol. 2011;9(2):e1000589.

82. Declerck N, Bouillaut L, Chaix D, Rugani N, Slamti L, Hoh F, et al. Structure of PlcR: Insights into virulence regulation and evolution of quorum sensing in Gram-positive bacteria. Proc Natl Acad Sci U A. 2007 Nov 20;104(47):18490–5.

83. Zouhir S, Perchat S, Nicaise M, Perez J, Guimaraes B, Lereclus D, et al. Peptide-binding dependent conformational changes regulate the transcriptional activity of the quorum-sensor NprR. Nucleic Acids Res. 2013 Sep;41(16):7920–33.

84. Jiang M, Grau R, Perego M. Differential processing of propeptide inhibitors of Rap phosphatases in Bacillus subtilis. J Bacteriol. 2000 Jan;182(2):303–10.

85. Perego M, Hanstein C, Welsh KM, Djavakhishvili T, Glaser P, Hoch JA. Multiple protein-aspartate phosphatases provide a mechanism for the integration of diverse signals in the control of development in *B. subtilis.* Cell. 1994 Dec 16;79(6):1047–55.

86. Smits WK, Bongiorni C, Veening JW, Hamoen LW, Kuipers OP, Perego M. Temporal separation of distinct differentiation pathways by a dual specificity Rap-Phr system in *Bacillus subtilis.* Mol Microbiol. 2007 Jul;65(1):103–20.

87. Auchtung JM, Lee CA, Grossman AD. Modulation of the ComA-Dependent Quorum Response in *Bacillus subtilis* by Multiple Rap Proteins and Phr Peptides. J Bacteriol. 2006 Jul 15;188(14):5273–85.

88. Ogura M, Shimane K, Asai K, Ogasawara N, Tanaka T. Binding of response regulator DegU to the aprE promoter is inhibited by RapG, which is counteracted by extracellular PhrG in Bacillus subtilis. Mol Microbiol. 2003;13.

89. Core L, Perego M. TPR-mediated interaction of RapC with ComA inhibits response regulator-DNA binding for competence development in Bacillus subtilis. Mol Microbiol. 2003 Sep;49(6):1509–22.

90. Perego M, Brannigan JA. Pentapeptide regulation of aspartyl-phosphate phosphatases. Peptides. 2001 Oct;22(10):1541–7.

91. Perego M, Hoch JA. Negative regulation of Bacillus subtilis sporulation by the spo0E gene product. J Bacteriol. 1991 Apr;173(8):2514–20.

92. Reizer J, Reizer A, Perego M, Saier MH. Characterization of a family of bacterial response regulator aspartyl-phosphate (RAP) phosphatases. Microb Comp Genomics. 1997;2(2):103–11.

93. Ohlsen KL, Grimsley JK, Hoch JA. Deactivation of the sporulation transcription factor Spo0A by the Spo0E protein phosphatase. Proc Natl Acad Sci. 1994 Mar 1;91(5):1756–60.

94. Perego M. A new family of aspartyl phosphate phosphatases targeting the sporulation transcription factor Spo0A of Bacillus subtilis. Mol Microbiol. 2001 Oct;42(1):133–43.

95. Grenha R, Rzechorzek NJ, Brannigan JA, de Jong RN, Ab E, Diercks T, et al. Structural characterization of Spo0E-like protein-aspartic acid phosphatases that regulate sporulation in bacilli. J Biol Chem. 2006 Dec 8;281(49):37993–8003.

96. Diaz AR, Stephenson S, Green JM, Levdikov VM, Wilkinson AJ, Perego M. Functional role for a conserved aspartate in the Spo0E signature motif involved in the dephosphorylation of the Bacillus subtilis sporulation regulator Spo0A. J Biol Chem. 2008 Feb 1;283(5):2962–72.

97. Dubey GP, Narayan A, Mattoo AR, Singh GP, Kurupati RK, Zaman MohdS, et al. Comparative genomic study of spo0E family genes and elucidation of the role of Spo0E in Bacillus anthracis. Arch Microbiol. 2009 Mar;191(3):241–53.

98. Stephenson SJ, Perego M. Interaction surface of the Spo0A response regulator with the Spo0E phosphatase: Spo0A interaction surface with Spo0E. Mol Microbiol. 2002 Jun 18;44(6):1455–67.

99. Bongiorni C, Stoessel R, Perego M. Negative Regulation of Bacillus anthracis Sporulation by the Spo0E Family of Phosphatases. J Bacteriol. 2007 Apr 1;189(7):2637–45.

100. Edwards AN, Wetzel D, DiCandia MA, McBride SM. Three orphan histidine kinases inhibit *Clostridioides difficile* sporulation [Internet]. Microbiology; 2021 Nov [cited 2021 Dec 1]. Available from: http://biorxiv.org/lookup/doi/10.1101/2021.11.18.469199

101. Worner K, Szurmant H, Chiang C, Hoch JA. Phosphorylation and functional analysis of the sporulation initiation factor Spo0A from Clostridium botulinum. Mol Microbiol. 2006 Feb;59(3):1000–12.

102. Mearls EB, Lynd LR. The identification of four histidine kinases that influence sporulation in Clostridium thermocellum. Anaerobe. 2014 Aug;28:109–19.

103. Steiner E, Dago AE, Young DI, Heap JT, Minton NP, Hoch JA, et al. Multiple orphan histidine kinases interact directly with Spo0A to control the initiation of endospore formation in Clostridium acetobutylicum. Mol Microbiol. 2011 May;80(3):641–54.

104. Freedman JC, Li J, Mi E, McClane BA. Identification of an Important Orphan Histidine Kinase for the Initiation of Sporulation and Enterotoxin Production by Clostridium perfringens Type F Strain SM101. MBio. 2019 Jan 22;10(1).

105. Underwood S, Guan S, Vijayasubhash V, Baines SD, Graham L, Lewis RJ, et al. Characterization of the sporulation initiation pathway of *Clostridium difficile* and its role in toxin production. J Bacteriol. 2009 Dec;191(23):7296–305.

106. Edwards AN, Tamayo R, McBride SM. A novel regulator controls Clostridium difficile sporulation, motility and toxin production. Mol Microbiol. 2016 Jun;100(6):954–71.

107. Edwards AN, Anjuwon-Foster BR, McBride SM. RstA Is a Major Regulator of Clostridioides difficile Toxin Production and Motility. MBio. 2019 Mar 12;10(2).

108. Jumper J, Evans R, Pritzel A, Green T, Figurnov M, Ronneberger O, et al. Highly accurate protein structure prediction with AlphaFold. Nature. 2021 Aug 26;596(7873):583–9.

109. He D, Hagen SJ, Pothoulakis C, Chen M, Medina ND, Warny M, et al. Clostridium difficile toxin A causes early damage to mitochondria in cultured cells. Gastroenterology. 2000;119(1):139–50.

110. Mani N, Dupuy B. Regulation of toxin synthesis in Clostridium difficile by an alternative RNA polymerase sigma factor. Proc Natl Acad Sci U A. 2001 May 8;98(10):5844–9.

111. Matamouros S, England P, Dupuy B. Clostridium difficile toxin expression is inhibited by the novel regulator TcdC. Mol Microbiol. 2007 Jun;64(5):1274–88.

112. Govind R, Dupuy B. Secretion of Clostridium difficile toxins A and B requires the holin-like protein TcdE. PLoS Pathog. 2012;8(6):e1002727.

113. Govind R, Fitzwater L, Nichols R. Observations on the Role of TcdE Isoforms in Clostridium difficile Toxin Secretion. J Bacteriol. 2015 Aug 1;197(15):2600–9.

114. Olling A, Seehase S, Minton NP, Tatge H, Schroter S, Kohlscheen S, et al. Release of TcdA and TcdB from Clostridium difficile cdi 630 is not affected by functional inactivation of the tcdE gene. Microb Pathog. 2012 Jan;52(1):92–100.

115. Tan KS, Wee BY, Song KP. Evidence for holin function of tcdE gene in the pathogenicity of Clostridium difficile. J Med Microbiol. 2001 Jul;50(7):613–9.

116. Carter GP, Chakravorty A, Pham Nguyen TA, Mileto S, Schreiber F, Li L, et al. Defining the Roles of TcdA and TcdB in Localized Gastrointestinal Disease, Systemic Organ Damage, and the Host Response during Clostridium difficile Infections. Ballard J, Collier RJ, editors. mBio. 2015 Jul;6(3):e00551-15.

117. Gerding DN, Johnson S, Rupnik M, Aktories K. *Clostridium difficile* binary toxin CDT: Mechanism, epidemiology, and potential clinical importance. Gut Microbes. 2014 Jan;5(1):15–27.

118. Cowardin CA, Buonomo EL, Saleh MM, Wilson MG, Burgess SL, Kuehne SA, et al. The binary toxin CDT enhances Clostridium difficile virulence by suppressing protective colonic eosinophilia. Nat Microbiol. 2016 Aug;1(8):16108.

119. Schwan C, Stecher B, Tzivelekidis T, van Ham M, Rohde M, Hardt WD, et al. Clostridium difficile Toxin CDT Induces Formation of Microtubule-Based Protrusions and Increases Adherence of Bacteria. Blanke SR, editor. PLoS Pathog. 2009 Oct 16;5(10):e1000626.

Chapter 2: Identification of functional Spo0A residues critical for sporulation in

Clostridioides difficile

Michael A. DiCandia[1], Adrianne N. Edwards[1], Joshua B. Jones[1], Grace L. Swaim[2], Brooke D. Mills[1], and Shonna M. McBride[1]

[1] Department of Microbiology and Immunology, Emory University School of Medicine, Emory Antibiotic Resistance Center, Atlanta, GA, USA.

[2] Current address: Department of Neuroscience and Cell Biology, Yale University Graduate School of Arts and Sciences, New Haven, CT, USA.

M.A.D. performed experiments and contributed to the writing and editing of the manuscript.

A.N.E. performed experiments and contributed to the writing and editing of the manuscript.

J.B.J. performed experiments.

G.L.S. assisted with experiments.

B.D.M. assisted with experiments.

S.M.M. performed experiments and contributed to the writing and editing of the manuscript.

ABSTRACT

Clostridioides difficile is an anaerobic, Gram-positive pathogen that is responsible for *C. difficile* infection (CDI). To survive in the environment and spread to new hosts, *C. difficile* must form metabolically dormant spores. The formation of spores requires activation of the transcription factor Spo0A, which is the master regulator of sporulation in all endospore-forming bacteria. Though the sporulation initiation pathway has been delineated in the Bacilli, including the model spore-former *Bacillus subtilis*, the direct regulators of Spo0A in *C. difficile* remain undefined. *C. difficile* Spo0A shares highly conserved protein interaction regions with the *B. subtilis* sporulation proteins Spo0F and Spo0A, although many of the interacting factors present in *B. subtilis* are not encoded in *C. difficile.* To determine if comparable Spo0A residues are important for *C. difficile* sporulation initiation, site-directed mutagenesis was performed at conserved receiver domain residues and the effects on sporulation were examined. Mutation of residues important for homodimerization and interaction with positive and negative regulators of *B. subtilis* Spo0A and Spo0F impacted *C. difficile* Spo0A function. The data also demonstrated that mutation of many additional conserved residues altered *C. difficile* Spo0A activity, even when the corresponding *Bacillus* interacting proteins are not apparent in the *C. difficile* genome. Finally, the conserved aspartate residue at position 56 of *C. difficile* Spo0A was determined to be the phosphorylation site that is necessary for Spo0A activation. The finding that Spo0A interacting motifs maintain functionality suggests that *C. difficile* Spo0A interacts with yet unidentified proteins that regulate its activity and control spore formation.

INTRODUCTION

Sporulation initiation is a complex developmental process that allows for prolonged survival when environmental conditions become unfavorable. Some members of the Firmicutes phylum transition into metabolically dormant endospores (spores) that remain inert until environmental conditions are favorable again and the spore germinates to produce vegetative cells. Sporulation is energetically costly and, as such, highly regulated (1-5). Sporulation initiation is controlled by the conserved transcription factor, Spo0A, the essential regulator of the sporulation gene expression program. Spo0A consists of a receiver domain and a DNA-binding domain and is encoded in all endospore-forming species (**Fig. S1**) (6, 7). Spo0A is a response regulator, and its DNA-bindng activity is regulated by phosphorylation of a conserved aspartate residue (8). In the activated form, phosphorylated Spo0A undergoes a conformational change that facilitates self-dimerization. Activated Spo0A can then bind specific promoter regions, referred to as "0A boxes", to regulate gene expression and trigger entry into the sporulation pathway (9, 10).

Sporulation initiation has been extensively studied in the model spore-former, *Bacillus subtilis*. In *B. subtilis* and other Bacilli, the phosphorylation status of Spo0A is controlled through a multicomponent phosphorelay, with the orphan sensor histidine kinases, KinA, KinB, KinC, KinD, and KinE, transferring phosphate to the intermediate response regulator, Spo0F. Spo0F in turn mediates the flow of phosphate to the phosphotransferase Spo0B (11). Spo0B then directly phosphorylates Spo0A, which activates sporulation-specific gene expression (2). The Rap phosphatases, such as RapA, RapB, and RapH, can dephosphorylate Spo0F, while the Spo0E family of proteins dephosphorylate Spo0A (**Fig. 1A**). The ability of Spo0B to interact with both Spo0F and Spo0A at shared, highly conserved motifs suggests a critical role for these residues in the regulation of Spo0A activity (12, 13).

Like the Bacilli, all spore-forming members of the anaerobic Clostridia encode *spo0A* (14). However, the mechanisms of Spo0A regulation in the Clostridia, including *C. difficile*, are poorly characterized. The Spo0F-Spo0B phosphorelay is not apparent in clostridial genomes, suggesting that there are divergent mechanisms of Spo0A activation (15). In some clostridial species, phosphotransfer proteins interact directly with Spo0A to activate or inactivate sporulation in a manner consistent with a traditional two-component system (16-19). *C. difficile* encodes five orphan putative histidine kinases, three of which resemble the *B. subtilis* Spo0A-associated kinases and negatively regulate sporulation (PtpA, PtpB, and PtpC), and two that are not involved in sporulation (20, 21). While one orphan kinase, PtpC, was reported to phosphorylate Spo0A *in vitro* (22), it was recently shown that a *ptpC* null mutant exhibits variably increased sporulation, demonstrating that PtpC negatively impacts Spo0A activity in the conditions tested (20) (**Fig. 1B**). As none of the *C. difficile* orphan kinases are verified activators of Spo0A, it is challenging to predict the specific strategy of *C. difficile* Spo0A regulation.

Although Spo0F and Spo0B are not found in *C. difficile*, the regions of the Spo0A receiver domain that interact with these and other *Bacillus* regulators appear to be conserved in *C. difficile*. We hypothesized that conserved *Bacillus* Spo0A and Spo0F residues are also functionally important for *C. difficile* Spo0A regulation. To better understand how *C. difficile* Spo0A activity is regulated, we performed site-directed mutagenesis of conserved regions of the receiver domain that are functionally important for *B. subtilis* Spo0A and Spo0F, or are in areas likely to be important for functional interactions, and examined the effects on sporulation. Here we report on the residues and potential interaction surfaces that are important for regulation of *C. difficile* Spo0A activity.

RESULTS

The Spo0A *B. subtilis* and *C. difficile* N-terminal receiver domains are highly conserved.

In *B. subtilis*, Spo0A and Spo0F share similar response regulator receiver domains (residues 6 – 116 in Spo0F and 6 – 120 in Spo0A), and both proteins interact with the phosphotransfer protein Spo0B using conserved secondary structure (12, 23-26). The residues of *B. subtilis* Spo0F and Spo0A that are important for signal transduction were previously identified and characterized (4, 12, 13, 27-30). We aligned the amino acid sequence of the *B. subtilis* Spo0A (**Fig. 2**) and Spo0F receiver domains (**Fig. S2**) to *C. difficile* Spo0A to predict orthologous functional residues. After identifying corresponding functional residues in the *C. difficile* Spo0A amino acid sequence, including many residues not previously investigated in Spo0A proteins and solely in Spo0F, we performed site-directed mutagenesis of 30 *C. difficile* Spo0A residues to alanine, with the exception of native alanine residues, which were mutated to serine (**Fig. 2B**). Mutated *spo0A* alleles driven by the *C. difficile spo0A* native promoter were expressed in a *C. difficile spo0A* mutant (31). To assess the stability of mutant Spo0A proteins, we performed western blotting using an anti-Spo0A antibody (32) and found that all mutant Spo0A proteins, except those containing the Q17A, V18A, and P60A mutations, were stable under sporulating conditions (**Fig. S3**).

Conserved amino acid residues impact Spo0A function in *C. difficile*

To determine the functional significance of the individual mutant Spo0A proteins, the ability for these proteins to restore sporulation when expressed in a *C. difficile spo0A* mutant was assessed. The sporulation frequencies for the mutant *C. difficile spo0A* alleles tested are displayed in **Table 1**. The corresponding *B. subtilis* Spo0A amino acid residue location and the functional significance of each site-directed mutant are also included for reference (**Table 1**).

The strains containing the D14A, Q90A, K92A, and P109A Spo0A site-directed mutants exhibited significantly increased sporulation compared to the control strain expressing wildtype *spo0A* allele (**Fig. 3A, 3C**). The strains containing the F15A, K36A, and D91A Spo0A site-directed mutants also displayed increased sporulation but were not statistically significant (**Table 1**). The *C. difficile* Spo0A Q90A gain-of-function sporulation phenotype was similar to the increased sporulation phenotype observed with the *B. subtilis* Spo0A Q90R mutant, which facilitates interaction with the activating protein KinC (33-35). The increased sporulation phenotype displayed by the *C. difficile* Spo0A D14A mutant was similar to the sporulation phenotype observed when the orthologous *B. subtilis* Spo0A residue E14 is mutated (28, 33). The *B. subtilis* Spo0A E14A mutant confers resistance to hyperactive Spo0E, resulting in increased Spo0A phosphorylation and activity (28, 33). The gain of function phenotype of the *C. difficile* D14A mutant suggests that this residue may also be important for recognition by Spo0E in *C. difficile* (28, 33). The *B. subtilis* Spo0F residues G14, L87, and P105 are all important for positively influencing sporulation through interaction with Spo0B (**Table 1**), yet the corresponding *C. difficile* site-directed mutants (Spo0A D14A, D91A, and P109A) all exhibited increased sporulation, suggesting that these residues serve a divergent role in *C. difficile* Spo0A activation (12).

Conversely, 15 of the 30 Spo0A site-directed mutants had reduced sporulation compared to expression the wildtype *spo0A* allele, representing a much larger proportion of the mutants assessed (**Table 1, Fig. 3B, 3D**). Expression of eleven of the mutant *spo0A* alleles resulted in significantly reduced sporulation: D10A, D11A, C16A, E21A, A35S, D56A, M59A, H61A, S86A, A92S, and K108A. Spo0A Q17A, V18A, and P60A demonstrated sporulation frequencies below the limit of detection (>0.0002%); however, through western blotting we found these Spo0A site-directed mutants were not stably produced (**Table 1, Fig. S3**).

The *C. difficile* Spo0A mutants that demonstrate a loss-of-function sporulation phenotype may represent amino acid residues that facilitate direct interactions with positive regulators of sporulation. The *C. difficile* Spo0A C16A and E21A mutations are located within the α1 region (**Fig. 3D**). The *B. subtilis* Spo0F equivalents, R16 and E21, promote direct interactions with KinA and Spo0B (13), while *B. subtilis* Spo0A E21 is also expected to interact with Spo0B (12). Altogether, these data suggest that *C. difficile* C16 and E21 coordinate the interaction with a positive regulator of Spo0A activity. The *B. subtilis* Spo0A residues D10, D11, I58, and K108 form the aspartyl pocket and are important for Spo0A homodimerization, which is necessary for DNA-binding activity (25, 36). Mutation of the *C. difficile* Spo0A equivalent residues D10, D11, and K108 all produced severe sporulation defects. The *C. difficile* Spo0A I58A mutant had decreased sporulation, although these results were not statistically significant (**Table 1**).

The aspartate residue at position 56 of *B. subtilis* Spo0A serves as the phosphorylation site and is critical for sporulation, consistent with findings for the conserved aspartate residue in other species' Spo0A orthologs (4, 16-19, 37). As expected, mutation of the predicted *C. difficile* Spo0A phosphorylation site (D56A) resulted in dramatically reduced sporulation (>1000-fold decrease, **Table 1**), suggesting that this aspartate residue is required for *C. difficile* Spo0A phosphorylation and activation. *C. difficile* Spo0A I58, M59, and H61 are located immediately adjacent to the phosphorylation site in the open face between β3-α3 (**Fig. 3D**). Mutation of the *B. subtilis* Spo0F K56 residue results in a loss-of-function phenotype, and several residues in this region facilitate *B. subtilis* Spo0A and Spo0F interactions with kinases or phosphatases (12, 13). These data correspond with the low sporulation frequencies of the orthologous *C. difficile* Spo0A I58A, M59A, and H61A mutants (**Fig. 3B**), suggesting that this region functions similarly in *C. difficile*. The β4 region of *B. subtilis* Spo0A is important for phosphotransfer between Spo0F or Spo0B. The *C. difficile* Spo0A S86 and A87 residues are located at the C-terminal end of β4 (**Fig.**

3D), and site-directed mutagenesis of these residues significantly reduced sporulation frequency (**Table 1**), suggesting that the β4 region is likewise important for phosphotransfer to *C. difficile* Spo0A (12, 38). Additionally, the *B. subtilis* Spo0F residue T82 is equivalent to *C. difficile* Spo0A S86, and is involved in stabilizing the phosphorylation of Spo0F (39). Since both threonine and serine have polar side chains, *C. difficile* S86 may also facilitate phosphorylation of the Spo0A active site. Finally, the *C. difficile* Spo0A A35 residue is conserved in both *B. subtilis* Spo0A (A35) and Spo0F (A33), though the function of these residues in Bacilli have not been determined.

The Spo0A mutants N12A, K13A, L19A, L62A, F110A, and D111A had sporulation frequencies that were comparable to the wildtype Spo0A allele. N12, K13, and L19 appear to be dispensable for sporulation, even though residues located in this region are important for interaction of *B. subtilis* Spo0A and Spo0F with both positive and negative regulators (**Table 1**) (13, 33). However, the Spo0A L19A mutant exhibited a translucent plate morphology on sporulation agar, suggesting some functional importance in other physiological processes outside of sporulation (**Table 2**). This result is not surprising given the pleiotropic effects Spo0A displays in *C. difficile* and other species (10, 19, 40-46). Mutation of the *Bacillus* Spo0A and Spo0F residues that are comparable to *C. difficile* Spo0A L62 result in gain-of-function phenotypes but was not important for *C. difficile* Spo0A activity (**Table 1**). The *C. difficile* Spo0A residues F110A and D111A are located at the open face of β5-α5 in a motif (KPFD) that is highly conserved in the CheY superfamily of response regulators (12, 47). Our data indicate that this region is also important for *C. difficile* Spo0A regulation, as the K108A mutant had decreased sporulation and the P109A mutant had increased sporulation (**Table 1**). While the F110A or D111A mutants did not affect sporulation, mutation of these residues produced a translucent and crushed plate morphologies, respectively (**Table 2**), suggesting they impact Spo0A function. Lastly, we used RoseTTAFold to model Spo0A site-directed mutants with the greatest changes in sporulation

relative to wildtype, and did not observe major predicted changes to Spo0A structure in the site-directed mutants relative to wildtype Spo0A, suggesting that the changes in sporulation in the site-directed mutants are not likely to be due to major structural differences (**Fig. S4)** (48).

Altered growth and morphology of Spo0A mutants

Fourteen of the mutated *spo0A* alleles produced phenotypes that impacted growth in BHIS broth and growth and morphology on sporulation agar (**Table 2**). The most commonly observed phenotype was a stringy, mucoidal morphology that was observed for ten of the mutants after 24 h growth on sporulation plates (Spo0A D14A, F15A, C16A, E21A, A35S, H61A, A87S, Q90A, D91A, and P109A). The mucoidal phenotype was observed in both hyper- and hyposporulating strains, indicating that mucoidy is not directly correlated with the sporulation outcome. The Spo0A L19A and F110A mutants produced flat, translucent lawns, but sporulation was not affected in either mutant background. Similarly, the Spo0A D111A mutant did not affect sporulation, but produced a rigid, crushed lawn morphology. Strains expressing *spo0A* Q17A, E21A, A35S, H61A, and A87S exhibited poor growth in BHIS liquid compared to expression of the wildtype *spo0A* (data not shown). The Spo0A mutants with poor growth all had reduced sporulation (**Table 1**). However, only 5 of the 14 hyposporulating mutants grew slowly, indicating that defects in Spo0A that reduce sporulation do not necessarily retard growth.

C. difficile **Spo0A requires phosphorylation of the conserved aspartate for activation.**

In *B. subtilis*, Spo0A is phosphorylated at the conserved aspartate residue D56, which is required for activation (36, 49). In the activated state, Spo0A homodimerizes and binds to specific DNA sequences, or "0A boxes", to regulate Spo0A-dependent gene expression (50, 51). Sequence comparison to *B. subtilis* Spo0A and other response regulators implicated D56 as the conserved site of *C. difficile* Spo0A phosphorylation and activation. The *C. difficile* Spo0A D56A

site-directed mutation also dramatically reduced sporulation, further supporting the necessity of this residue for activity (**Fig. 3B**). To determine if *C. difficile* Spo0A is also phosphorylated at the conserved aspartate residue, we isolated total protein from strains expressing either p*spo0A*-3XFLAG 3x-FLAG-Spo0A or p*spo0A*-D56A-3XFLAG and separated phosphorylated and unphosphorylated Spo0A species using phos-tag SDS-polyacrylamide gel electrophoresis followed by western blotting with an α-FLAG antibody (52-54) (**Fig. 4A**). In the phos-tag assay, higher molecular weight bands that are present in the unheated sample but absent in the heated sample represent phosphorylated protein, as phosphoryl groups are heat-labile. In the strain expressing wildtype *spo0A*, two bands were observed in the unheated sample, with the upper band denoting phosphorylated Spo0A and the lower band corresponding to unphosphorylated Spo0A. In contrast, the Spo0A D56A mutant displayed only the lower, unphosphorylated band in both the unheated and heated samples, indicating that D56 is the primary site of phosphorylation. The ratio of phosphorylated Spo0A to total Spo0A is significantly greater in the wildtype compared to the Spo0A D56A mutant (**Fig. 4B**). Altogether, the sporulation defect and the absence of Spo0A phosphorylation of the D56A mutant demonstrate that residue D56 is the primary site of Spo0A phosphorylation.

Residues necessary for Spo0A dimerization in other species have conserved functions in *C. difficile*.

Residues that are important for Spo0A homodimerization were previously identified in Bacilli (25, 36, 47). The residues of *C. difficile* Spo0A that facilitate dimerization have not been characterized; however, *C. difficile* Spo0A contains five residues that are identical to those involved in dimerization in *B. subtilis* and other aerobic spore-formers: D10, D11, D56, I58, and K108. The alanine mutants of these five residues all produced defects in sporulation, indicating that they are important for Spo0A function. To test if these residues are involved in Spo0A

dimerization *in vivo*, we performed split-luciferase reporter assays. Here, luciferase enzyme is fragmented into either a SmBit or LgBit subunit and fused to a gene(s) of interest to test for protein-protein interaction (55, 56). We constructed C-terminal fusions of the SmBit and LgBit luciferase subunits to the wildtype, D10A, D11A, D56A, I58A, and K108A mutant *spo0A* alleles. All five site-directed mutants had less activity than the wildtype Spo0A fusions, with the D10A and D56A alleles exhibiting significantly less output (**Fig. 5A, Table S1**), indicating that these Spo0A site-directed mutations reduce the ability for these mutant proteins to form homodimers. The D10, D11, I58, and K108 residues are all oriented around the D56 activation site (**Fig. 5B**), further supporting the importance of these residues for Spo0A homodimerization (25). These results demonstrate that the functional residues that are involved in Bacilli Spo0A dimerization are also important for *C. difficile* Spo0A dimerization.

DISCUSSION

In this study, we employed alanine-scanning mutagenesis to define the regions of the *C. difficile* Spo0A receiver domain that are important for regulation of sporulation. Altogether, we examined the ability of *C. difficile* Spo0A to initiate sporulation through mutational analysis of 30 residues located within 10 different regions of the Spo0A receiver domain secondary structure (**Fig. 2**). The results demonstrated that mutation of many residues that influence *B. subtilis* Spo0A and Spo0F activation also have profound effects on *C. difficile* Spo0A function, even though few of the interacting partner proteins are conserved between these species. We also established Spo0A residues that are important for homodimerization and found altered growth and morphology phenotypes by mutating the receiver domain of Spo0A.

The receiver domain of the *C. difficile* Spo0A shares 47% identity with the *B. subtilis* Spo0A and 30% identify with *B. subtilis* Spo0F, but the protein architectures of the receiver motifs are highly conserved. By probing the function of conserved regions and residues that have been implicated in protein interaction in Bacilli, we demonstrate conservation of sporulation phenotypes in many *C. difficile* Spo0A residues relative to *Bacillus* Spo0F and Spo0A (**Table 1**) (12, 13, 25, 27, 30, 34). As in Bacilli, we found that the receiver domain α-helices and the β1-α1, β3-α3, β4-α4, and β5-α5 open faces are all important for *C. difficile* Spo0A activity (**Table 1**) (12, 13, 25). The majority of residues that were mutated in this study that produced major changes in sporulation are orientated on the same face as the site of activation, an effect observed for other response regulator receiver domains (**Fig. 3**) (13, 47, 57).

C. difficile Spo0A and *B. subtilis* Spo0A perform the same sporulation function, but there are gaps in knowledge about the contribution of specific residues to Spo0A activity in both species. Our data demonstrate that most residues within the receiver domains of *B. subtilis* and *C. difficile* Spo0A proteins have similar impacts on sporulation. However, many of the characterized *B. subtilis* Spo0A site-directed mutants are gain-of-function suppressor mutations that are not alanine substitutions or were characterized in strain backgrounds lacking elements of the phosphorelay (27, 33). Additionally, many of the described residues that are important for sporulation in *B. subtilis* Spo0F have not been characterized in Spo0A. Our sporulation results in *C. difficile* suggest open questions remain about the function of the following *B. subtilis* Spo0A residues: L15, V16, S17, L18, E21, A35, I58, M59, P60, H61, T86, A87, Q90, E91, D92, K108, and P109. These residues may also be important for Spo0A function in *B. subtilis* and other spore-forming Firmicutes.

The receiver domain of *B. subtilis* Spo0F has been more extensively characterized than Spo0A and more is understood about the impact of specific Spo0F residues on the regulation of

sporulation (12, 13, 39). We found several differences in the sporulation outcomes for mutations in conserved residues of *B. subtilis* Spo0F and *C. difficile* Spo0A, which is not surprising, considering the differences in these species' sporulation pathways. Mutation of *C. difficile* Spo0A residues K13, F15, Q17, L62, V88, Q90, D91, and F110 resulted in different impacts on sporulation relative to similar mutations in Spo0F (**Table 1**). Some of these residues are important for Spo0F interaction with factors that are not present in *C. difficile*, such as the Rap phosphatases, Spo0B, and the specific sporulation kinases of *Bacillus* (**Fig. 1**, **Table 1**). In particular, the *C. difficile* Spo0A mutants F15A, Q90A, and D91A displayed higher sporulation, while corresponding residues in *B. subtilis* Spo0F (I15A, E86A, L87A) resulted in sporulation defects (13). *C. difficile* Spo0A V88A and F110A maintained wildtype sporulation levels, while *B. subtilis* Spo0F Y84A and F106A resulted in sporulation defects (13). These results suggest that the importance of these residues is maintained for both proteins, although the interacting partners and the resulting effects on sporulation differ.

Distinct effects on growth and colony morphology were observed for the 14 Spo0A mutants listed in **Table 2**. The growth and morphology phenotypes are likely due to altered Spo0A regulation or function, as we found that deletion of *spo0A* in *C. difficile* does not change growth or morphology under the conditions tested, as previously observed (22, 40, 41). The mucoidal phenotype observed on sporulation agar was the most commonly observed effect and was found in 10 of the 30 characterized Spo0A mutants. Mucoidy was only observed when the mutants grew for at least 12 hours as a lawn on sporulation agar, suggesting this phenotype is linked to either a facet of sporulation or conditions that facilitate sporulation (data not shown). However, the mucoidal phenotype was present in both hyposporulating and hypersporulating mutants and did not have an obvious impact on the capacity to sporulate. Additional changes in morphology, but not sporulation, were observed in Spo0A L19A, F110A and D111A. The L19A and F110A mutants

produced flat, translucent lawns on sporulation agar, and the D111A mutant had a crushed morphology on sporulation agar. While our findings were unexpected, changes in plate morphology in *C. difficile spo0A* mutants in various strain backgrounds, including 630Δ*erm*, have been previously described (40). However, altered morphology was described explicitly in *spo0A* null mutants, not specific site-directed mutants, and we did not observe changes in morphology in our *spo0A* null mutant. Further, the mutants Q17A, E21A, A35S, H61A, and A87S all had poor growth in BHIS broth relative to both the wildtype and *spo0A* mutant, and all had defects in sporulation. To our knowledge, this is the first report that specific Spo0A residues impact colony morphology or growth. While it is unclear why Spo0A mutant alleles would affect morphology or growth, the simplest explanation is that the altered Spo0A alleles can interact with additional partner proteins that control these cellular processes. Future experiments to determine the differences in binding partners between wildtype Spo0A and site-directed Spo0A mutants with altered morphology or growth may help explain the impact specific Spo0A site-directed mutants have *in vivo* in processes outside of sporulation. It remains unknown if the morphology and growth phenotypes of specific Spo0A site-directed mutants are unique to *C. difficile* or if these phenotypes are conserved for Spo0A of other spore-forming Firmicutes.

We found that Spo0A is phosphorylated at the conserved site of activation (D56), and that a D56A mutation results in loss of phosphorylation (**Fig. 4**). Interestingly, the D56A mutant does exhibit reduced, but not total loss, of sporulation. This could be a result of low Spo0A DNA-binding activity present in unphosphorylated Spo0A. Although all studied Spo0A are regulated by phosphorylation and dephosphorylation, the proteins that directly interact with Spo0A vary considerably within the Clostridia and the Spo0A proteins in these species have diverged (**Fig. S5A, S5B**). In other Clostridia in which Spo0A regulation has been studied*,* Spo0A is directly phosphorylated by orphan histidine kinases or phosphatases to regulate Spo0A activity, and all

encode at least one kinase that induces sporulation (16-20, 58, 59). While a Spo0A-activating kinase has not yet been identified in *C. difficile*, our data confirm that phosphorylation of Spo0A at the conserved site of activation is critical for Spo0A activity. Despite the lack of evidence of an activating kinase to date, we expect that Spo0A is directly phosphorylated by at least one histidine kinase to positively regulate sporulation.

To our knowledge, this represents the first report on residues important for Spo0A dimerization in *C. difficile* (**Fig. 5**) (25, 36). The fact that the mechanism of dimerization is maintained in *C. difficile* is likely due to the conserved architecture of response regulator receiver domains, defined by $(\beta/\alpha)_5$ folding and functional residues that are orientated near the site of activation (25, 36, 47, 57).

The Bacilli and Clostridia diverged roughly 2.4 billion years ago during the Great Oxidation Event (60). While the mechanism(s) of *C. difficile* Spo0A regulation remains unclear, we have identified conserved regions of Spo0A that are important for activity. Because the phosphorelay interactions are not retained in *C. difficile*, our results suggest that *C. difficile* Spo0A uses functionally conserved regions for interaction with both positive and negative regulators that are not part of the Bacilli mechanism for Spo0A regulation. Elucidation of the factors that regulate Spo0A in *C. difficile* will provide greater insight on the biology and lifestyle of this clinically important pathogen.

MATERIALS AND METHODS

Bacterial strains and growth conditions

Bacterial strains and plasmids used in this study are listed in (**Table 3**). *C. difficile* strains were routinely grown in BHIS broth or on BHIS agar supplemented with 2-5 µg ml^{-1} thiamphenicol (Sigma-Aldrich) as needed (61). *C. difficile* cultures were supplemented with 0.2% fructose and 0.1% taurocholate (Sigma-Aldrich) to prevent sporulation and induce germination as indicated (32, 61). *C. difficile* was grown on 70:30 agar to assess sporulation frequency as previously described (32). *C. difficile* strains were grown in a 37°C anaerobic chamber (Coy) with an atmosphere consisting of 10% H$_2$, 5% CO$_2$, and 85% N$_2$, as previously described (62). Strains of *Escherichia coli* were cultured in LB at 37°C (63) and supplemented with 100 µg ml^{-1} ampicillin or 20 µg ml^{-1} chloramphenicol as needed. Kanamycin 100 µg ml^{-1} was used for counterselection of *E. coli* HB101 pRK24 after conjugation with *C. difficile* (64).

Strain and plasmid construction

Table 4 contains oligonucleotides used in this study. *C. difficile* 630 strain (GenBank accession number **AJP10906.1**) was used as a template for primer design and *C. difficile* 630Δ*erm* genomic DNA was used for PCR amplification. *C. difficile* 630Δ*erm* has a known 18 nucleotide duplication outside of the Spo0A receiver domain and was used for strain creation (10). Strain construction is described in **Table S2**.

Dendrogram

The Spo0A dendrogram rooted *to B. subtilis* Spo0A was created using the MUSCLE Multiple Alignment plugin and Geneious Tree Builder in Geneious Prime v2020.2.2. Spo0A amino acid sequences from *C. difficile* 630 (GenBank accession **AJP10906.1**), *C. perfringens* SM101 (GenBank **CP000312.1**), *C. acetobutylicum* ATCC 824 (GenBank **NC_003030.1**), *A. thermocellus* DSM 1313 (GenBank **NC_017304.1**), *C. botulinum* A str. ATCC 3502 (GenBank **NC_009495.1**), and *B. subtilis* str. 168 (GenBank **NC_000964.3**) were retrieved, aligned, and assembled into a

dendrogram. The percentage of identity for each Spo0A protein relative to *B. subtilis* and the heatmap comparing Spo0A percent identities to each species was generated using Geneious Tree Builder in Geneious Prime v2020.2.2. (https://www.geneious.com).

Sporulation assays

C. difficile ethanol resistance sporulation assays were performed on 70:30 sporulation agar supplemented with 2 µg ml^{-1} thiamphenicol for plasmid maintenance, as previously described (65-67). Following growth on sporulation agar for 24 h, cells were resuspended in BHIS broth to an OD_{600} of 1.0. To determine total vegetative cell counts ml^{-1}, cultures were serially diluted in BHIS and plated on BHIS agar with 2 µg ml^{-1} thiamphenicol. Concurrently, 0.5 ml of resuspended cells were treated with a mixture of 0.3 ml 95% ethanol and 0.2 ml dH$_2$O for 15 min to kill all vegetative cells, then serially diluted in a mixture of 1X PBS and 0.1% taurocholate and plated onto BHIS agar with 2 µg ml^{-1} thiamphenicol and 0.1% taurocholate to enumerate the total number of spores per ml. After 48 h growth, CFU were calculated and the sporulation frequency was determined as the number of spores that germinated following ethanol treatment divided by the total number of spores and vegetative cells (65). A *spo0A* mutant complemented with wildtype *spo0A* driven from its native promoter on a plasmid was used as a positive control (MC848), and a *spo0A* null mutant containing the empty vector was used as the negative control (MC855). Statistical analyses were performed using the Welch's ANOVA with Dunnett's multiple comparisons test to compare *spo0A* site-directed mutants to the wildtype control (MC848) using GraphPad Prism v8.0.

Western blotting

C. difficile strains were grown in BHIS supplemented with 5 μg ml^{-1} thiamphenicol, 0.2% fructose, and 0.1% taurocholate. Cultures were then diluted, grown to an OD_{600} of 0.5, and 250

μL of culture was plated on 70:30 agar. After 12 h, 5 ml of cells were scraped from agar, pelleted, and then washed with 1x PBS. Cells were resuspended in 1X sample buffer (10% glycerol, 5% 2-mercaptoethanol, 62.5 mM upper tris, 3% SDS, 5 mM PMSF) and lysed using a Biospec BeadBeater. Total protein concentration was then measured using a BCA protein assay kit (Pierce), and 2.5 μg of protein was separated by SDS-PAGE using pre-cast TGX 4-15% gradient gels (BioRad) and performed in triplicate. Stain-free imaging using BioRad ChemiDoc MP System was performed for densitometric analysis, and protein was then transferred to a 0.45 μm nitrocellulose membrane. Spo0A was detected using anti-Spo0A antibody (32). Goat anti-mouse IgG Alexa fluor 488 (Invitrogen) was used as a secondary antibody, and western blots were visualized using a BioRad ChemiDoc MP System. Densitometry calculations were performed using Image Lab 6.0.1 (BioRad). Detected Spo0A protein was normalized to a major band on the stain-free image located at ~40 kDa as a loading control, and then each site-directed mutant was normalized to the Spo0A detected in the parental control strain.

Spo0A modeling for structural changes

RoseTTAFold was used for 3D predictive modeling of wildtype Spo0A and the following Spo0A site-directed mutants: D10A, D11A, D14A, Q17A, V18A, D56A, P60A, A87S, Q90A, K92A, and P109A using default settings and full-length Spo0A amino acid sequences (48). The angstroms error estimate values for wildtype and the corresponding Spo0A site-directed mutants were derived from the first generated model (Model 1), and the confidence values of the accuracy of the predicted structures were recorded to demonstrate the similarities of the wildtype and mutant Spo0A predicted structures.

Phos-tag blotting

C. difficile strains were cultured as described for western blotting. Cells from two plates for each strain were collected and pelleted. Cell pellets were suspended in 1 ml of 1X sample buffer (5% SDS, 93 mM Tris, 10% glycerol, 100 mM DTT). Protease Inhibitor Cocktail II (Sigma-Aldrich) was included in the sample buffer to inhibit protein degradation. Cells were lysed using a bead beater as described above. Total protein was measured using a BCA protein assay kit (Pierce). 10 µg protein aliquots were kept at 4°C or heated to 99°C for 10 min to dephosphorylate Spo0A prior to loading onto a 12.5% SuperSep Phos-tag gel (Fujifilm Wako)(53, 54). Total protein was electrophoresed at 125 V for two hours at 4°C. The gel was rinsed three times in transfer buffer with 10% methanol and 10 mM EDTA to remove zinc present within the gel, and subsequently transferred to a low-fluorescence PVDF membrane (Thermo Scientific) in transfer buffer containing 10% methanol and 0.5% SDS overnight at 4°C. Western blot analysis was conducted with anti-FLAG M2 antibody (Sigma-Aldrich), followed by goat anti-mouse Alexa Fluor 488-conjugated antibody (Invitrogen) as the secondary. Experiments were performed in triplicate, and imaging was performed using the BioRad ChemiDoc MP system. Densitometry calculations were performed using ImageJ 1.53a.

Two-hybrid luciferase assays

Two-hybrid assays were performed using a *C. difficile* codon-optimized split luciferase system previously described (55, 56). *C. difficile* strains were grown in 70:30 broth supplemented with 2 μg ml^{-1} thiamphenicol. Cultures were grown to an OD_{600} of 0.8 – 0.9, then induced with 50 ng ml^{-1} anhydrous tetracycline for 1 hour. After induction, the OD_{600} were recorded, and 100 μL of each culture was added in technical duplicate to a chimney-style 96 well plate. Split-luciferase assay was then performed per manufacturer's instructions (Promega). Luminescence output was immediately recorded at 135 nm using a BioTek plate reader. Output was normalized to cell density (OD_{600}). A one-way ANOVA with Dunnett's multiple comparisons test was performed to

determine the statistical significance of luminescence outputs of the site-directed mutants relative to the wildtype using GraphPad Prism v8.0.

ACKNOWLEDGEMENTS

1   **Table 1. Sporulation frequencies of *C. difficile* Spo0A site-directed mutants**

C. difficile Spo0A allele	Spo0A region	Corresponding *B. subtilis* Spo0A residue	Corresponding *B. subtilis* Spo0F residue	Spo0A function in *B. subtilis*	Spo0F function in *B. subtilis*	Average sporulation frequency (%)[a,c]	Mutant phenotype in *B. subtilis*[b]
Wildtype	-	-	-	Interaction with Spo0B, Spo0E	Interaction with KinA, KinB, KinC, KinD, and KinE, interaction with Spo0B	12.1±1.0	-
spo0A::erm	-	-	-	-	-	0.00	
D10A	β1-α1	D10	D10	Forms aspartyl pocket, Spo0A dimerization, divalent cation binding, predicted Spo0E interaction (4, 25, 36, 68)	Forms aspartyl pocket, divalent cation binding (57)	0.0002±0.0001[**]	n.d.
D11A	β1-α1	D11	D11	Forms aspartyl pocket, Spo0A dimerization, divalent cation binding, predicted Spo0E interaction (4, 25, 36, 68)	Forms aspartyl pocket, divalent cation binding (57)	0.00055±0.0004[**]	n.d.
N12A	β1-α1	N12	Q12	Interaction with Spo0E, N12K is resistant to hyperactive Spo0E, predicted Spo0B interaction (12, 28, 33-35, 68)	Interaction with Spo0B, inferred interaction with KinA (12, 13, 39, 69)	14.8±1.86	**Spo0A gain-of-function**
K13A	α1	R13	Y13	n.d.	Interaction with RapA and RapB, Y13S is resistant to RapB (70-73)	19.1±3	**Spo0F gain-of-function**
D14A	α1	E14	G14	E14A allows direct interaction with KinC, resistant to hyperactive Spo0E (28, 33)	Interaction with Spo0B, and RapB (12, 71-73)	49.7±6.5[*]	Spo0A gain-of-function
F15A	α1	L15	I15	n.d.	Interaction with KinA, Spo0B, and RapB (12, 13, 71-73)	23.1±1.7	**Spo0F decreased sporulation**
C16A	α1	V16	R16	n.d.	Interaction with KinA, Spo0B, and RapB (12, 13, 71)	0.7±0.3[*]	Spo0F decreased sporulation

Q17A	α1	S17	I17	n.d.	Interaction with RapB (13, 69, 71-73)	<LOD**	**Spo0F gain-of-function**
V18A	α1	L18	L18	n.d.	Interaction with KinA, Spo0B, RapB (12, 13, 71-73)	<LOD**	Spo0F decreased sporulation
L19A	α1	L19	L19	n.d.	Inferred structural importance (13)	6.4±1.5	Spo0F decreased sporulation
E21A	α1	E21	E21	Inferred to interact with Spo0B (12)	Interaction with Spo0B, inferred interaction with KinA (12, 39)	0.01±0.01**	n.d.
A35S	β2	A35	A33	n.d.	n.d.	0.15±0.1*	n.d.
K36A	β2-α2	Y36	A34		Interaction with Spo0B (12)	26.4±5.7	n.d.
D56A	β3	D56	D54	Site of phosphorylation by Spo0B, forms aspartyl pocket, Spo0A dimerization, predicted to interact with Spo0E (4, 25, 36, 68)	Site of phosphorylation by KinA, KinB, KinC, KinD, and KinE,(27), forms aspartyl pocket (4, 25, 36, 57)	0.008±0.001**	Spo0A
I58A	β3-α3	I58	K56	Stabilizes aspartyl pocket, Spo0A dimerization (25)	Interaction with KinA, Spo0B, and RapB, stabilizes aspartyl pocket (12, 13, 57, 71)	2±0.9	Spo0F decreased sporulation
M59A	β3-α3	M59	I57	n.d.	Interaction with KinA (13)	0.006±0.001**	Spo0F decreased sporulation
P60A	β3-α3	P60	P58	Interaction with Spo0E, P60S is resistant to hyperactive Spo0E; active without phosphorelay (28, 33)	Interaction with Spo0B (12)	<LOD**	**Spo0A gain-of-function**
H61A	β3-α3	H61	G59	n.d.	Interaction with Spo0B (12)	0.6±0.2*	n.d.
L62A	β3-α3	L62	M60	Interaction with Spo0E, L62P is resistant to hyperactive Spo0E (28)	M60A results in reduced *spoIIG* transcription (12)	11.5±1.8	**Spo0A gain-of-function**
S86A	β4	T86	T82	Stabilizes phosphorylation of active site (47)	Interaction with KinA, interaction with RapH, interaction with Spo0B (13, 38, 39, 74)	0.1±0.1*	Spo0F decreased sporulation

A87S	β4	A87	A83	n.d.	Interaction with Spo0B (12)	0.01±0.01[**]	n.d.
V88A	β4-α4	F88	Y84	Interaction with Spo0E; F88L is resistant to hyperactive Spo0E (28)	Interaction with Spo0B, KinA, RapH, Y84A is resistant to RapB, RapH (13, 38, 71)	17.9±1.0	**Spo0F reduced sporulation**
G89A	β4-α4	G89	G85	Inferred to interact with Spo0B (12)	Interaction with Spo0B (12)	5.6±2.1	n.d.
Q90A	β4-α4	Q90	E86	Q90R allows for direct interaction with KinC, and resistant to hyperactive Spo0E (34, 35)	Interaction with Spo0B, interaction with KinA (12, 13)	59.3±10.7[*]	**Spo0F reduced sporulation**, Spo0A gain-of-function
D91A	α4	E91	L87	n.d.	Interaction with Spo0B, interaction with KinA (12, 13)	37.8±12.5	**Spo0F reduced sporulation**
K92A	α4	D92	D88	D92Y is resistant to hyperactive Spo0E and is functional without phosphorelay (27, 33)	n.d.	33±2.7[*]	Spo0A gain-of-function
K108A	β5	K108	K104	Stabilizes aspartyl pocket, Spo0A dimerization, predicted Spo0E and Spo0B interaction (12, 25, 68)	Interaction with Spo0B, stabilizes aspartyl pocket, inferred interaction with KinA (12, 39, 57)	0.6±0.2[*]	n.d.
P109A	β5-α5	P109	P105	Spo0E and Spo0B interaction (12, 68)	Interaction with Spo0B (12)	76.9±9.3[*]	n.d.
F110A	β5-α5	F110	F106	Predicted Spo0E interaction (68)	Interaction with Spo0B (12)	17.9±2.1	**Spo0F reduced sporulation**
D111A	β5-α5	D111	D107	Predicted Spo0E interaction (68)	Interaction with Spo0B, inferred interaction with KinA (12, 39)	7.6±0.9	n.d.

2   [a] *, $P = > .05$; **, $P = > .01$

3   [b] *B. subtilis* phenotype that differs from *C. difficile* phenotype noted in bold

4   [c] Spo0A site-directed mutant sporulation frequency where protein was undetectable by western blot is underlined

5   n.d., not determined

Table 2. Spo0A site-directed mutant morphology and growth phenotypes

Spo0A mutant	Morphology phenotype
D14A	Mucoidal
F15A	Mucoidal
C16A	Mucoidal
Q17A	Poor growth
L19A	Translucent
E21A	Mucoidal, poor growth
A35S	Mucoidal, poor growth
H61A	Mucoidal, poor growth
A87S	Mucoidal, poor growth
Q90A	Mucoidal
D91A	Mucoidal
P109A	Mucoidal
F110A	Translucent
D111A	Crushed

Table 3. Bacterial Strains and plasmids

Plasmid or Strain	Relevant genotype or features	Source, construction or reference
Strains		
E. coli		
HB101	F⁻ *mcrB mrr hsdS20*(r$_B^-$ m$_B^-$) *recA13 leuB6 ara-14 proA2 lacY1 galK2 xyl-5 mtl-1 rpsL20*	B. Dupuy
C. difficile		
630Δ*erm*	Erm^S derivative of strain 630	N. Minton (75)
MC310	630Δ*erm spo0A*::*erm*	(31)
MC324	630Δ*erm* pMC123	(31)
MC848	630Δ*erm spo0A*::*erm* pMC566	This study
MC849	630Δ*erm spo0A*::*erm* pMC567	This study
MC855	630Δ*erm spo0A*::*erm* pMC123	This study
MC961	630Δ*erm spo0A*::*erm* pMC656	This study
MC962	630Δ*erm spo0A*::*erm* pMC657	This study
MC981	630Δ*erm spo0A*::*erm* pMC663	This study
MC1003	630Δ*erm spo0A*::*erm* pMC674	This study
MC1033	630Δ*erm spo0A*::*erm* pMC684	This study
MC1036	630Δ*erm spo0A*::*erm* pMC685	This study
MC1057	630Δ*erm spo0A*::*erm* pMC697	This study
MC1058	630Δ*erm spo0A*::*erm* pMC698	This study
MC1059	630Δ*erm spo0A*::*erm* pMC699	This study
MC1060	630Δ*erm spo0A*::*erm* pMC700	This study
MC1061	630Δ*erm spo0A*::*erm* pMC701	This study
MC1062	630Δ*erm spo0A*::*erm* pMC702	This study
MC1063	630Δ*erm spo0A*::*erm* pMC703	This study

MC1064	630Δ*erm spo0A*::*erm* pMC704	This study
MC1184	630Δ*erm spo0A*::*erm* pMC768	This study
MC1185	630Δ*erm spo0A*::*erm* pMC770	This study
MC1527	630Δ*erm* pMC917	This study
MC1529	630Δ*erm* pMC930	This study
MC1618	630Δ*erm spo0A*::*erm* pMC732	This study
MC1619	630Δ*erm spo0A*::*erm* pMC742	This study
MC1620	630Δ*erm spo0A*::*erm* pMC769	This study
MC1621	630Δ*erm spo0A*::*erm* pMC771	This study
MC1664	630Δ*erm spo0A*::*erm* pMC967	This study
MC1665	630Δ*erm spo0A*::*erm* pMC969	This study
MC1666	630Δ*erm spo0A*::*erm* pMC970	This study
MC1670	630Δ*erm spo0A*::*erm* pMC965	This study
MC1671	630Δ*erm spo0A*::*erm* pMC966	This study
MC1690	630Δ*erm spo0A*::*erm* pMC971	This study
MC1711	630Δ*erm spo0A*::*erm* pMC975	This study
MC1712	630Δ*erm spo0A*::*erm* pMC976	This study
MC1713	630Δ*erm spo0A*::*erm* pMC986	This study
MC1778	630Δ*erm spo0A*::*erm* pMC968	This study
MC1846	630Δ*erm spo0A*::*erm* pMC1055	This study
MC1904	630Δ*erm spo0A*::*erm* pMC922	This study
MC1905	630Δ*erm spo0A*::*erm* pMC924	This study
MC1906	630Δ*erm spo0A*::*erm* pMC944	This study
MC1991	630Δ*erm spo0A*::*erm* pMC1097	This study
MC1992	630Δ*erm spo0A*::*erm* pMC1098	This study
MC1993	630Δ*erm spo0A*::*erm* pMC1099	This study
MC1994	630Δ*erm spo0A*::*erm* pMC1100	This study
MC1995	630Δ*erm spo0A*::*erm* pMC1101	This study
MC1996	630Δ*erm spo0A*::*erm* pMC1102	This study

MC1997	630Δ*erm spo0A*::*erm* pMC1103	This study
MC1998	630Δ*erm spo0A*::*erm* pMC1104	This study
MC1999	630Δ*erm spo0A*::*erm* pMC1105	This study
MC2000	630Δ*erm spo0A*::*erm* pMC1106	This study
MC2001	630Δ*erm spo0A*::*erm* pMC1107	This study
MC2002	630Δ*erm spo0A*::*erm* pMC1108	This study
MC2003	630Δ*erm spo0A*::*erm* pMC1109	This study
MC2004	630Δ*erm spo0A*::*erm* pMC1110	This study
MC2005	630Δ*erm spo0A*::*erm* pMC1111	This study

Plasmids

pRK24	Tra+, Mob+; *bla, tet*	(76)
pUC19	Cloning vector; *bla*	(77)
pMC123	*E. coli-C. difficile* shuttle vector; *bla, catP*	(59)
pMC566	pMC123 WT Spo0A	This study
pMC567	pMC123 Spo0A D56A	This study
pMC656	pMC123 Spo0A N12A	This study
pMC657	pMC123 Spo0A K13A	This study
pMC663	pMC123 Spo0A I58A	This study
pMC674	pMC123 Spo0A 3xFLAG	This study
pMC684	pMC123 Spo0A V18A	This study
pMC685	pMC123 Spo0A H61A	This study
pMC697	pMC123 Spo0A C16A	This study
pMC698	pMC123 Spo0A E21A	This study
pMC699	pMC123 Spo0A A35S	This study
pMC700	pMC123 Spo0A P60A	This study
pMC701	pMC123 Spo0A A87S	This study
pMC702	pMC123 Spo0A V88A	This study
pMC703	pMC123 Spo0A G89A	This study

pMC704	pMC123 Spo0A K108A	This study
pMC742	pMC123 Spo0A D91A	This study
pMC768	pMC123 Spo0A M59A	This study
pMC769	pMC123 Spo0A L62A	This study
pMC770	pMC123 Spo0A K92A	This study
pMC771	pMC123 Spo0A P109A	This study
pMC915	pAF 256 HupA-SmBit-LgBit	Wiep Klaas Smits (56)
pMC916	pAF257 SmBit-HupA-LgBit	Wiep Klaas Smits (56)
pMC917	pAF 259 BitLuc	Wiep Klaas Smits (56)
pMC918	pAP118 HupA-SmBit-HupA-LgBit	Wiep Klaas Smits (56)
pMC922	pAP118 Spo0A-SmBit-LgBit	This study
pMC924	pAP118 SmBit-Spo0A-LgBit	This study
pMC930	pAF256 SmBit-LgBit	This study
pMC932	pAF257 Spo0A-SmBit-LgBit	This study
pMC944	pMC932 Spo0A-SmBit-Spo0A-LgBit	This study
pMC965	pMC123 Spo0A D11A	This study
pMC966	pMC123 Spo0A D14A	This study
pMC967	pMC123 Spo0A F15A	This study
pMC968	pMC123 Spo0A Q17A	This study
pMC969	pMC123 Spo0A L19A	This study
pMC970	pMC123 Spo0A D111A	This study
pMC971	pMC123 Spo0A D56A 3xFLAG	This study
pMC975	pMC123 Spo0A K36A	This study
pMC976	pMC123 Spo0A Q90A	This study
pMC986	pMC123 Spo0A F110A	This study
pMC1055	pMC123 Spo0A S86A	This study
pMC1088	pMC123 Spo0A D10A	This study
pMC1097	pAF256 Spo0A D10A-SmBit	This study
pMC1098	pAF256 Spo0A D11A-SmBit	This study

pMC1099	pAF256 Spo0A D56A-SmBit	This study
pMC1100	pAF256 Spo0A I58A-SmBit	This study
pMC1101	pAF256 Spo0A K108A-SmBit	This study
pMC1102	pAF257 Spo0A D10A-LgBit	This study
pMC1103	pAF257 Spo0A D11A-LgBit	This study
pMC1104	pAF257 Spo0A D56A-LgBit	This study
pMC1105	pAF257 Spo0A I58A-LgBit	This study
pMC1106	pAF257 Spo0A K108A-LgBit	This study
pMC1107	pAP118 D10A-SmBit-D10A-LgBit	This study
pMC1108	pAP118 D11A-SmBit-D11A-LgBit	This study
pMC1109	pAP118 D56A-SmBit-D56A-LgBit	This study
pMC1110	pAP118 I58A-SmBit-I58A-LgBit	This study
pMC1111	pAP118 K108A-SmBit-K108A-LgBit	This study

Table 4. Oligonucleotides

Primer	Sequence (5'→3')[a, b]	Use/locus tag/reference
oMC305	CACAGGAGGTATCGTACAG	Forward primer for sequencing Spo0A
oMC306	GCGAAACGGTATAACCCTAG	Reverse for sequencing Spo0A
oMC1249	GTCGA<u>GGATCC</u>GATGACAAGTTATTGGAATACACAG	Forward primer for Spo0A expression from pMC123
oMC1250	GACTC<u>GAATTC</u>CCCTAGTGGTTATACCGTTTCG	Reverse primer for Spo0A expression from pMC123
oMC1251	ATTAATACTAG**C**TGTAATAATGCCACATC	Forward SOEing primer for Spo0A D56A
oMC1252	GAT GTGGCATTATTACA**G**CTAGTATTAAT	Reverse SOEing primer for Spo0A D56A
oMC1513	GTTTTAGCAGATGAC**GC**TAAGGATTTTTGTCAG	Forward SOEing primer for Spo0A N12A
oMC1514	CTGACAAAAATCCTTA**GC**GTCATCTGCTAAAAC	Reverse SOEing primer for Spo0A N12A
oMC1515	TTAGCAGATGACAAT**GCA**GATTTTTGTCAGGTA	Forward SOEing primer for Spo0A K13A
oMC1516	TACCTGACAAAAATC**TGC**ATTGTCATCTGCTAA	Reverse SOEing primer for Spo0A K13A
oMC1517	AAGGATTTTTGTCAGG**C**ATTAAAAGAGTATTTG	Forward SOEing primer for Spo0A V18A
oMC1518	CAAATACTCTTTTAAT**G**CCTGACAAAAATCCTT	Reverse SOEing primer for Spo0A V18A

oMC1519	TTAATACTAGATGTA**GC**AATGCCACATCTAGAT	Forward SOEing primer for Spo0A I58A
oMC1520	ATCTAGATGTGGCATT**GC**TACATCTAGTATTAA	Reverse SOEing primer for Spo0A I58A
oMC1547	GATGC<u>GAATTC</u>TCACTTGTCATCGTCATCCTTGTAA TCTATGTCATGATCTTTATAATCACCGTCATGGT CTTTGTAGTCACCTCCTTTAACCATACTATGTTC TAGTCTTAA	Reverse primer for Spo0A with 3x FLAG tag and homology to pMC123
oMC1583	GATGTAATAATGCCA**GCA**CTAGATGGATTAGGT	Forward SOEing primer for Spo0A H61A
oMC1584	ACCTAATCCATCTAG**TGC**TGGCATTATTACATC	Reverse SOEing primer for Spo0A H61A
oMC2354	AGGTTATAGACTTTTTGAAGAAATTCTATAGCT <u>CGATCG</u>GTGTAAAAAGTTTAGTTTTCTGTAATA AGAAGATGT	Forward primer to amplify Spo0A fused to LgBit fragment
oMC2437	CTTGATCGTAGCGTTAACAGATCT<u>GAGCTC</u>GTG TAAAAAGTTTAGTTTTCTGTAATAAGAAGATGT	Forward primer to amplify Spo0A fused to SmBit fragment
oMC2439	CACCACCACTAGAACCCC<u>CTCGAG</u>ATTTAACCAT ACTATGTTCTAGTCTTAATTTATCAGC	Reverse primer to amplify Spo0A fused to SmBit fragment
oMC2447	ACCACCACCACTAGAACCT<u>GCGGCCGC</u>TCCTTTAA CCATACTATGTTCTAGTCTTAATTTATCAGC	Reverse primer to amplify Spo0A fused to LgBit fragment

aRestriction sites underlined

bNucleotides for site-directed mutagenesis are noted in bold

Supplementary Material

Table S1. Luminescence outputs from split-luciferase assay.

Strain	Average LU/OD$_{600}$
Positive control (bitLuc^{opt})	9422.6 ± 1035.5
Negative control (SmBit-LgBit)	1051.6 ± 328.0
Spo0A-SmBit	1820.5 ± 692.9
Spo0A-LgBit	845.7 ± 188.2
Spo0A-SmBit-Spo0A-LgBit	934244.3 ± 47268.6
Spo0A D10A-SmBit	2517.3 ± 456.7
Spo0A D10A-LgBit	1307.8 ± 64.2
Spo0A D10A-SmBit-Spo0A D10A-LgBit	341759.3 ± 145113
Spo0A D11A-SmBit	969.4 ± 195.5
Spo0A D11A-LgBit	1378.3 ± 44.6
Spo0A D11A-SmBit-Spo0A D11A-LgBit	399696.3 ± 145900
Spo0A D56A-SmBit	998.9 ± 141.4
Spo0A D56A-LgBit	1203.4 ± 370.1
Spo0A D56A-SmBit-Spo0A D56A-LgBit	242346.6 ± 89320.3
Spo0A I58A-SmBit	2200.3 ± 788.8
Spo0A I58A-LgBit	1609.2 ± 199.9
Spo0A I58A-SmBit-Spo0A I58A-LgBit	442895.4 ± 269303
Spo0A K108A-SmBit	2648.6 ± 196.3
Spo0A K108A-LgBit	1592.4 ± 54.6
Spo0A K108A-SmBit-Spo0A K108A-LgBit	542192.7 ± 443215

Table S2. Cloning and vector construction details

pMC566: A 1.2 kb *spo0A* PCR product amplified with primers oMC1249/oMC1250 was cloned into pMC123 using BamHI/EcoRI sites.

pMC567: A single amino acid mutation (D56A) within a 1.2 kb *spo0A* PCR product amplified with primers oMC1249/oMC1250 was made in a SOEing PCR reaction with two fragments generated by using primer set oMC1251/oMC1252 and cloned into pMC123 using BamHI/EcoRI sites.

pMC656: A single amino acid mutation (N12A) within a 1.2 kb *spo0A* PCR product amplified with primers oMC1249/oMC1250 was made in a SOEing PCR reaction with two fragments generated by using primer set oMC1513/oMC1514 and cloned into pMC123 using BamHI/EcoRI sites.

pMC657: A single amino acid mutation (K13A) within a 1.2 kb *spo0A* PCR product amplified with primers oMC1249/oMC1250 was made in a SOEing PCR reaction with two fragments generated by using primer set oMC1515/oMC1516 and cloned into pMC123 using BamHI/EcoRI sites.

pMC663: A single amino acid mutation (I58A) within a 1.2 kb *spo0A* PCR product amplified with primers oMC1249/oMC1250 was made in a SOEing reaction with two fragments generated by using primer set oMC1519/oMC1520 and cloned into pMC123 using BamHI/EcoRI sites.

pMC674: A 1.3 kb *spo0A* PCR product with C-terminal 3xFLAG amplified with primers oMC1249/oMC1547 was cloned into pMC123 using BamHI/EcoRI sites.

pMC684: A single amino acid mutation (V18A) within a 1.2 kb *spo0A* PCR product amplified with primers oMC1249/oMC1250 was made in a SOEing PCR reaction with two fragments generated by using primer set oMC1517/oMC1518 and cloned into pMC123 using BamHI/EcoRI sites.

pMC685: A single amino acid mutation (H61A) within a 1.2 kb *spo0A* PCR product amplified with primers oMC1249/oMC1250 was made in a SOEing PCR reaction with two fragments generated by using primer set oMC1583/oMC1584 and cloned into pMC123 using BamHI/EcoRI sites.

pMC697: A 1.2 kb *spo0A* C16A allele (TGT -> GCT) synthesized by Genscript was cloned into pMC123 using BamHI/EcoRI sites.

pMC698: A 1.2 kb *spo0A* E21A allele (GAG -> GCT) synthesized by Genscript was cloned into pMC123 using BamHI/EcoRI sites.

pMC699: A 1.2 kb *spo0A* A35S allele (GCT -> TCT) synthesized by Genscript was cloned into pMC123 using BamHI/EcoRI sites.

pMC700: A 1.2 kb *spo0A* P60A allele (CCA -> GCA) synthesized by Genscript was cloned into pMC123 using BamHI/EcoRI sites.

pMC701: A 1.2 kb *spo0A* A87S allele (GCA -> TCA) synthesized by Genscript was cloned into pMC123 using BamHI/EcoRI sites.

pMC702: A 1.2 kb *spo0A* V88A allele (GTA -> GCA) synthesized by Genscript was cloned into pMC123 using BamHI/EcoRI sites.

pMC703: A 1.2 kb *spo0A* G89A allele (GGT -> GCT) synthesized by Genscript was cloned into pMC123 using BamHI/EcoRI sites.

pMC704: A 1.2 kb *spo0A* K108A allele (AAG -> GCA) synthesized by Genscript was cloned into pMC123 using BamHI/EcoRI sites.

pMC742: A 1.2 kb *spo0A* D91A allele (GAT -> GCT) synthesized by Genscript was cloned into pMC123 using BamHI/EcoRI sites.

pMC768: A 1.2 kb *spo0A* M59A allele (ATG -> GCA) synthesized by Genscript was cloned into pMC123 using BamHI/EcoRI sites.

pMC769: A 1.2 kb *spo0A* L62A allele (CTA -> GCA) synthesized by Genscript was cloned into pMC123 using BamHI/EcoRI sites.

pMC770: A 1.2 kb *spo0A* K92A allele (AAG -> GCA) synthesized by Genscript was cloned into pMC123 using BamHI/EcoRI sites.

pMC771: A 1.2 kb *spo0A* P109A allele (CCA -> GCA) synthesized by Genscript was cloned into pMC123 using BamHI/EcoRI sites.

pMC922: Two PCR fragments were generated with oMC2437/2439 (950 bp) + oMC2441/2442 (600 bp) to create *spo0A*-SmBit-LgBit and Gibson assembled as BamHI/SacI into pAP118.

pMC924: Three PCR fragments were generated with oMC2443/2356 (150 bp) + oMC2354/2447 (950 bp) + oMC2445/2442 (550 bp) to create SmBit-*spo0A*-LgBit and Gibson assembled as BamHI/SacI into pAP118.

pMC930: Two PCR fragments were combined in SOEing PCR reaction from oMC2443/2449 and oMC2442/2448 (600 bp) and Gibson assembled into pAF256 to create SmBit-LgBit fusion.

pMC932: Two PCR fragments were combined in SOEing PCR reaction from oMC2437/2439 and oMC2441/2356 (1050 bp) and cloned into the SacI/PvuI sites of pAF257 to create *spo0A*-SmBit.

pMC944: Two PCR fragments were combined in SOEing PCR reaction from oMC2354/2447 and oMC2445/2442 (1850 bp) and cloned into the BamHI/PvuI sites of pMC932 to create *spo0A*-SmBit-*spo0A*-LgBit.

pMC965: A 1.2 kb *spo0A* D11A allele (GAC -> GCA) synthesized by Genscript was cloned into pMC123 using BamHI/EcoRI sites.

pMC966: A 1.2 kb *spo0A* D14A allele (GAT -> GCT) synthesized by Genscript was cloned into pMC123 using BamHI/EcoRI sites.

pMC967: A 1.2 kb *spo0A* F15A allele (TTT -> GCT) synthesized by Genscript was cloned into pMC123 using BamHI/EcoRI sites.

pMC968: A 1.2 kb *spo0A* Q17A allele (CAG -> GCT) synthesized by Genscript was cloned into pMC123 using BamHI/EcoRI sites.

pMC969: A 1.2 kb *spo0A* L19A allele (TTA -> GCA) synthesized by Genscript was cloned into pMC123 using BamHI/EcoRI sites.

pMC970: A 1.2 kb *spo0A* D111A allele (GAT -> GCT) synthesized by Genscript was cloned into pMC123 using BamHI/EcoRI sites.

pMC971: *spo0A* D56A-3XFLAG (SOEing product from oMC1249/1252 and oMC1251/1547) was made and cloned into pMC123 using BamHI/EcoRI.

pMC975: A 1.2 kb *spo0A* K36A allele (AAG -> GCA) synthesized by Genscript was cloned into pMC123 using BamHI/EcoRI sites.

pMC976: A 1.2 kb *spo0A* Q90A allele (CAA -> GCA) synthesized by Genscript was cloned into pMC123 using BamHI/EcoRI sites.

pMC986: A 1.2 kb *spo0A* F110A allele (TTT -> GCT) synthesized by Genscript was cloned into pMC123 using BamHI/EcoRI sites.

pMC1055: A 1.2 kb *spo0A* S86A allele (TCA -> GCA) synthesized by Genscript was cloned into pMC123 using BamHI/EcoRI sites.

pMC1088: A 1.2 kb *spo0A* D10A allele (GAT -> GCT) synthesized by Genscript was cloned into pMC123 using BamHI/EcoRI sites.

pMC1097: An 850 bp *spo0A* D10A PCR fragment was amplified from pMC1088 using oMC2437/oMC2439 and was Gibson assembled into pAF256.

pMC1098: An 850 bp *spo0A* D11A PCR fragment was amplified from pMC965 using oMC2437/oMC2439 and was Gibson assembled into pAF256.

pMC1099: An 850 bp *spo0A* D56A PCR fragment was amplified from pMC567 using oMC2437/oMC2439 and was Gibson assembled into pAF256.

pMC2000: An 850 bp *spo0A* I58A PCR fragment was amplified from pMC663 using oMC2437/oMC2439 and was Gibson assembled into pAF256.

pMC2001: An 850 bp *spo0A* K108A PCR fragment was amplified from pMC704 using oMC2437/oMC2439 and was Gibson assembled into pAF256.

pMC2002: An 850 bp *spo0A* D10A PCR fragment was amplified from pMC1088 using oMC2354/oMC2447 and was Gibson assembled into pAF257.

pMC2003: An 850 bp *spo0A* D11A PCR fragment was amplified from pMC965 using oMC2354/oMC2447 and was Gibson assembled into pAF257.

pMC2004: An 850 bp *spo0A* D56A PCR fragment was amplified from pMC567 using oMC2354/oMC2447 and was Gibson assembled into pAF257.

pMC2005: An 850 bp *spo0A* I58A PCR fragment was amplified from pMC663 using oMC2354/oMC2447 and was Gibson assembled into pAF257.

pMC2006: An 850 bp *spo0A* K108A PCR fragment was amplified from pMC704 using oMC2354/oMC2447 and was Gibson assembled into pAF257.

pMC2007: An 850 bp *spo0A* D10A PCR fragment was amplified from pMC1088 using oMC2437/oMC2439 and was Gibson assembled into pAP118. An 850 bp *spo0A* D10A PCR fragment was then amplified from pMC1088 using oMC2354/oMC2447 and cloned into pAP118 using NotI and PvuI sites.

pMC2008: An 850 bp *spo0A* D11A PCR fragment was amplified from pMC965 using oMC2437/oMC2439 and was Gibson assembled into pAP118. An 850 bp *spo0A* D11A PCR fragment was then amplified from pMC965 using oMC2354/oMC2447 and cloned into pAP118 using NotI and PvuI sites.

pMC2009: An 850 bp *spo0A* D56A PCR fragment was amplified from pMC567 using oMC2437/oMC2439 and was Gibson assembled into pAP118. An 850 bp *spo0A* D56A PCR fragment was then amplified from pMC567 using oMC2354/oMC2447 and cloned into pAP118 using NotI and PvuI sites.

pMC2010: An 850 bp *spo0A* I58A PCR fragment was amplified from pMC663 using oMC2437/oMC2439 and was Gibson assembled into pAP118. An 850 bp *spo0A* I58A PCR fragment was then amplified from pMC663 using oMC2354/oMC2447 and cloned into pAP118 using NotI and PvuI sites.

pMC2011: An 850 bp *spo0A* K108A PCR fragment was amplified from pMC704 using oMC2437/oMC2439 and was Gibson assembled into pAP118. An 850 bp *spo0A* K108A PCR fragment was then amplified from pMC704 using oMC2354/oMC2447 and cloned into pAP118 using NotI and PvuI sites.
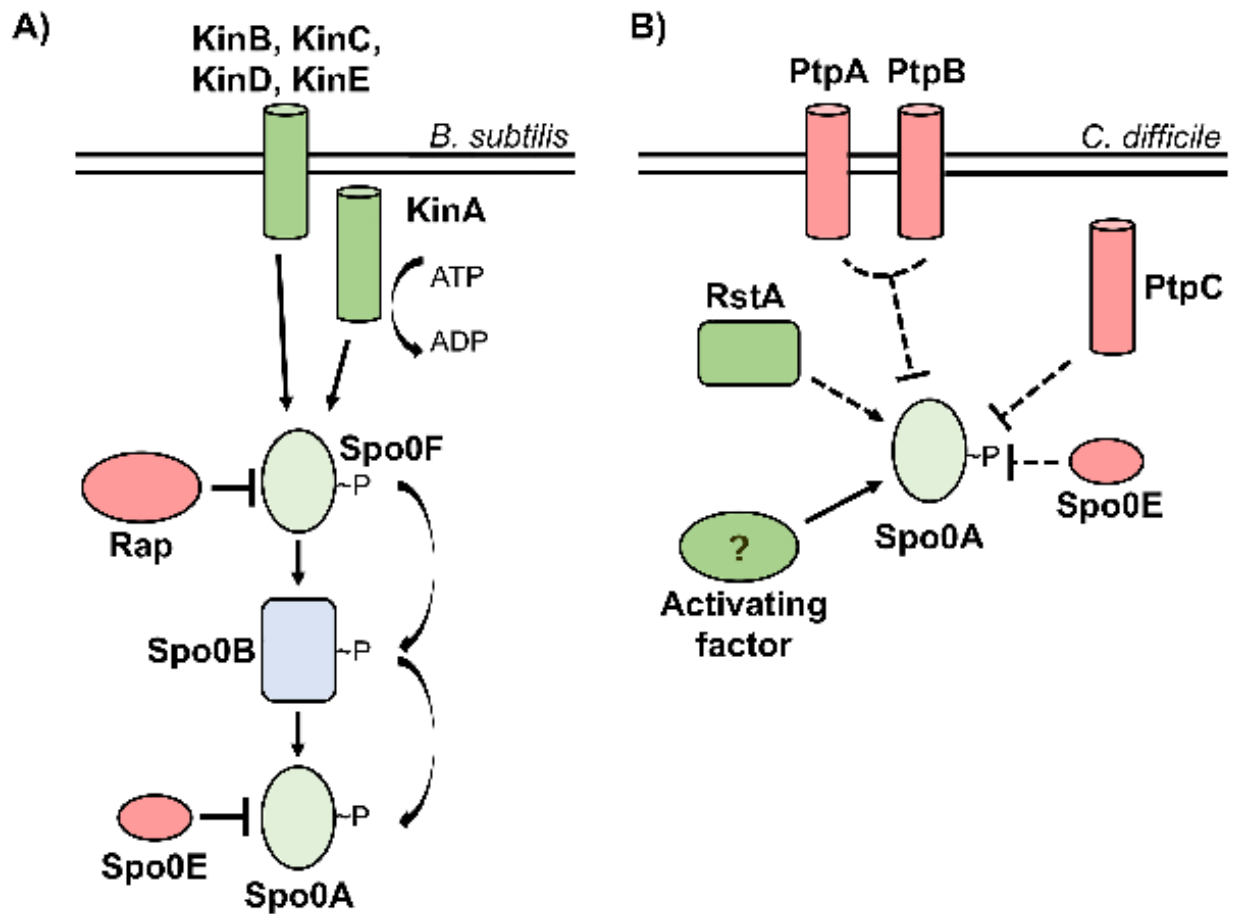
Figures

Fig. 1. Evolutionarily divergent strategies for Spo0A activation. A) In *Bacillus* species, Spo0A is activated via the phosphorelay, with kinases KinA, KinB, KinC, KinD, and KinE transferring phosphate to Spo0A via Spo0F and Spo0B, while the Rap and Spo0E phosphatases repress Spo0A activation. **B)** In *C. difficile*, the phosphotransfer proteins PtpA and PtpB act in coordination to prevent Spo0A activation, with PtpC and Spo0E also acting to repress Spo0A activity. RstA promotes sporulation through an unknown mechanism, and a yet unidentified activating factor is hypothesized to phosphorylate Spo0A.
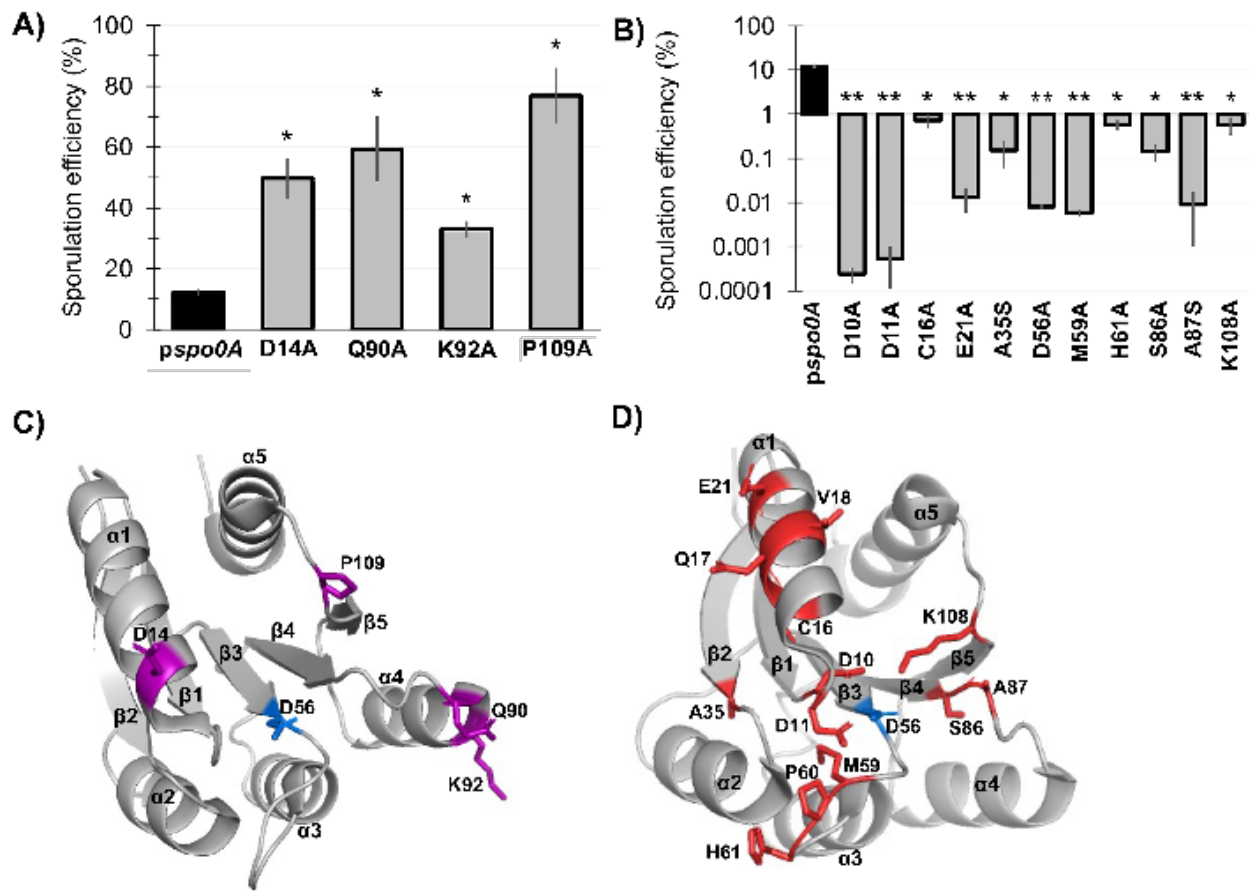
Fig. 2. Conservation of the Spo0A receiver domains in _B. subtilis_ and _C. difficile_. A) Graphic

representation of Spo0A domain structure. Functional residues responsible for protein - protein

interaction and Spo0A activation are located in the N-terminal receiver domain. The C-terminal

region of Spo0A is defined by a helix-turn-helix (HTH) DNA-binding domain. **B)** Amino acid

sequences of the Spo0A receiver domains for _B. subtilis str. 168_ (BSU_24220, top) and _C. difficile_

630 (CD630_12140, bottom). Residues important for activity that were chosen for mutation in _C._

difficile are highlighted in yellow. The blue star (*) is the conserved site of phosphorylation.

Alignment performed using Clustal Omega. Arrows represent beta sheets, and waved rectangles

represent alpha helices.

Fig. 3. Mutagenesis of conserved Spo0A residues results in both increased and decreased

***C. difficile* sporulation frequency. A)** Ethanol-resistant spore formation of 630Δ*erm spo0A*

p*spo0A* (MC848) expressed on a plasmid compared to the Spo0A site-directed mutants D14A

(MC1671), Q90A (MC1712), K92A (MC1185), and P109A (MC1621) with increased sporulation

frequency. **B)** Ethanol-resistant spore formation of 630Δ*erm spo0A* p*spo0A* (MC848) expressed

on a plasmid compared to the Spo0A site-directed mutants D10A (MC1618), D11A (MC1703),

C16A (MC1057), E21A (MC1058), A35S (MC1059), D56A (MC849), M59A (MC1184), H61A

(MC1036), S86A (MC1846), A87S (MC1061), and K108A (MC1064) with decreased sporulation

frequency, displayed on $\log_{10}$ scale. Sporulation assays were performed independently at least

four times. Statistical significance was determined using Kruskal-Wallis test and uncorrected

Dunn's test (*, $P = > 0.05$; **, $P = > 0.01$). **C)** 3D structure of Spo0A with residues (highlighted

purple) that cause increased sporulation when mutated, orientated around the activation site

(D56, highlighted blue). **D)** 3D structure of Spo0A with residues (highlighted red) that reduce sporulation when mutated, orientated around the active site (D56, highlighted blue). Spo0A PDB code 5WQ0, edited in PyMOL (The PyMOL Molecular Graphics System, Version 2.4.0 Schrödinger, LLC).
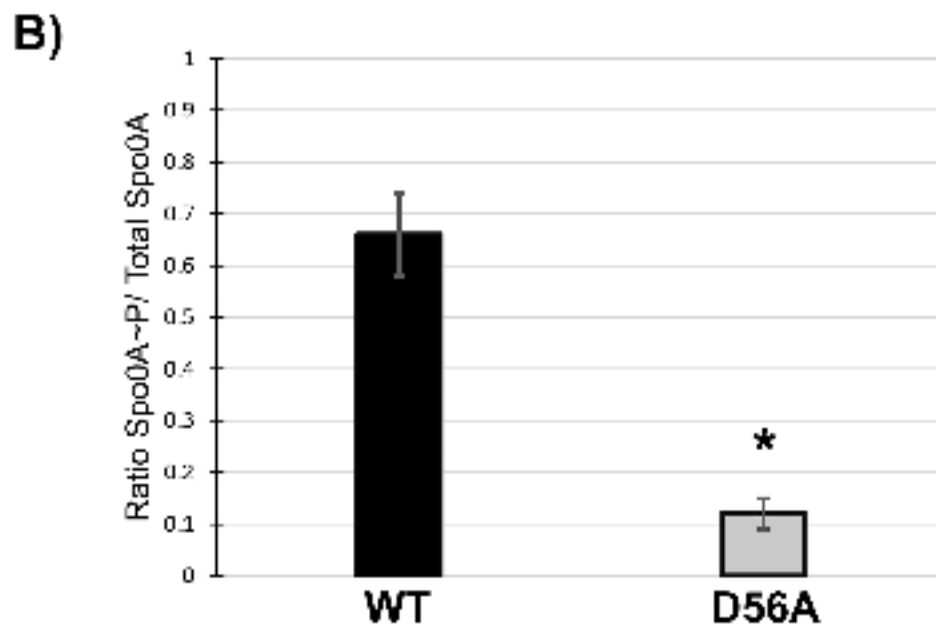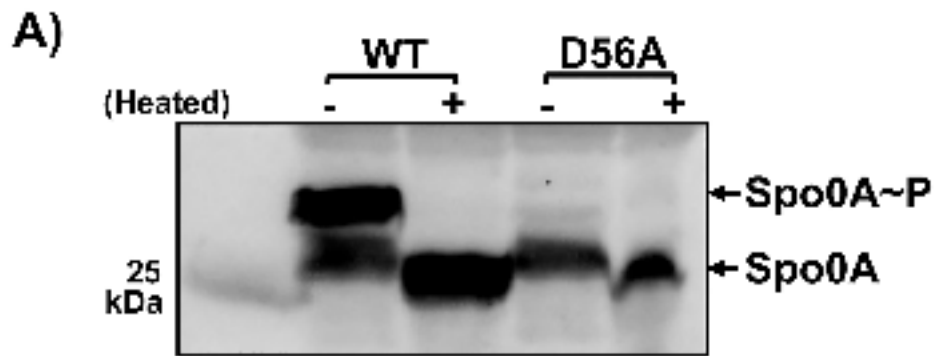
Fig. 4. The conserved aspartate residue of *C. difficile* Spo0A is phosphorylated. A) Anti-FLAG western blot after phos-tag gel separation of unphosphorylated and phosphorylated Spo0A (Spo0A~P) species in 630Δ*erm spo0A* p*spo0A*-3XFLAG (MC1003) and 630Δ*erm spo0A* p*spo0A* D56A-3XFLAG (MC1690) grown on sporulation agar. Phos-tag SDS-PAGE was performed on protein extracts (10 ug) and visualized using an anti-FLAG antibody. The molecular weight marker (25 kDa) is indicated on the left of the panel and experiments were performed 3 independent times. **B**) Ratio of phosphorylated Spo0A to total Spo0A. Densitometry calculations were performed using ImageJ 1.53a. (*, $P = < 0.01$) as determined by unpaired two-tailed Student's t-test
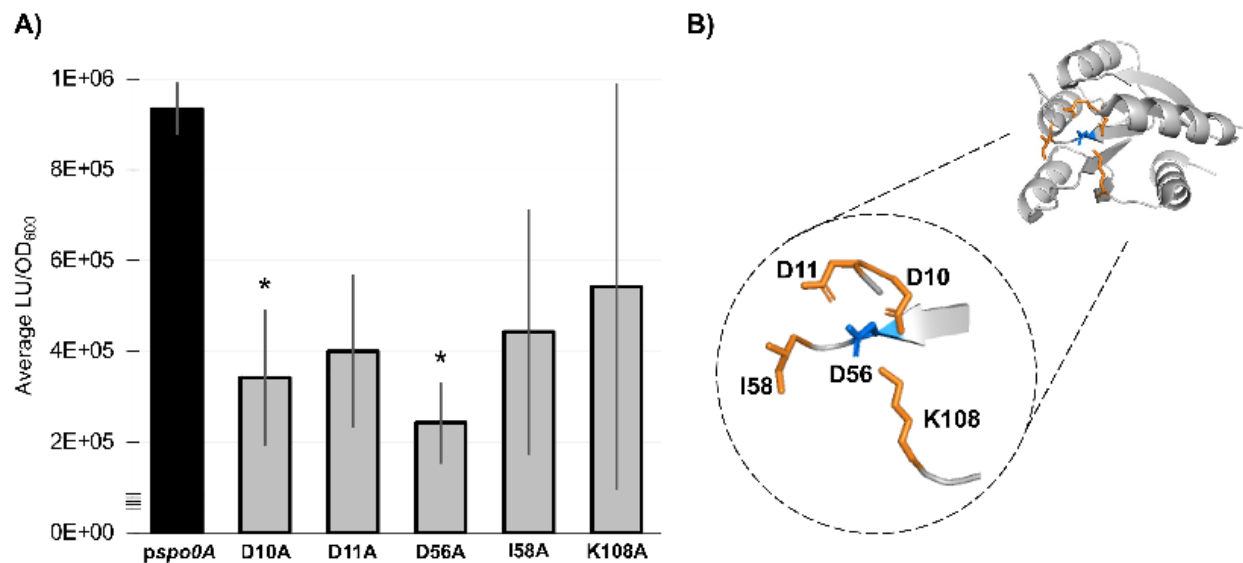
Fig. 5. Residues necessary for Spo0A dimerization in other Firmicutes are functionally conserved in *C. difficile*. A) Split-luciferase activity in strains 630Δ*erm spo0A* p*spo0A* (MC1906) and the Spo0A site-directed mutants D10A (MC2001), D11A (MC2002), D56A (MC2003), I58A (MC2004), and K108A (MC2005) fused to SmBit and LgBit fragments after cultures were grown in 70:30 sporulation broth to $OD_{600} = 0.8 – 0.9$ and induced with anhydrous tetracycline (ATc) for 1 h. Average luminescence outputs are normalized to optical densities (LU/OD_{600}). Error bars represent the standard deviation of three independent experiments (*, $P = < 0.05$) as determined by a one-way ANOVA with Dunnett's multiple comparisons test. **B)** 3D structure of Spo0A with the residues that form the aspartyl pocket and facilitate dimerization highlighted orange near the site of activation (D56, highlighted blue). Spo0A PDB code 5WQ0, edited in PyMOL (The PyMOL Molecular Graphics System, Version 2.4.0 Schrödinger, LLC).
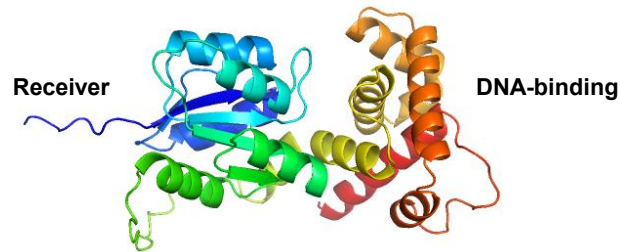
Fig. S1. Predicted Spo0A structure and domain architecture. AlphaFold predicted model of

C. difficile Spo0A (UniProt accession P52938). Spo0A consists of an N-terminal receiver

domain used for protein-protein interaction and a C-terminal helix-turn-helix domain used for

DNA-binding. The AlphaFold-generated predicted Spo0A PDB (AF-P52938-F1-model_v2) was

color-edited using PyMOL (The PyMOL Molecular Graphics System, Version 2.4.0 Schrödinger,

LLC).

```
B.s. Spo0F    MMNEKILIVDDQYGIRILLNEVFNKEG-YQ-TFQAANGLQALDIVTKERPDLVLL
B.s. Spo0A    MEKIKVCVADDNRELVSLLSEYIEGQEDMEVIGVAYNGQECLSLFKEKDPDVLVL
C.d. Spo0A    VEKIKIVLADDNKDFCQVLKEYLSNEDDIDILGIAKDGIEALDLVKKTQPDLLIL
              : : *: :.**:   :  :*.* :. :    :    * :* :.*.:..:  **:::*
                   |         |         |         |         |         |
                   10        20        29        38        48
                   10        20        30        40        50


B.s. Spo0F    DMKIPGMDGIEILKRMKVID--ENIRVIIMTAYGELDMIQESKELGALTHFAKPFDIDEI
B.s. Spo0A    DIIMPHLDGLAVLERLRESDLKKQPNVIMLTAFGQEDVTKKAVDLGASYFILKPFDMENL
C.d. Spo0A    DVIMPHLDGLGVIEKLNTMDIPKMPKIIVLSAVGQDKITQSAINLGADYYIVKPFDFVVF
              *: :* :**: :::::.   *   :   .:*:::* *: .: :.: :*** .: ****:  :
                   |         |         |         |         |         |
                   58        68        76        86        96        106
                   60        70        80        90        100       110
```

Fig. S2. Alignment of receiver domain residues of _B. subtilis_ Spo0A and Spo0F, and _C. difficile_ Spo0A. Spo0A receiver domain of _C. difficile_ aligned to _B. subtilis_ Spo0F and receiver domain of Spo0A using Clustal Omega (_B.s._ = _B. subtilis_; _C.d._ = _C. difficile_). Conserved residues chosen for mutation in _C. difficile_ are highlighted in yellow. Amino acid sequences of Spo0F (BSU_37130) and of the Spo0A receiver domains for _B. subtilis str. 168_ (BSU_24220, top), and _C. difficile_ 630 (CD630_12140, bottom). The blue star (*) is the conserved site of phosphorylation.
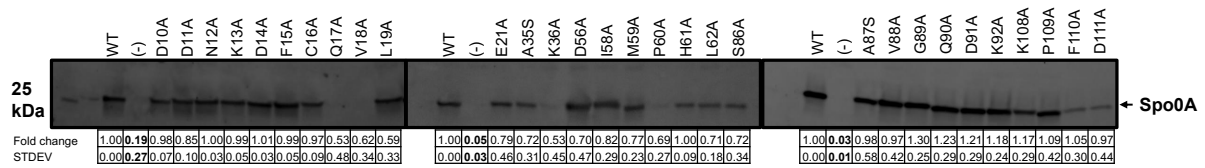
Fig. S3. Stability of Spo0A mutant alleles. SDS-PAGE western blot analysis of the 30 Spo0A point mutants to assess their stability using anti-Spo0A antibody. Strains harvested after 12 h growth on 70:30 sporulation medium and 2.5 μg of total protein was loaded for each sample. A wildtype (WT) positive control, *spo0A*::*erm* pSpo0A (MC848) and the *spo0A*::*erm* pMC123 (MC855) negative control strain (-) are included with each western blot. Each blot is representative of three independent experiments. The means and standard deviation of densitometric quantification normalized to WT on each membrane are shown, and bold values indicate $P \leq .05$ as determined by a one-way ANOVA with Dunnett's multiple comparisons test.

Spo0A site-directed mutation	Angstroms error estimate	Confidence in model	Sporulation frequency (%)
Wildtype	-	0.85	12.1±1.0
D10A	0.75 (0.71)	0.86	0.0002±0.0001
D11A	0.75 (0.74)	0.83	0.00055±0.0004
D14A	0.82 (0.81)	0.84	49.7±6.5
Q17A	0.78 (0.78)	0.86	<LOD
V18A	0.82 (0.77)	0.83	<LOD
D56A	0.71 (0.72)	0.85	0.008±0.001
P60A	0.74 (0.77)	0.86	<LOD
A87S	1.00 (1.22)	0.83	0.01±0.01
Q90A	1.16 (1.62)	0.84	59.3±10.7
K92A	1.32 (1.36)	0.85	33±2.7
P109A	0.99 (0.94)	0.87	76.9±9.3

Fig. S4. Predicted wild type and site-directed mutant Spo0A structures. The predicted effect on protein structure of a Spo0A site-directed mutant based on comparison of angstroms error estimate and confidence in the predicted model of site-directed mutants against corresponding wildtype residue values. Wild type residue angstroms error estimates are shown in parentheses adjacent to the corresponding Spo0A site-directed mutation. Predictions made using RoseTTAFold (Robetta).
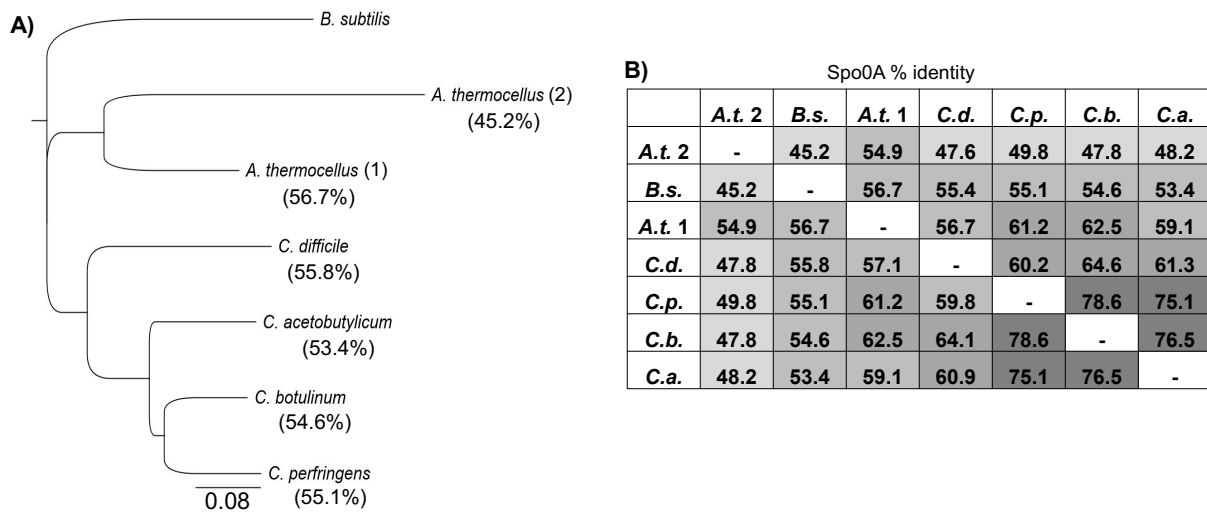
A)

B. subtilis

A. thermocellus (2)
(45.2%)

A. thermocellus (1)
(56.7%)

C. difficile
(55.8%)

C. acetobutylicum
(53.4%)

C. botulinum
(54.6%)

C. perfringens
(55.1%)

0.08

B) Spo0A % identity

	A.t. 2	B.s.	A.t. 1	C.d.	C.p.	C.b.	C.a.
A.t. 2	-	45.2	54.9	47.6	49.8	47.8	48.2
B.s.	45.2	-	56.7	55.4	55.1	54.6	53.4
A.t. 1	54.9	56.7	-	56.7	61.2	62.5	59.1
C.d.	47.8	55.8	57.1	-	60.2	64.6	61.3
C.p.	49.8	55.1	61.2	59.8	-	78.6	75.1
C.b.	47.8	54.6	62.5	64.1	78.6	-	76.5
C.a.	48.2	53.4	59.1	60.9	75.1	76.5	-

Fig. S5 Spo0A divergence in Firmicutes. A) Dendrogram of full-length Spo0A protein coding regions rooted to the outgroup *B. subtilis* Spo0A. Percentage identity of each species' Spo0A protein sequence is shown relative to *B. subtilis*. Spo0A alignment and dendrogram tree constructed using MUSCLE Alignment plugin and Geneious Tree Builder in Geneious Prime 2020.2.2. **B)** Heatmap of the comparisons of percent identities of Spo0A from each species in **(A)**. *B.s.* = *B. subtilis*, *A.t.*1 = *A. thermocellus* Spo0A 1, *A.t. 2* = *A. thermocellum* Spo0A 2, *C.d.* = *C. difficile*, *C.p.* = *C. perfringens*, *C.b.* = *C. botulinum*, and *C.a.* = *C. acetobutylicum*.

REFERENCES

1.   Ferrari FA, Trach K, LeCoq D, Spence J, Ferrari E, Hoch JA. Characterization of the *spo0A* locus and its deduced product. Proceedings of the National Academy of Sciences of the United States of America. 1985;82(9):2647-51.

2.   Perego M, Cole SP, Burbulys D, Trach K, Hoch JA. Characterization of the gene for a protein kinase which phosphorylates the sporulation-regulatory proteins Spo0A and Spo0F of *Bacillus subtilis*. Journal of bacteriology. 1989;171(11):6187-96.

3.   Perego M, Spiegelman GB, Hoch JA. Structure of the gene for the transition state regulator, abrB: regulator synthesis is controlled by the spo0A sporulation gene in Bacillus subtilis. Molecular microbiology. 1988;2(6):689-99.

4.   Burbulys D, Trach KA, Hoch JA. Initiation of sporulation in *B. subtilis* is controlled by a multicomponent phosphorelay. Cell. 1991;64(3):545-52.

5.   Strauch MA, Wu JJ, Jonas RH, Hoch JA. A positive feedback loop controls transcription of the spoOF gene, a component of the sporulation phosphorelay in Bacillus subtilis. Molecular microbiology. 1993;7(6):967-74.

6.   Jumper J, Evans R, Pritzel A, Green T, Figurnov M, Ronneberger O, et al. Highly accurate protein structure prediction with AlphaFold. Nature. 2021;596(7873):583-+.

7.   Varadi M, Anyango S, Deshpande M, Nair S, Natassia C, Yordanova G, et al. AlphaFold Protein Structure Database: massively expanding the structural coverage of protein-sequence space with high-accuracy models. Nucleic acids research. 2022;50(D1):D439-D44.

8.   Strauch MA, Hoch JA. Signal transduction in Bacillus subtilis sporulation. Current opinion in genetics & development. 1993;3(2):203-12.

9.   Zhao H, Msadek T, Zapf J, Madhusudan, Hoch JA, Varughese KI. DNA complexed structure of the key transcription factor initiating development in sporulating bacteria. Structure. 2002;10(8):1041-50.

10.   Rosenbusch KE, Bakker D, Kuijper EJ, Smits WK. *C. difficile* 630Delta*erm* Spo0A regulates sporulation, but does not contribute to toxin production, by direct high-affinity binding to target DNA. PloS one. 2012;7(10):e48608.

11.   Trach K, Burbulys D, Strauch M, Wu JJ, Dhillon N, Jonas R, et al. Control of the initiation of sporulation in *Bacillus subtilis* by a phosphorelay. Research in microbiology. 1991;142(7-8):815-23.

12.   Zapf J, Sen U, Madhusudan, Hoch JA, Varughese KI. A transient interaction between two phosphorelay proteins trapped in a crystal lattice reveals the mechanism of molecular recognition and phosphotransfer in signal transduction. Structure. 2000;8(8):851-62.

13.   Tzeng YL, Hoch JA. Molecular recognition in signal transduction: the interaction surfaces of the Spo0F response regulator with its cognate phosphorelay proteins revealed by alanine scanning mutagenesis. Journal of molecular biology. 1997;272(2):200-12.

14.   Brown DP, Ganova-Raeva L, Green BD, Wilkinson SR, Young M, Youngman P. Characterization of spo0A homologues in diverse Bacillus and Clostridium species identifies a probable DNA-binding domain. Molecular microbiology. 1994;14(3):411-26.

15.   Stephenson K, Hoch JA. Evolution of signalling in the sporulation phosphorelay. Molecular microbiology. 2002;46(2):297-304.

16.   Worner K, Szurmant H, Chiang C, Hoch JA. Phosphorylation and functional analysis of the sporulation initiation factor Spo0A from Clostridium botulinum. Molecular microbiology. 2006;59(3):1000-12.

17.   Mearls EB, Lynd LR. The identification of four histidine kinases that influence sporulation in Clostridium thermocellum. Anaerobe. 2014;28:109-19.

18.   Steiner E, Dago AE, Young DI, Heap JT, Minton NP, Hoch JA, et al. Multiple orphan histidine kinases interact directly with Spo0A to control the initiation of endospore formation in Clostridium acetobutylicum. Molecular microbiology. 2011;80(3):641-54.

19.   Freedman JC, Li J, Mi E, McClane BA. Identification of an Important Orphan Histidine Kinase for the Initiation of Sporulation and Enterotoxin Production by Clostridium perfringens Type F Strain SM101. mBio. 2019;10(1).

20.   Edwards AN, Wetzel D, DiCandia MA, McBride SM. Three orphan histidine kinases inhibit Clostridioides difficile sporulation. bioRxiv. 2021:2021.11.18.469199.

21.   Suarez JM, Edwards AN, McBride SM. The *Clostridium difficile cpr* locus is regulated by a noncontiguous two-component system in response to type A and B lantibiotics. Journal of bacteriology. 2013;195(11):2621-31.

22.   Underwood S, Guan S, Vijayasubhash V, Baines SD, Graham L, Lewis RJ, et al. Characterization of the sporulation initiation pathway of *Clostridium difficile* and its role in toxin production. Journal of bacteriology. 2009;191(23):7296-305.

23.   Bourret RB, Borkovich KA, Simon MI. Signal Transduction Pathways Involving Protein-Phosphorylation in Prokaryotes. Annual review of biochemistry. 1991;60:401-41.

24.   Stock JB, Ninfa AJ, Stock AM. Protein-Phosphorylation and Regulation of Adaptive Responses in Bacteria. Microbiological reviews. 1989;53(4):450-90.

25.   Lee CW, Park SH, Lee SG, Shin SC, Han SJ, Kim HW, et al. Crystal structure of the inactive state of the receiver domain of Spo0A from Paenisporosarcina sp TG-14, a psychrophilic bacterium isolated from an Antarctic glacier. J Microbiol. 2017;55(6):464-74.

26.   Feher VA, Zapf JW, Hoch JA, Whiteley JM, McIntosh LP, Rance M, et al. High-resolution NMR structure and backbone dynamics of the Bacillus subtilis response regulator, SpoOF: Implications for phosphorylation and molecular recognition. Biochemistry. 1997;36(33):10015-25.

27.   Quisel JD, Burkholder WF, Grossman AD. In vivo effects of sporulation kinases on mutant Spo0A proteins in Bacillus subtilis. Journal of bacteriology. 2001;183(22):6573-8.

28.   Stephenson SJ, Perego M. Interaction surface of the Spo0A response regulator with the Spo0E phosphatase. Molecular microbiology. 2002;44(6):1455-67.

29.   Strauch M, Webb V, Spiegelman G, Hoch JA. The SpoOA protein of Bacillus subtilis is a repressor of the abrB gene. Proceedings of the National Academy of Sciences of the United States of America. 1990;87(5):1801-5.

30.   Jiang M, Tzeng YL, Feher VA, Perego M, Hoch JA. Alanine mutants of the Spo0F response regulator modifying specificity for sensor kinases in sporulation initiation. Molecular microbiology. 1999;33(2):389-95.

31.   Edwards AN, Nawrocki KL, McBride SM. Conserved oligopeptide permeases modulate sporulation initiation in *Clostridium difficile*. Infection and immunity. 2014;82(10):4276-91.

32.   Putnam EE, Nock AM, Lawley TD, Shen A. SpoIVA and SipL are Clostridium difficile spore morphogenetic proteins. Journal of bacteriology. 2013;195(6):1214-25.

33.   Spiegelman G, Van Hoy B, Perego M, Day J, Trach K, Hoch JA. Structural alterations in the Bacillus subtilis Spo0A regulatory protein which suppress mutations at several spo0 loci. Journal of bacteriology. 1990;172(9):5011-9.

34.   Kobayashi K, Shoji K, Shimizu T, Nakano K, Sato T, Kobayashi Y. Analysis of a suppressor mutation ssb (kinC) of sur0B20 (spo0A) mutation in Bacillus subtilis reveals that kinC encodes a histidine protein kinase. Journal of bacteriology. 1995;177(1):176-82.

35.   LeDeaux JR, Grossman AD. Isolation and characterization of kinC, a gene that encodes a sensor kinase homologous to the sporulation sensor kinases KinA and KinB in Bacillus subtilis. Journal of bacteriology. 1995;177(1):166-75.

36.   Lewis RJ, Brannigan JA, Muchova K, Barak I, Wilkinson AJ. Phosphorylated aspartate in the structure of a response regulator protein. J Mol Biol. 1999;294(1):9-15.

37.   Bird TH, Grimsley JK, Hoch JA, Spiegelman GB. Phosphorylation of Spo0A activates its stimulation of in vitro transcription from the Bacillus subtilis spoIIG operon. Molecular microbiology. 1993;9(4):741-9.

38.   Parashar V, Mirouze N, Dubnau DA, Neiditch MB. Structural basis of response regulator dephosphorylation by Rap phosphatases. PLoS biology. 2011;9(2):e1000589.

39.   Varughese KI, Tsigelny I, Zhao HY. The crystal structure of beryllofluoride Spo0F in complex with the phosphotransferase Spo0B represents a phosphotransfer pretransition state (vol 188, pg 4970, 2006). Journal of bacteriology. 2007;189(8):3328-.

40.   Mackin KE, Carter GP, Howarth P, Rood JI, Lyras D. Spo0A differentially regulates toxin production in evolutionarily diverse strains of Clostridium difficile. PloS one. 2013;8(11):e79666.

41.   Deakin LJ, Clare S, Fagan RP, Dawson LF, Pickard DJ, West MR, et al. The *Clostridium difficile spo0A* gene is a persistence and transmission factor. Infection and immunity. 2012;80(8):2704-11.

42.   Pettit LJ, Browne HP, Yu L, Smits WK, Fagan RP, Barquist L, et al. Functional genomics reveals that Clostridium difficile Spo0A coordinates sporulation, virulence and metabolism. BMC genomics. 2014;15:160.

43.   Dawson LF, Valiente E, Faulds-Pain A, Donahue EH, Wren BW. Characterisation of Clostridium difficile biofilm formation, a role for Spo0A. PloS one. 2012;7(12):e50527.

44.   Molle V, Fujita M, Jensen ST, Eichenberger P, González-Pastor JE, Liu JS, et al. The Spo0A regulon of Bacillus subtilis. Molecular microbiology. 2003;50(5):1683-701.

45.   Huang IH, Waters M, Grau RR, Sarker MR. Disruption of the gene (spo0A) encoding sporulation transcription factor blocks endospore formation and enterotoxin production in enterotoxigenic Clostridium perfringens type A. FEMS microbiology letters. 2004;233(2):233-40.

46.   Mirouze N, Desai Y, Raj A, Dubnau D. Spo0A similar to P Imposes a Temporal Gate for the Bimodal Expression of Competence in Bacillus subtilis. PLoS genetics. 2012;8(3).

47.   Volz K. Structural conservation in the CheY superfamily. Biochemistry. 1993;32(44):11741-53.

48.   Baek M, DiMaio F, Anishchenko I, Dauparas J, Ovchinnikov S, Lee GR, et al. Accurate prediction of protein structures and interactions using a three-track neural network. Science. 2021;373(6557):871-+.

49.   Fujita M, Sadaie Y. Feedback loops involving Spo0A and AbrB in in vitro transcription of the genes involved in the initiation of sporulation in Bacillus subtilis. J Biochem. 1998;124(1):98-104.

50.   Asayama M, Yamamoto A, Kobayashi Y. Dimer form of phosphorylated Spo0A, a transcriptional regulator, stimulates the spo0F transcription at the initiation of sporulation in Bacillus subtilis. Journal of molecular biology. 1995;250(1):11-23.

51.   Lewis RJ, Scott DJ, Brannigan JA, Ladds JC, Cervin MA, Spiegelman GB, et al. Dimer formation and transcription activation in the sporulation response regulator Spo0A. Journal of molecular biology. 2002;316(2):235-45.

52.   Barbieri CM, Stock AM. Universally applicable methods for monitoring response regulator aspartate phosphorylation both in vitro and in vivo using Phos-tag-based reagents. Analytical biochemistry. 2008;376(1):73-82.

53.   Kinoshita E, Kinoshita-Kikuta E. Improved Phos-tag SDS-PAGE under neutral pH conditions for advanced protein phosphorylation profiling. Proteomics. 2011;11(2):319-23.

54.   Kinoshita-Kikuta E, Kusamoto H, Ono S, Akayama K, Eguchi Y, Igarashi M, et al. Quantitative monitoring of His and Asp phosphorylation in a bacterial signaling system by using Phos-tag Magenta/Cyan fluorescent dyes. Electrophoresis. 2019;40(22):3005-13.

55.   Oliveira Paiva AM, Friggen AH, Hossein-Javaheri S, Smits WK. The Signal Sequence of the Abundant Extracellular Metalloprotease PPEP-1 Can Be Used to Secrete Synthetic Reporter Proteins in Clostridium difficile. ACS synthetic biology. 2016;5(12):1376-82.

56.   Oliveira Paiva AM, Friggen AH, Qin L, Douwes R, Dame RT, Smits WK. The Bacterial Chromatin Protein HupA Can Remodel DNA and Associates with the Nucleoid in Clostridium difficile. Journal of molecular biology. 2019;431(4):653-72.

57.   Madhusudan, Zapf J, Whiteley JM, Hoch JA, Xuong NH, Varughese KI. Crystal structure of a phosphatase-resistant mutant of sporulation response regulator Spo0F from Bacillus subtilis (vol 4, pg 679, 1996). Structure. 1996;4(8):999-.

58.   Obana N, Nakao R, Nagayama K, Nakamura K, Senpuku H, Nomura N. Immunoactive Clostridial Membrane Vesicle Production Is Regulated by a Sporulation Factor. Infection and immunity. 2017;85(5).

59.   McBride SM, Sonenshein AL. Identification of a genetic locus responsible for antimicrobial peptide resistance in Clostridium difficile. Infection and immunity. 2011;79(1):167-76.

60.   Stephenson K, Lewis RJ. Molecular insights into the initiation of sporulation in Gram-positive bacteria: new technologies for an old phenomenon. FEMS microbiology reviews. 2005;29(2):281-301.

61.   Sorg JA, Dineen SS. Laboratory maintenance of Clostridium difficile. Current protocols in microbiology. 2009;Chapter 9:Unit9A 1.

62.   Edwards AN, Suarez JM, McBride SM. Culturing and maintaining *Clostridium difficile* in an anaerobic environment. Journal of visualized experiments : JoVE. 2013(79):e50787.

63.   Luria SE, Burrous JW. Hybridization between *Escherichia coli* and *Shigella.* Journal of bacteriology. 1957;74:461-76.

64.   Purcell EB, McKee RW, McBride SM, Waters CM, Tamayo R. Cyclic diguanylate inversely regulates motility and aggregation in Clostridium difficile. Journal of bacteriology. 2012;194(13):3307-16.

65.   Edwards AN, Tamayo R, McBride SM. A novel regulator controls Clostridium difficile sporulation, motility and toxin production. Molecular microbiology. 2016;100(6):954-71.

66.   Edwards AN, McBride SM. Determination of the in vitro Sporulation Frequency of Clostridium difficile. Bio Protoc. 2017;7(3).

67.   Childress KO, Edwards AN, Nawrocki KL, Woods EC, Anderson SE, McBride SM. The Phosphotransfer Protein CD1492 Represses Sporulation Initiation in Clostridium difficile. Infection and immunity. 2016.

68.   Diaz AR, Stephenson S, Green JM, Levdikov VM, Wilkinson AJ, Perego M. Functional role for a conserved aspartate in the Spo0E signature motif involved in the dephosphorylation of the Bacillus subtilis sporulation regulator Spo0A. The Journal of biological chemistry. 2008;283(5):2962-72.

69.   Cheng RR, Morcos F, Levine H, Onuchic JN. Toward rationally redesigning bacterial two-component signaling systems using coevolutionary information. Proceedings of the National Academy of Sciences of the United States of America. 2014;111(5):E563-E71.

70.   Perego M, Hanstein C, Welsh KM, Djavakhishvili T, Glaser P, Hoch JA. Multiple protein-aspartate phosphatases provide a mechanism for the integration of diverse signals in the control of development in *B. subtilis*. Cell. 1994;79(6):1047-55.

71.   Tzeng YL, Feher VA, Cavanagh J, Perego M, Hoch JA. Characterization of interactions between a two-component response regulator, Spo0F, and its phosphatase, RapB. Biochemistry. 1998;37(47):16538-45.

72.   McLaughlin PD, Bobaya BG, Regel EJ, Thompson RJ, Hoch JA, Cavanagh J. Predominantly buried residues in the response regulator Spo0F influence specific sensor kinase recognition. FEBS letters. 2007;581(7):1425-9.

73.   Perego M, Hoch JA. Cell-cell communication regulates the effects of protein aspartate phosphatases on the phosphorelay controlling development in Bacillus subtilis. Proceedings of the National Academy of Sciences of the United States of America. 1996;93(4):1549-53.

74.   Feher VA, Tzeng YL, Hoch JA, Cavanagh J. Identification of communication networks in SpoOF: a model for phosphorylation-induced conformational change and implications for activation of multiple domain bacterial response regulators. FEBS letters. 1998;425(1):1-6.

75.   Hussain HA, Roberts AP, Mullany P. Generation of an erythromycin-sensitive derivative of Clostridium difficile strain 630 (630Δerm) and demonstration that the conjugative transposon Tn916ΔE enters the genome of this strain at multiple sites. Journal of medical microbiology. 2005;54(2):137-41.

76.   Thomas CM, Smith CA. Incompatibility group P plasmids: genetics, evolution, and use in genetic manipulation. Annu Rev Microbiol. 1987;41:77-101.

77.   Yanisch-Perron C, Vieira J, Messing J. Improved M13 phage cloning vectors and host strains: nucleotide sequences of the M13mp18 and pUC19 vectors. Gene. 1985;33(1):103-19.

Chapter 3: Identification of a Conserved Switch that Controls Sporulation, Toxin, and Motility in *C. difficile*

Michael A. DiCandia[1], Adrianne N. Edwards[1], Cheyenne D. Lee[1], Marcos P. Monteiro[1], Pritha Bagchi[2], and Shonna M. McBride*[1]

[1]Department of Microbiology and Immunology, Emory University School of Medicine, Emory Antibiotic Resistance Center, Atlanta, GA, USA.
[2]Emory Integrated Proteomics Core, Emory University, Atlanta, GA, USA

In preparation

M.A.D. designed and performed experiments and wrote and edited the manuscript.

A.N.E. designed and performed experiments and wrote and edited the manuscript.

C.D.L. designed and performed experiments and wrote and edited the manuscript.

M.P.M. designed and performed experiments and wrote and edited the manuscript.

P.B. performed LC-MS/MS and assisted with data analysis.

S.M.M. designed and performed experiments and wrote and edited the manuscript.

SUMMARY

Clostridioides difficile spore formation is required for environmental survival and transmission. In all spore formers, sporulation is regulated through activation of the master response regulator, Spo0A. However, the factors that directly regulate *C. difficile* Spo0A activity are not defined. In *Bacillus*, Spo0A is directly inactivated by Spo0E, a small phosphatase. To understand Spo0E function in *C. difficile*, we created a null mutation of the *spo0E* ortholog and assessed sporulation and physiology. The *spo0E* mutant produced significantly more spores, demonstrating Spo0E represses *C. difficile* sporulation. Unexpectedly, the *spo0E* mutant also exhibited increased motility, toxin production, and virulence in animal infections. We uncovered that Spo0E interacts with both Spo0A and the toxin/motility regulator, RstA. Interactions between Spo0A, Spo0E, and RstA constitute a previously unknown molecular switch that coordinates sporulation with motility and toxin production. Reinvestigation of *B. subtilis* revealed that Spo0E also repressed motility, demonstrating conserved multi-function of the protein. Further, we found Spo0E orthologs are widespread among prokaryotes, suggesting that Spo0E performs conserved regulatory functions in diverse bacteria.

INTRODUCTION

Clostridioides difficile is an anaerobic gastrointestinal pathogen that requires spore formation for transmission (1). While spores are highly resistant to environmental insults, the formation of endospores is both energetically costly and can result in long-term dormancy of the bacterium. Consequently, the initiation of spore development has evolved tight regulatory controls that prevent unnecessary dormancy. While the regulatory pathways that control sporulation initiation in *Bacillus* species have been well characterized, the factors required for regulation of initiation in anaerobes, like *C. difficile*, are poorly conserved and remain incompletely defined (2–15).

One factor that is highly conserved and required for sporulation initiation in all spore formers is the transcriptional regulator, Spo0A (10,16). In *Bacillus* species, Spo0A is directly inactivated by a small phosphatase known as Spo0E, which results in repression of spore formation (17–22,22,23). However, Spo0E function has not been studied in the Clostridia or any other anaerobes, and as these systems regulate Spo0A through divergent mechanisms, the function of Spo0E in these organisms cannot be assumed (23,24).

In this work, we investigated the role of a predicted Spo0E ortholog, CD3271, to determine its effect on sporulation initiation in *C. difficile*. Analysis of a *spo0E* mutant revealed that Spo0E represses sporulation of *C. difficile*, as was observed in *Bacillus*. Unexpectedly, we also observed that Spo0E repressed motility and toxin production. Further investigation of Spo0E function revealed that Spo0E interacted specifically with Spo0A, as predicted, but also interacted with the regulator, RstA. RstA was previously shown to directly decrease motility and toxin production as a transcriptional repressor and to induce sporulation through an undetermined mechanism. These results reveal that Spo0E acts as a lynchpin in a mechanism that governs sporulation through interaction with Spo0A and concomitantly regulates toxin production and motility through its interaction with RstA.

Additionally, we determined that Spo0E also repressed motility in *Bacillus subtilis*, indicating that Spo0E functions as a regulator of sporulation and motility in both species. A further search for Spo0E orthologs revealed widespread distribution among Gram-positive and Gram-negative bacteria. Together, these results suggest that Spo0E-like proteins are conserved among prokaryotes and represent an overlooked regulatory mechanism in bacteria.

RESULTS

Spo0E represses sporulation, toxin production, and motility in *C. difficile*. To determine if the Spo0E ortholog has a role in *C. difficile* sporulation, we disrupted the predicted *spo0E* gene

(**Fig. S1 A-C**) and assessed spore production in the mutant. The *spo0E* mutant sporulated at about three-fold greater than the wild-type (WT) parent strain, indicating Spo0E substantially represses sporulation in *C. difficile,* similar to *B. subtilis* (**Fig. 1A, B**)*.* The *spo0E* phenotypes were fully complemented with the reintroduction of wild-type *spo0E* (**Fig. S2**).

Unexpectedly, it was also observed that colonies of the *spo0E* mutant appeared mucoid and spreading, which was not reported previously for *Bacillus* species (8,22,24,25). The *spo0E* mutant colony phenotypes suggested that Spo0E could impact additional cellular processes. To explore this further, motility assays were performed on soft agar to assess the dissemination of the *spo0E* mutant over time, relative to the WT. As the spreading *spo0E* colony phenotype hinted, the *spo0E* mutant demonstrated increased motility on soft agar (**Fig. 1C**), implicating *C. difficile* Spo0E in the function of a non-sporulation process.

The primary driver of motility in *C. difficile* is the sigma factor, SigD, which promotes expression of the toxins TcdA and TcdB by transcription of the toxin sigma factor, TcdR (26,27). Considering the direct link between motility and toxin regulation, we next examined toxin production in the *spo0E* mutant using a TcdA/TcdB ELISA assay. The *spo0E* mutant produced markedly greater toxin than the parent strain (**Fig. 1D**), with toxin values averaging more than 15-fold higher in the mutant. The increases in toxin and motility observed for the *spo0E* mutant strongly suggested that Spo0E represses SigD activity. The only factor that Spo0E-like proteins are known to interact with is the sporulation regulator Spo0A. However, such dramatic increases in toxin or motility are not observed for *spo0A* mutants, indicating that the effects of Spo0E on SigD-dependent regulation are independent of Spo0A, and thus, occur through an undescribed mechanism (28).

Disruption of *spo0E* increases early production of toxins and morbidity during infection.
The production of the toxins TcdA and TcdB are responsible for *C. difficile* pathogenesis; thus, an increase in toxin synthesis within the host is expected to increase virulence. To determine if

the *spo0E* mutant impacts virulence, a Syrian golden hamster model of *C. difficile* infection

(CDI) was used to examine colonization, toxin production, and overall pathogenesis. Hamsters

were infected with spores of 630Δ*erm* (WT) or the *spo0E* mutant, as described in the Methods,

and monitored for symptoms of disease. Hamsters infected with the *spo0E* mutant spores

succumbed to infection faster than WT-infected animals (**Fig. 2A**; median time to morbidity: 46.7

h for WT, 36.8 h for *spo0E*). To assess toxin production in the infected animals, fecal samples

were collected 24 h post-infection and assayed for toxin content (**Fig. 2C**), which revealed that

the *spo0E* mutant generated significantly higher toxin loads within the intestine earlier in

infection than WT. However, an analysis of toxin levels from moribund animals (**Fig. 2D**)

showed no overall increase in the toxin present between the *spo0E* mutant and parent strain,

suggesting that the maximum threshold of toxicity is reached earlier in animals infected with the

spo0E mutant. Further, examination of the *C. difficile* burden in moribund animals demonstrated

that the *spo0E* mutant was not carried at higher levels than the WT strain (**Fig. 2B**), indicating

that the increase in toxin production by the mutant was not due to greater colonization or

carriage. Together, these results corroborate the *in vitro* toxin results and indicate that the

spo0E mutant produces more toxin per bacterium *in vivo*, leading to more rapid morbidity.

Spo0E binds to regulators of sporulation, toxin, and motility. As Spo0E has not been

examined outside of sporulation, nothing is known about Spo0E interacting partners that would

facilitate motility or toxin phenotypes. To this end, we investigated the Spo0E interactome.

Using FLAG-tagged Spo0E expressed in the *spo0E* mutant, we performed co-

immunoprecipitation (co-IP) from sporulating *C. difficile* and determined proteins bound to

Spo0E by MS/MS analysis. Few proteins were enriched in the Spo0E-FLAG samples relative to

negative controls **(Table 1; Table S1; Fig. S3)**. As expected, the most enriched bound protein

was Spo0A, which suggests that *C. difficile* Spo0E directly regulates Spo0A activity, as in

Bacillus. But in addition, the regulator RstA was also bound to Spo0E and highly enriched in co-

IP samples. RstA is a multifunctional RRNPP family protein that directly represses toxin and

motility gene expression, and promotes sporulation through an unknown mechanism (9,30,31).

The binding of Spo0E and RstA strongly implies that Spo0E controls toxin and motility through

interaction with RstA, and conversely, that RstA promotes sporulation by interacting with Spo0E,

which would prevent Spo0E inactivation of Spo0A (**Fig. S4**). Lastly, the translation factor EF-4

(LepA) was also highly enriched in the Spo0E pulldown.

To complement the Spo0E co-IP, we performed Spo0A-FLAG pulldowns from

sporulating cells and found that Spo0E is highly enriched (**Table 1**, **Table S2**). This finding

further supports a model by which Spo0E influences sporulation, toxin, and motility through

interactions with both Spo0A and RstA. In addition, the phosphotransfer protein PtpC co-purified

with Spo0A, as previously characterized, and CD630_12310, a predicted site-specific

recombinase, was also highly enriched in the Spo0A pulldown.

Multiple regulatory functions of Spo0E are conserved across species. Considering the

evidence that Spo0E interfaces with multiple regulatory factors to control different physiological

processes in *C. difficile*, we questioned whether Spo0E has similar functions in other species

that were missed in prior studies. For this, we revisited the original resource for Spo0E function,

B. subtilis. B. subtilis is the model organism for endospore formation and is motile, however, it

does not produce human pathogenic toxins. As *B. subtilis spo0E* mutants already have a

verified hypersporulation phenotype, we assessed the mutant for motility. Using *B. subtilis* wild-

type and an isogenic *spo0E* deletion mutant, we examined motility on soft agar plates for 24 h

(**Fig. 3A**). The *B. subtilis spo0E* mutant consistently exhibited greater motility on soft agar,

demonstrating that the motility regulatory effects of Spo0E are conserved with *C. difficile.* In

addition, we examined motility of a *B. subtilis spo0A* mutant and a *spo0A spo0E* double mutant

to determine if the *spo0E* motility phenotype was linked to *spo0A.* The *spo0A* mutant displayed

similar motility to the parental strain, while the *spo0A spo0E* double mutant demonstrated

increased motility, similar to the *spo0E* mutant. Together, these data establish that *B. subtilis* Spo0E has a conserved motility regulatory function that is independent of its interaction with Spo0A.

Spo0E-like proteins are conserved and prevalent across phylogenies.

To understand the greater role of Spo0E, we searched for Spo0E orthologs in other species. The Spo0E family of proteins contain a signature five amino acid motif (SQELD), with invariant serine and aspartate residues (19,21–24). To identify Spo0E orthologs, we probed for the Spo0E signature motif using AlphaFold and PSI-BLAST, and filtered by proteins that were between 40 – 100 amino acids in length (*C. difficile* Spo0E is 53 amino acids in length) (**Fig. 4A**) (20,24,32,33). We then predicted the 3D structure of proteins that met these criteria using Phyre2, comparing to the known *Bacillus* Spo0E structure that is comprised of two α-helices connected by a loop (**Fig. 4B - C**) (23). The presence of Spo0E orthologs encoded in the genomes of Gram-positive and Gram-negative bacteria with and without motility and sporulation abilities (**Fig. 4A**) suggests that Spo0E-like proteins perform diverse regulatory functions that are species specific.

DISCUSSION

In this study, we identified an ortholog to the *Bacillus* Spo0E protein and investigated its role in *C. difficile* physiology and pathogenesis. We established that *C. difficile* Spo0E represses sporulation, as was observed in *Bacillus* species (8,19,22,24). In addition, we found that Spo0E represses *C. difficile* toxin production and motility, which was not recognized in prior Spo0E studies of *Bacillus*. By assessing the Spo0E interactome, we discovered interactions between Spo0E and Spo0A, as well as Spo0E and the regulator RstA. Identification of this interacting triad illuminates the molecular mechanism through which RstA promotes spore formation and Spo0E represses toxin production and motility in *C. difficile*. This mechanism supports a new

model for regulatory coordination of motility, virulence, and dormancy in *C. difficile*. The identification of Spo0E dual roles in *B. subtilis* motility and sporulation suggests broad conservation of Spo0E function as a regulator of these processes in endosporulating Firmicutes.

While our data indicate Spo0A-Spo0E and RstA-Spo0E interactions, the details of these exchanges remain to be elucidated. RstA has three apparent domains: a HTH DNA-binding domain that regulates motility and sporulation, followed by a series of tetratricopeptide (TPR) repeats that are annotated as a Spo0F-like binding domain, and a series of TPR repeats at the C-terminus that are predicted to bind quorum sensing peptides (9,30,31). Based on the predicted RstA structure and functions, it is likely that Spo0E binds to the Spo0F-like domain of RstA. Spo0E in *Bacillus* requires the second helix containing the SQELD phosphatase motif to interface with Spo0A, which may also occur in *C. difficile.* Examination of *C. difficile* Spo0A functional residues suggests that Spo0E interacts with Spo0A at conserved Spo0E-interfacing residues within the receiver domain that impact Spo0A activity (10,21). The Spo0E interface with RstA is not known.

The discovery of this mechanism introduces many questions about the regulatory role of Spo0E in other species. The interaction of Spo0E with the RRNPP regulator, RstA, suggests that Spo0E orthologs may bind to other RRNPP-family proteins. RRNPP regulators control diverse physiological processes in bacteria, including toxin expression, nutrient acquisition, biofilm formation, solventagenesis, motility, sporulation, and competence in response to binding small peptide quorum sensing signals (34–39). Many of the RRNPPs interact with response regulators or directly facilitate transcription of genes that direct the above processes (*e.g.,* Rap, Rgg, NprR, PrgX, PlcR) (37). Spo0E ortholog interactions with response regulators or RRNPPs, or both, could add a layer of regulatory control that interfaces with other physiological processes, as Spo0E does in *C. difficile.* However, the specific interactions and interfaces between RRNPP proteins and response regulators are not well conserved, and given the

divergence in Spo0E ortholog sequences, we expect similar diversity in the interactions between Spo0E and their partners in other species.

Through phylogenetic analyses, we identified Spo0E-like proteins in many Gram-positive and Gram-negative bacteria, as well as in the Archaea (**Fig 4**). The presence of Spo0E in species that do not sporulate or are non-motile, suggests the evolution of different roles for Spo0E in other systems. While the role of these Spo0E orthologs is not known, a plausible interaction in any of these systems would involve contact with a conserved partner protein, such as a response regulator.

MATERIALS AND METHODS

Bacterial strains and growth conditions

Bacterial plasmids and strains used in this study are listed in (**Table S3**). *C. difficile* was routinely grown in BHIS or BHIS supplemented with 2-5 μg ml^{-1} thiamphenicol as needed (Sigma) (40). Active *C. difficile* cultures were supplemented with 0.1% taurocholate (Sigma) and 0.2% fructose to prevent sporulation and stimulate germination as needed (40,41). *C. difficile* was grown on 70:30 agar to determine sporulation frequencies as previously described (41). *C. difficile* was grown in a 37°C anaerobic chamber (Coy) with an atmosphere consisting of 10% H_2, 5% CO_2, and 85% N_2 as previously described (42). *B. subtilis* strains were grown in LB at 37°C, supplemented with kanamycin 7 μg ml^{-1} or spectinomycin 100 μg ml^{-1} as needed. Strains of *Escherichia coli* were grown in LB at 37°C, supplemented with chloramphenicol 20 μg ml^{-1}, ampicillin 100 μg ml^{-1}, or spectinomycin 100 μg ml^{-1} as needed (43). Kanamycin 100 μg ml^{-1} was used for *B. subtilis* BS49 and *E. coli* HB101 pRK24 counterselection after conjugation with *C. difficile* (44).

Strain and plasmid construction

(**Table S3**) contains strains used in this study. (**Table S4**) contains oligonucleotides used in this study. *C. difficile* 630 strain (GenBank accession **AJP10906.1**) was used as a template for primer design and *C. difficile* 630Δ*erm* genomic DNA was used for PCR amplifications. The *spo0E* null mutant was generated by retargeting the group II intron from pCE240 to *spo0E* using the primers specified in (**Table S4**). Strain construction is outlined in (**Table S5**).

Sporulation assays

Ethanol-resistance sporulation assays were performed on 70:30 sporulation media and supplemented with 2 μg ml^{-1} thiamphenicol as previously described (9,45,46). After growth on sporulation agar for 24 hours, wildtype or *spo0E* (MC1615) cells were resuspended in BHIS liquid to an OD_{600} = 1.0. To enumerate total vegetative cells per ml^{-1}, *C. difficile* cultures were serially diluted into BHIS and plated on BHIS agar supplemented with 2 μg ml^{-1} thiamphenicol as needed. Concomitantly, 0.5 ml of resuspended cells were exposed to a mix of 0.3 ml 95% ethanol and 0.2 ml dH$_2$O for 15 minutes to kill vegetative cells. Ethanol-treated cultures were then serially diluted in 1X PBS and 0.1% taurocholate and plated onto BHIS agar with 0.1% taurocholate and 2 μg ml^{-1} thiamphenicol as needed to determine the total spores per ml. After 48 hours, sporulation frequency was calculated as the proportion of spores that germinated after ethanol treatment divided by the total number of spores and vegetative cells (9). Statistical significance was determined using a one-way ANOVA with Dunnett's multiple comparisons test in GraphPad Prism v9.0.

***In vitro* toxin ELISA**

Cultures of wildtype or *spo0E C. difficile* were grown overnight in TY media, supplemented with 2 μg ml^{-1} thiamphenicol as needed. Total levels of both TcdA and TcdB toxins were enumerated using a *C. difficile* ELISA kit (tgcBIOMICS). Toxin ELISAs were performed according to manufacturer's instructions (tgcBIOMICS). Samples were pelleted, and 1 ml supernatant was collected, then diluted 1:10 using Dilution Buffer, and 100 μl of samples were added in duplicate

to a flat-bottom 96 well plate. 50 μl of anti-TcdA/TcdB—HRP was then added to each well, and

the plate was incubated at 37°C for 1 hour. Following washing with Wash Buffer, 100 μl

Substrate was added to each well and incubated for 10 minutes at room temperature, then 50 μl

Stop Solution was added to each well. Measurements for 450 nm and 620 nm were made using

a BioTek plate reader. A two-tailed Student's t-test was performed to determine statistical

significance using GraphPad Prism.

In vivo hamster infections

Male and female Syrian golden hamsters (*Mesocricetus auratus*) were purchased from Charles

River Laboratories and housed in sterile, individual cages in an animal biosafety level 2 facility

in the Emory University Division of Animal Resources as previously described (47). Hamsters

were fed a standard rodent diet and had unlimited access to water. Seven days prior to

challenge with *C. difficile* spores, hamsters were treated with one dose of clindamycin (30 mg

kg^{-1} body weight) by oral gavage to initiate *C. difficile* infection. Hamsters were inoculated with

5,000 spores from either wildtype or *spo0E* backgrounds and monitored for progression of

disease symptoms (lethargy, weight loss, wet tail, diarrhea). Spores were stored in 1X PBS

solution with 0.1% BSA as previously described (48,49). Negative control hamsters were given

clindamycin to induce susceptibility to disease but were not treated with *C. difficile* spores. Prior

to infection, spores were heated for 20 minutes and allowed to cool to room temperature. After

administration of spores, hamsters were weighed at least daily, and fecal samples were

collected daily to determine total *C. difficile* CFU, and an additional fecal sample from each

hamster was collected 24 hours after infection for *in vivo* toxin ELISAs. Hamsters were

considered moribund if they had lost 15% of their highest weight, or presented advanced

symptoms of lethargy, wet tail, or diarrhea. Hamsters that met these criteria were euthanized by

CO_2 asphyxiation, followed by thoracotomy. At the time of death, animals were necropsied, and

cecal contents were collected and stored in a 1:1 ethanol-acetone solution, and an additional

100 μl of cecal sample was taken from each hamster for toxin ELISAs. Both fecal and cecal contents were enumerated by plating samples on TCCFA agar (50,51). Differences in *C. difficile* CFU recovered in cecal and fecal contents were determined by a Student's two-tailed t-test, and differences in hamster survival time between 630Δ*erm* or *spo0E* infection were analyzed by log-rank test in GraphPad Prism.

In vivo toxin ELISA

To quantify toxin production *in vivo*, fecal samples were collected from hamsters 24 hours after infection, and 100 μl cecal contents were recovered immediately after euthanization and stored at 4°C, and total levls of TcdA and TcdB toxin were enumerated using the tgcBIOMICS toxin ELISA kit. Fecal samples were weighed to calculate toxin levels per gram of feces, then resuspended in 450 μl Dilution Buffer. Cecal contents were diluted either 1:10 or 1:40 in Dilution Buffer. Toxin was quantified for both the fecal and cecal samples as described above. A two-tailed Student's t-test was performed to determine statistical significance in toxin levels between both wildtype and *spo0E* fecal samples and cecal samples using GraphPad Prism.

C. difficile motility assays

Cultures of wildtype and *spo0E C. difficile* were grown overnight in BHIS liquid supplemented with 0.1% taurocholate and 0.2% fructose as described above. Cultures were then diluted in BHIS and grown to an OD_{600} = 0.5, and 2 μl culture was injected into the center of ½ BHI plates with 0.3% agar concentration in duplicate. The swimming diameter was measured every 24 hours for a total of five days and replicate values were averaged. A two-tailed Student's t-test was performed to determine statistical significance using GraphPad Prism.

B. subtilis motility assays

Cultures of *B. subtilis* were grown overnight in LB broth and diluted to an OD_{600} = 0.5, then 2 μl of culture was injected into 0.5x BHI plates with 0.3% agar in technical duplicate. The swimming diameter was measured after 24 hours. A one-way ANOVA with Dunnett's multiple comparisons

test was used to determine statistical significance relative to the parental control in GraphPad

Prism.

Co-immunoprecipitation

C. difficile cultures of wildtype vector control (MC324), Spo0E-3xFLAG (MC1968), or Spo0A-

3xFLAG (MC1003) were grown overnight in BHIS broth supplemented with 2 μg ml^{-1}

thiamphenicol and diluted to an OD$_{600}$ = 0.5, then plated on 70:30 agar supplemented with 2 μg

ml^{-1} thiamphenicol. After 12 hours of growth, cells were harvested from plates, pelleted, and

washed with 1X PBS and stored at -80°C. Cells were then thawed on ice and resuspended in

mBS/THES buffer (50 mM HEPES, 25 mM CaCl$_2$, 250 mM KCl, 50 mM Tris-HCl pH 7.5, 2.5 mM

EDTA, 140 mM NaCl, 0.7% Protease Inhibitor Cocktail II [Sigma], 0.1% Phosphatase Inhibitor

Cocktail II [Sigma], and 1% glycerol) supplemented with DNase I (New England Biosciences)

and RNase A (Thermo Fisher). Cells were lysed by a freeze-thaw consisting of incubating

samples for 3 minutes in a dry ice-ethanol bath and 2 minutes in 37°C water, 25 times, then

pelleted at max speed at 4°C and supernatants were collected. Anti-FLAG beads (Sigma) were

equilibrated and then washed in TBS buffer, then subsequently washed in mBS/THES buffer.

Sample supernatants were then incubated with washed anti-FLAG beads on a mechanical rotor

for 4 hours at room temperature. Beads were then collected in a 1.5 mL Protein LoBind tube

(Eppendorf) and supernatants were discarded. Beads were then washed in mBS/THES buffer,

transferred to a new 1.5 mL Protein LoBind tube, washed with 1X PBS, then resuspended in 1X

PBS and stored at -20°C.

Western blotting

Western blotting was performed to confirm that FLAG-tagged protein was present only in the

test Spo0E-3xFLAG or Spo0A-3xFLAG pulldown samples. Samples of wildtype, Spo0E-

3xFLAG, and Spo0A-3xFLAG collected during co-immunoprecipitation were suspended in 1X

sample buffer (10% glycerol, 62.5 mM Upper Tris, 3% SDS, 5 mM PMSF, and 5% 2-

mercaptoethanol) then separated by SDS-PAGE using pre-cast TGX 4-20% gradient gels (BioRad), and protein was then transferred to a 0.45 μm nitrocellulose membrane (BioRad). Spo0A and Spo0E were detected using an anti-FLAG antibody (Thermo Fisher). Goat anti-mouse IgG Alexa Fluoro 488 (Invitrogen) was used as a secondary antibody, and western blots were resolved using a BioRad ChemiDoc MP System.

Silver staining

To visualize total protein in the pulldowns, silver staining was performed using the Pierce Silver Staining Kit according to manufacturer's instructions (Thermo Fisher) on samples collected during co-immunoprecipitation. Samples were suspended in 1X sample buffer and separated by SDS-PAGE using pre-cast TGX 4-20% gradient gels (BioRad). After separation, gels were washed in ultrapure water, then fixed in a 30% ethanol:10% acetic acid solution. Gels were sensitized using the Pierce Sensitizer Working Solution, then stained using the Pierce Stain Working Solution. Gels were washed with ultrapure water, and protein bands were developed following incubation in the Pierce Developer Working Solution. After stopping developing bands using 5% acetic acid, protein bands were imaged using a BioRad ChemiDoc MP System.

On-bead digestion for LC-MS/MS:

For on-bead digestion, a published protocol was followed (52). To the bead, digestion buffer (50 mM NH$_4$HCO$_3$) was added, and the mixture was then treated with 1 mM dithiothreitol (DTT) at room temperature for 30 minutes, followed by 5 mM iodoacetimide (IAA) at room temperature for 30 minutes in the dark. Proteins were digested with 2 μg of lysyl endopeptidase (Wako) at room temperature for overnight and were further digested overnight with 2 μg trypsin (Promega) at room temperature. Resulting peptides were desalted with HLB column (Waters) and were dried under vacuum.

LC-MS/MS

The data acquisition by LC-MS/MS was adapted from a published procedure (53). Derived peptides were resuspended in the loading buffer (0.1% trifluoroacetic acid, TFA) and were separated on a Water's Charged Surface Hybrid (CSH) column (150 μm internal diameter (ID) x 15 cm; particle size: 1.7 μm). The samples were run on an EVOSEP liquid chromatography system using the 15 samples per day preset gradient (88 min) and were monitored on a Q-Exactive Plus Hybrid Quadrupole-Orbitrap Mass Spectrometer (Thermo Fisher). The mass spectrometer cycle was programmed to collect one full MS scan followed by 20 data dependent MS/MS scans. The MS scans (400-1600 m/z range, 3 x 10^6 AGC target, 100 ms maximum ion time) were collected at a resolution of 70,000 at m/z 200 in profile mode. The HCD MS/MS spectra (1.6 m/z isolation width, 28% collision energy, 1 x 10^5 AGC target, 100 ms maximum ion time) were acquired at a resolution of 17,500 at m/z 200. Dynamic exclusion was set to exclude previously sequenced precursor ions for 30 seconds. Precursor ions with +1, and +7, +8 or higher charge states were excluded from sequencing.

MaxQuant

Label-free quantification analysis of protein pulldown samples was adapted from a published procedure (53). Spectra were searched using the search engine Andromeda, integrated into MaxQuant, against *C.difficile* Uniprot database (3,969 target sequences). Methionine oxidation (+15.9949 Da), asparagine and glutamine deamidation (+0.9840 Da), and protein N-terminal acetylation (+42.0106 Da) were variable modifications (up to 5 allowed per peptide); cysteine was assigned as a fixed carbamidomethyl modification (+57.0215 Da). Only fully tryptic peptides were considered with up to 2 missed cleavages in the database search. A precursor mass tolerance of ±20 ppm was applied prior to mass accuracy calibration and ±4.5 ppm after internal MaxQuant calibration. Other search settings included a maximum peptide mass of 6,000 Da, a minimum peptide length of 6 residues, 0.05 Da tolerance for orbitrap and 0.6 Da tolerance for

ion trap MS/MS scans. The false discovery rate (FDR) for peptide spectral matches, proteins, and site decoy fraction were all set to 1 percent. Quantification settings were as follows: re-quantify with a second peak finding attempt after protein identification has completed; match MS1 peaks between runs; a 0.7 min retention time match window was used after an alignment function was found with a 20-minute RT search space. Quantitation of proteins was performed using summed peptide intensities given by MaxQuant. The quantitation method only considered razor plus unique peptides for protein level quantitation.

LC-MS/MS data analysis

To determine statistical significance between experimental (Spo0A-FLAG, Spo0E-FLAG) and negative control groups, Perseus software (Version 1.6.15.0) was used to analyze Intensity data (54). Intensity values were $\log_2$ transformed, and data was filtered to remove: contaminants, proteins only identified by site, and reverse hits. Imputation of data was performed based on normal distribution with downshift of 1.8 and width of 0.3. A two-way Student's *t*-test was performed to determine significantly enriched proteins in the experimental group (Spo0A-3xFLAG or Spo0E-3xFLAG) and negative control. P-values were then adjusted with permutation based false discovery rate (FDR) for proteins that were identified in at least three of four replicates. Scatter plots were generated in Perseus. Proteins enriched with a P-value ≤ 0.05 were considered statistically significant. Proteins were additionally filtered by a cutoff of 1.2 $\log_2$ transformed Intensity ratio relative to the negative control.

DNA extraction and hybrid sequencing analysis

Genomic DNA was extracted from *spo0E* as previously described (55). Library prep and sequencing for both Illumina and Oxford Nanopore Technologies (ONT) samples was performed by SeqCenter (seqcenter.com). Whole genome sequencing variant calling was performed using paired-end reads generated by Illumina sequencing (2x151bp) on the

NextSeq2000 platform. Reads were trimmed using the BBDuk plug-in in Geneious Prime

v2022.2.2, then mapped to the reference genome (**NC_009089.1**) (https://www.geneious.com).

The Bowtie2 plugin was used to search for the presence of SNPs or InDels under default

settings with a minimum variant frequency set at 0.95, and no additional variants were identified

(56). A *de novo* assembly of Illumina and ONT reads (MinION) was then performed to confirm

the genomic location of the TargeTron solely within the coding region of *spo0E*. Assembly was

performed using Unicycler under default settings (57). The assembled genome was annotated

to the reference genom**e** using Geneious Prime. Circos plot was generated using PATRIC web

resources (58,59). Genome sequence files were deposited to the NCBI Sequence Read Archive

(SRA) BioProject PRJNA896704 under accession numbers SRX18115370 and SRX18115371.

Phylogenetic comparisons

Putative Spo0E orthologs were identified using PSI-BLAST to probe for the conserved Spo0E

motif, and AlphaFold to search for predicted Spo0E-like proteins (32,33). Protein alignments

were performed using ClustalW under default settings (60). An unrooted Neighbor-Joining tree

using full-length Spo0E and Spo0E-like protein sequences was created using MEGA11 (61).

Predicted 3D protein structures were generated using Phyre2, and the resultant output PDB

files were edited using PyMOL (The PyMOL Molecular Graphics System, Version 2.4.0

Schrödinger, LLC) (62). Protein accession numbers of Spo0E-like proteins used in the

phylogenetic analysis are as follows: *C. difficile* (**WP_009891746.1**), *Intestinibacter bartlettii*

(**WP_216572026.1**), *Paeniclostridium sordellii* (**WP_021126610.1**), *Bacillus subtilis*

(**NP_389247.1**), *Streptococcus pneumoniae* (**CJR48991.1**), *Staphylococcus epidermidis*

(**WP_145378230.1**), *Clostridium botulinum* (**WP_106898918.1**), *Clostridium perfringens*

(**UBL05073.1**), *Pseudomonas amygdali* (**WP_016766164.1**), *Escherichia coli*

(**WP_224654603.1**), *Vibrio vulnificus* (**TDL93146.1**), *Mycobacterium tuberculosis*

(**WP_079178562.1**), *Methanosaeta* (**OPY55450**), *Chlamydia trachomatis* (**CRH64375.1**),

Bacillus anthracis (**PFB78764.1**), *Bacillus cereus* (**AUZ26151.1**), *Listeria monocytogenes* (**ECO1678074.1**), *Mycobacteroides abscessus* (**SLB39125.1**), and *Rhodococcus qingshengii* (**SLB39125.1**).

Tables

Table 1. Enriched factors identified by co-immunoprecipitation.

co-IP Target	Bound Proteins	Log$_2$ Intensity/control	-Log P-value
Spo0E-FLAG	Spo0A	1.4	8.0
	LepA	1.3	7.0
	Spo0E	1.7	6.7
	RstA	1.3	5.5
Spo0A-FLAG	PtpC	1.5	5.5
	Spo0A	1.3	5.5
	Spo0E	1.5	5.3
	CD630_12310	1.2	5.2

Table S1. Filtered proteins identified in Spo0E-FLAG co-immunoprecipitation

Gene Locus	-Log P value[a]	Log$_2$ Intensity/control[b]
CD630_12140 (Spo0A)	8.0	1.4
CD630_24670 (LepA)	7.0	1.3
CD630_32710 (Spo0E)	6.7	1.7
CD630_36680 (RstA)	5.5	1.3
CD630_21730	5.4	1.4
CD630_20070	5.3	1.4
CD630_29560	5.2	1.3
CD630_35120	5.0	1.4
CD630_21230	4.5	1.3
CD630_03400	4.4	1.2
CD630_29800	4.2	1.2
CD630_00511	4.2	1.9
CD630_08210	4.0	1.3
CD630_22640	3.7	1.2
CD630_26460	3.2	1.3
CD630_34700	3.1	1.2
CD630_22090	2.6	1.4
CD630_03410	2.6	1.2
CD630_05590	2.1	1.2

[a]Negative log of *t*-test between average protein intensities of Spo0E-FLAG and negative control pulldown

[b]Ratio of averaged log$_2$ transformed intensities between Spo0E-FLAG and negative control pulldown

Table S2. Filtered proteins identified in Spo0A-FLAG co-immunoprecipitation

Gene locus	-Log P value[a]	Log$_2$ Intensity/control[b]
CD630_15790 (PtpC)	5.5	1.5
CD630_12140 (Spo0A)	5.5	1.3
CD630_32710 (Spo0E)	5.3	1.5
CD630_12310	5.2	1.2
CD630_03410	4.9	1.2
CD630_35230	4.8	1.3
CD630_24040	4.7	1.2
CD630_21230	4.6	1.3
CD630_P10	3.8	1.4
CD630_20070	3.8	1.4
CD630_19320	3.8	1.2
CD630_13060	3.7	1.3
CD630_25220	3.6	1.3
CD630_23980	3.6	1.3
CD630_05230	3.5	1.2
CD630_00200	3.3	1.2
CD630_01500	3.2	1.2
CD630_35940	3.0	1.2
CD630_18490	2.9	1.3
CD630_35460	2.9	1.2
CD630_19670	2.6	1.2
CD630_19640	2.4	1.2
CD630_21800	2.4	1.2
CD630_12470	2.4	1.2
CD630_19660	1.8	1.2

[a]Negative log of *t*-test between average protein intensities of Spo0A-FLAG and negative control pulldown

[b]Ratio of averaged log$_2$ transformed intensities between Spo0A-FLAG and negative control pulldown

Table S3. Bacterial Strains and plasmids

Plasmid or Strain	Relevant genotype or features	Source, construction or reference
Strains		
E. coli		
HB101	F- *mcrB mrr hsdS20*(r$_B^-$ m$_B^-$) *recA13 leuB6 ara-14 proA2 lacY1 galK2 xyl-5 mtl-1 rpsL20*	B. Dupuy
C. difficile		
630Δ*erm*	Erm^S derivative of strain 630	(63)
RT1075	630Δ*erm sigD*::*erm*	(64)
MC324	630Δ*erm* pMC123	(47)
MC855	630Δ*erm spo0A*::*erm* pMC123	(10)
MC1003	630Δ*erm spo0A*::*erm* Spo0A-3xFLAG	
MC1615	630Δ*erm spo0E*::*erm*	This study
MC1698	630Δ*erm spo0E*::*erm* pMC980	This study
MC1699	630Δ*erm spo0E*::*erm* pMC123	This study
MC1968	630Δ*erm spo0E*::*erm* pMC1093	This study
B. subtilis		
IAI	Wildtype *B. subtilis* str. 168	(65)
MC2235	IAIΔ*spo0E sacA*::*cat*	This study
MC2260	IAIΔ*spo0A*::*kan* Δ*spo0E*	This study
MC2261	IAIΔ*spo0A*::*kan*	This study
Plasmids		
pRK24	Tra$^+$, Mob$^+$; *bla, tet*	
pUC19	Cloning vector; *bla*	(75)
pCE240	*C. difficile* TargeTron® construct based on pJIR750ai (group II intron, *ermB::*RAM, *ltrA*); *catP*	C. Ellermeier
pMSR	pMTL-SC7315	J. Peltier
pMC123	*E. coli-C. difficile* shuttle vector; *bla, catP*	(66)
pMC228	pMC123 + *spo0E* TT7 derived from pMC232	This study
pMC232	pCE240 + *spo0E* TT7	This study
pMC980	pMC123 *CD3272-spo0E* complement	This study
pMC1093	pMC123 *spo0E*-3xFLAG	This study

Table S4. Oligonucleotides

Primer	Sequence (5'→3')[a]	Use/locus tag/reference
oMC513	GC<u>GGATCC</u>GACAAAATATAATATTGTTTGATAAAATG	Forward primer to amplify *CD630_32710* to confirm TargeTron insertion
oMC514	GAC<u>GGATCC</u>CTGTGGGCTATTTGCTTAGG	Reverse primer to amplify *CD630_32710* to confirm TargeTron insertion
oMC515	AAAAGCTTTTGCAACCCACGTCGATCGTGAA-AACTCTTCTTGA-GTGCGCCCAGATAGGGTG	*CD630_32710* IBS 75as to target TargeTron to *spo0E*
oMC516	CAGATTGTACAAATGTGGTGATAACAGATAAGTC-TCTTGAAA-TAACTTACCTTTCTTTGT	*CD630_32710* EBS1 75as to target TargeTron to *spo0E*
oMC517	CGCAAGTTTCTAATTTCGGTT-GAGTT-TCGATAGAGGAAAGTGTCT	*CD630_32710* EBS2 75as to target TargeTron to *spo0E*
oMC2589	AG<u>GGATCC</u>ATCACTAAAATTGTAACAAGTATGATAC	Forward primer 178 bp upstream *CD630_32720* to create *CD630_32720-CD630_CD32710* complement
oMC2590	CAG<u>GAATTC</u>ACAGATAATTTACACATCAGAAATAC	Reverse primer 111 bp downstream *CD630_32710* to create *CD630_32720-CD630_CD32710* complement

[a]Restriction sites underlined

Table S5. Cloning and vector construction details

pMC228: A (5.48 kb) TargeTron insert derived from pMC232 was subcloned into pMC123 using SphI and SnaBI sites.

pMC232: A (403 bp) TargeTron insert was cloned into pMC232 using primers oMC515, oMC516, and oMC517 using (BsrgI and HindIII sites).

pMC980: A 963 bp product containing full-length operon *CD630_32720-spo0E* to complement the *spo0E* mutant was generated using primers oMC2589 and oMC2590 and cloned into pMC123 using BamHI and EcoRI sites.

pMC1093: A 683 bp fragment containing *spo0E* with a C-terminal 3xFLAG tag driven by the *spo0E* native promoter was synthesized by Genscript and cloned into pMC123 using BamHI and EcoRI sites.

Figures
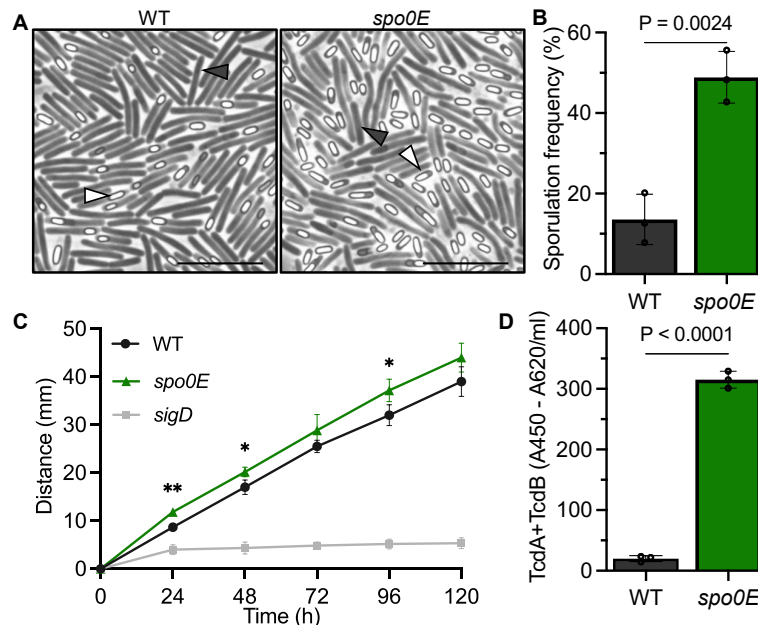
Fig 1. Spo0E represses sporulation, motility, and toxin production in *C. difficile.* A) Representative phase-contrast microscopy and **B)** sporulation frequencies of strain 630Δ*erm* (WT) and *spo0E* mutant (MC1615), grown on sporulation agar for 24 h. White triangles indicate phase bright spores, and dark triangles indicate vegetative cells. Scale bar: 10 µm **C)** Swimming motility of 630Δ*erm* (WT), the *spo0E* mutant (MC1615), and the non-motile *sigD* mutant (RT1075; negative control). Active cultures were injected into soft agar and swim diameters measured daily for five days. **D)** Quantification of TcdA and TcdB from supernatants of 630Δ*erm* (WT), the *spo0E* mutant (MC1615) grown in TY for 24 h. The means and SD of at least three independent experiments are shown unpaired *t* test was performed for B-D; *P = <0.05, **P = <0.01.
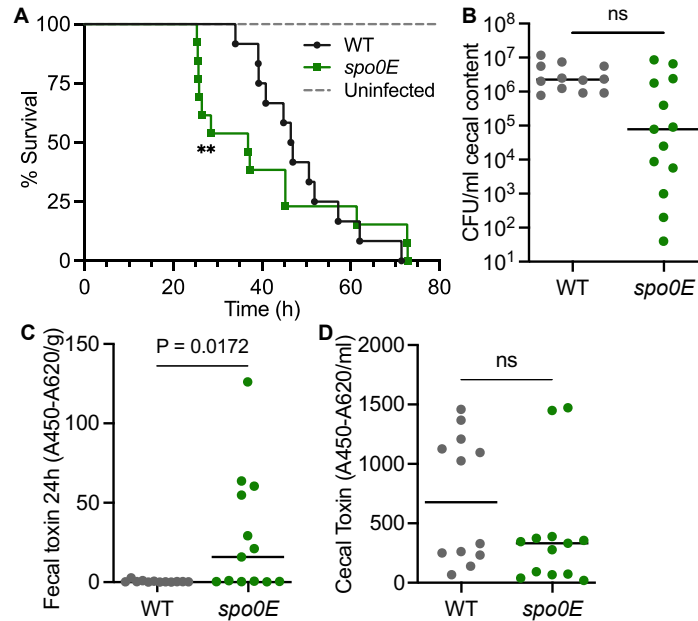
Fig 2. Disruption of *spo0E* increases morbidity and early production of toxins during infection. A) Kaplan-Meier survival curve representing the results from two independent experiments using Syrian golden hamsters inoculated with 5000 spores of *C. difficile* strain 630Δ*erm* (WT, n = 12) or *spo0E* mutant (MC1615, n = 13). Mean times to morbidity: WT, 48.7 ± 10.7 h; *spo0E*, 40.7 ± 17.8 h. **P < 0.001, Log-rank test. **B)** Total *C. difficile* CFU/ml of cecal content recovered post-mortem (ns = not significant; unpaired *t* test). ELISA quantification of TcdA and TcdB toxin per **C)** gram of fecal sample collected 24 h post-infection or **D)** per ml of cecal content collected post-mortem. Mid-line indicates median toxin values; unpaired *t* test.
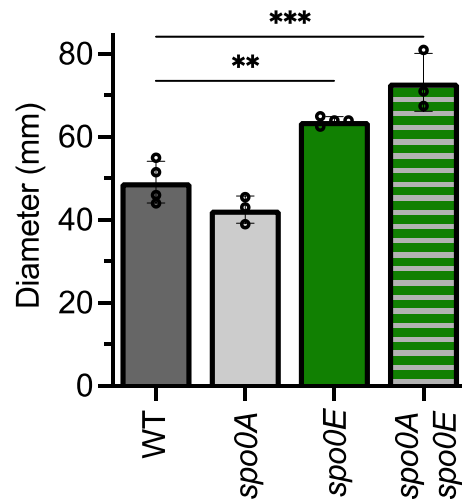
Fig 3. Spo0E repression of motility is conserved. Swimming motility of *B. subtilis* IAI (WT), *spo0A* (MC2261), *spo0E* (MC2235), and the double mutant *spo0A spo0E* (MC2260). Active cultures were injected into soft agar and swim diameters measured after 24 h. The means and SD of at least three independent experiments are shown. A one-way ANOVA with Dunnett's multiple comparisons test was performed; ***P* = <0.01, ****P* = <0.005.
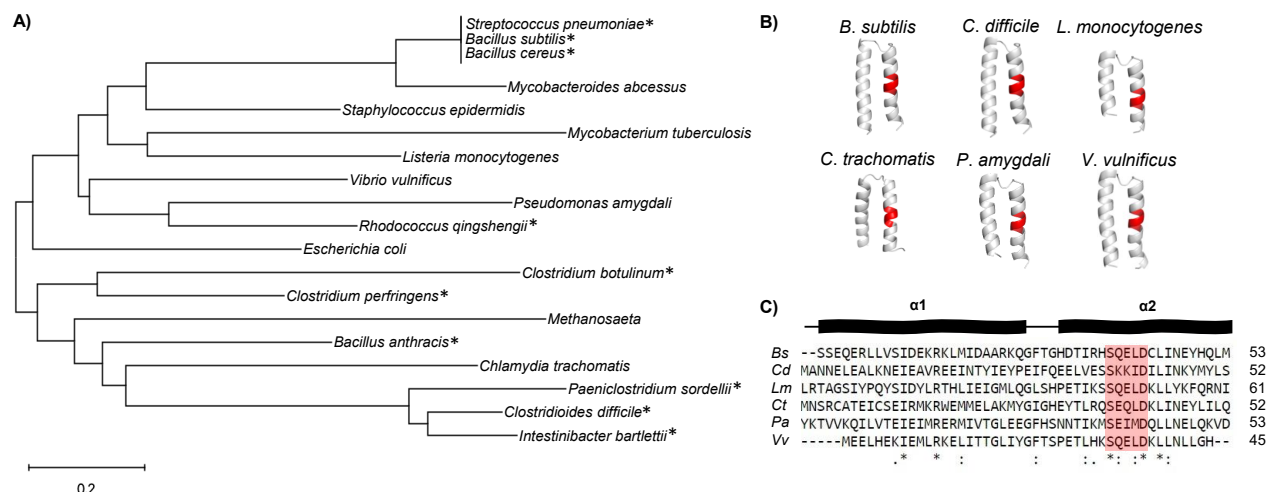
Figure 4. Spo0E-like proteins are conserved and prevalent in Gram-positive and Gram-negative bacteria. A) Unrooted neighbor-joining tree based on the full amino acid sequence of Spo0E and Spo0E-like proteins. Spore-forming species denoted with an asterisk (*). Tree generated using MEGA 11. **B)** The predicted Spo0E 3D structures generated with Phyre2 from representative Gram-positive and Gram-negative species. The residues comprising the signature Spo0E motif (SQELD) are colored red in each structure. Structures were edited in PyMOL (The PyMOL Molecular Graphics System, Version 2.4.0 Schrödinger, LLC). **C)** Multiple sequence alignment of Spo0E and Spo0E-like proteins overlayed against *B. subtilis* Spo0E secondary structure determined by AlphaFold and consisting of two α-helices. Spo0E motif residues are shaded red. Multiple sequence alignment performed using ClustalW.
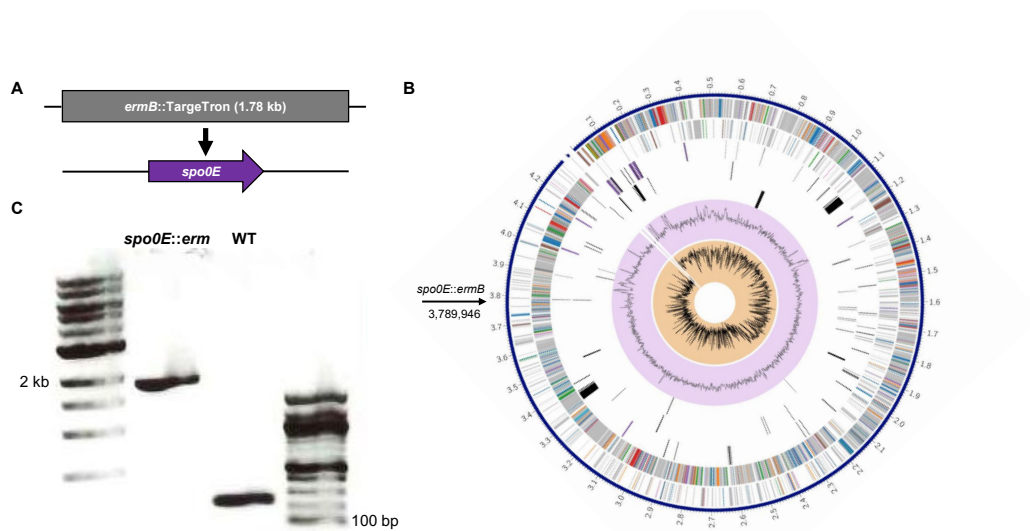
Fig S1. Construction and confirmation of the *spo0E* mutant. A) The retargeted group II intron (TargeTron) conferring erythromycin resistance (*ermB*) was inserted 59 bp into the coding region of *spo0E*. **B)** Circos plot of *de novo* assembly of the *spo0E* mutant genome using Illumina and Nanopore reads to confirm the TargeTron inserted solely into the *spo0E* locus. Reads were assembled into two contigs (4.29 Mb genome and 7.8 kb endogenous plasmid, respectively) using Unicycler and the assembly was annotated using Geneious Prime v2022.2.2. Circos plot generated using PATRIC web resources. Dashes/lines from outermost to innermost ring are: contigs with genomic position, (+) strand CDS, (-) strand CDS, RNA CDS, predicted antimicrobial resistance genes, predicted virulence factors, GC content, and GC skew, respectively. **C)** PCR confirmation of successful integration of the 1,781 bp TargeTron into *spo0E*.
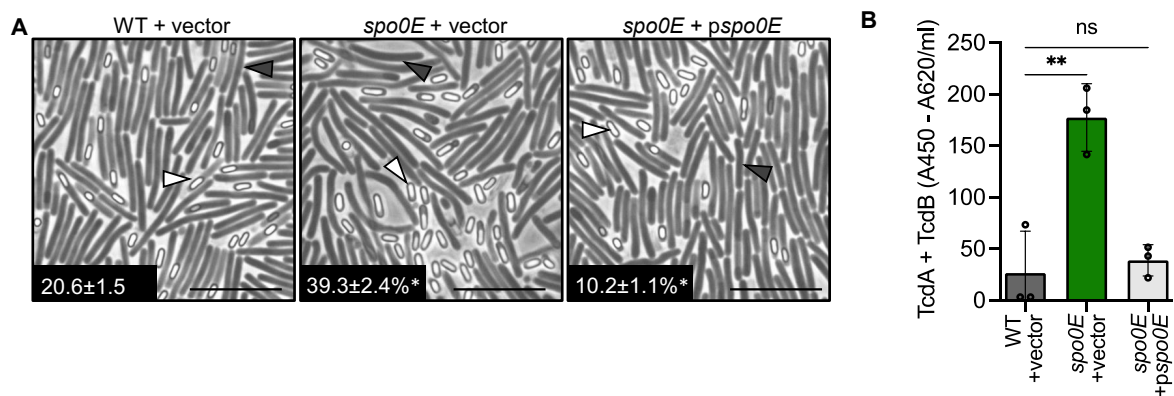
Fig S2. *spo0E* phenotypes are complemented with reintroduction of *spo0E*. A)

Representative phase-contrast microscopy and sporulation frequencies of strain 630Δ*erm* +

pMC123 (MC324), *spo0E* + pMC123 (MC1699), and complemented mutant *spo0E* + p*spo0E*

(MC1698) grown on sporulation agar supplemented with 2 μg ml^{-1} thiamphenicol for 24 h. n=4

White triangles indicate phase bright spores, and dark triangles indicate vegetative cells. Scale

bar: 10 μm **B)** Quantification of TcdA and TcdB from supernatants of strain 630Δ*erm* + pMC123

(MC324), *spo0E* + pMC123 (MC1699), and complemented mutant *spo0E* + p*spo0E* (MC1698)

in TY supplemented with 2 μg ml^{-1} thiamphenicol for 24 h. The means and SD of at least three

independent experiments are shown and one-way ANOVA with Dunnett's multiple comparisons

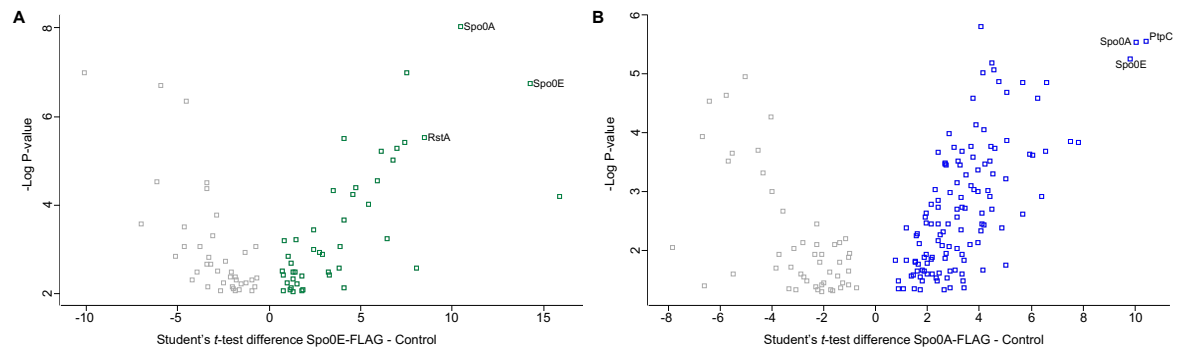test was performed for B-D; *P = <0.05, **P = <0.01.

Fig. S3. Spo0E co-purifies with regulators of sporulation, toxin, and motility. A) Scatter plot of enriched proteins identified in the Spo0E pulldown comparing mass spec profiles of Spo0E-FLAG (MC1968, green) and vector control (MC324, gray) and **B)** Spo0A pulldown comparing mass spec profiles of Spo0A-FLAG (MC1003, blue) and vector control (MC324, gray). P ≤ 0.05. Scatter plots generated using Perseus Version 1.6.15.0.

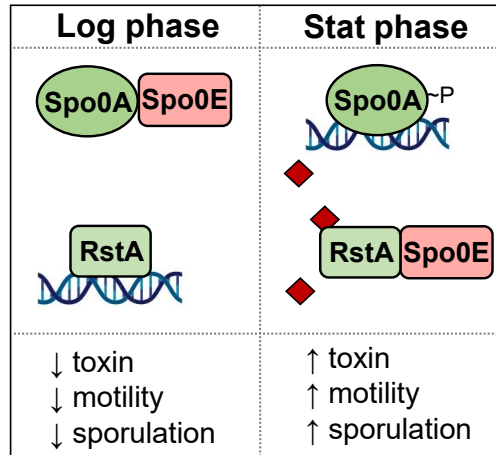| Log phase	Stat phase
↓ toxin ↓ motility ↓ sporulation	↑ toxin ↑ motility ↑ sporulation

Fig. S4. Model of Spo0E influence on sporulation initiation in *C. difficile*. During exponential growth, RstA binds DNA and represses expression of genes involved in toxin and motility (P*flgB*, P*tcdR*, P*tcdA*, P*tcdB*), while Spo0E binds Spo0A, preventing Spo0A activation and sporulation. At the transition to stationary phase, RstA is predicted to bind a quorum sensing peptide (◆), resulting in derepression of toxin and motility gene, and allowing for interaction with Spo0E. RstA-QS is then able to bind Spo0E, allowing for Spo0A phosphorylation and initiation of sporulation.

REFERENCES

1. Deakin LJ, Clare S, Fagan RP, Dawson LF, Pickard DJ, West MR, et al. The *Clostridium difficile spo0A* gene is a persistence and transmission factor. Infect Immun. 2012 Aug;80(8):2704–11.

2. Ferrari FA, Trach K, LeCoq D, Spence J, Ferrari E, Hoch JA. Characterization of the *spo0A* locus and its deduced product. Proc Natl Acad Sci U A. 1985 May;82(9):2647–51.

3. Perego M, Cole SP, Burbulys D, Trach K, Hoch JA. Characterization of the gene for a protein kinase which phosphorylates the sporulation-regulatory proteins Spo0A and Spo0F of *Bacillus subtilis*. J Bacteriol. 1989 Nov;171(11):6187–96.

4. Perego M, Spiegelman GB, Hoch JA. Structure of the gene for the transition state regulator, abrB: regulator synthesis is controlled by the spo0A sporulation gene in Bacillus subtilis. Mol Microbiol. 1988 Nov;2(6):689–99.

5. Burbulys D, Trach KA, Hoch JA. Initiation of sporulation in *B. subtilis* is controlled by a multicomponent phosphorelay. Cell. 1991 Feb 8;64(3):545–52.

6. Strauch MA, Wu JJ, Jonas RH, Hoch JA. A positive feedback loop controls transcription of the spoOF gene, a component of the sporulation phosphorelay in Bacillus subtilis. Mol Microbiol. 1993 Mar;7(6):967–74.

7. Trach K, Burbulys D, Strauch M, Wu JJ, Dhillon N, Jonas R, et al. Control of the initiation of sporulation in *Bacillus subtilis* by a phosphorelay. Res Microbiol. 1991 Oct;142(7–8):815–23.

8. Perego M, Hoch JA. Negative regulation of Bacillus subtilis sporulation by the spo0E gene product. J Bacteriol. 1991 Apr;173(8):2514–20.

9. Edwards AN, Tamayo R, McBride SM. A novel regulator controls Clostridium difficile sporulation, motility and toxin production. Mol Microbiol. 2016 Jun;100(6):954–71.

10. DiCandia MA, Edwards AN, Jones JB, Swaim GL, Mills BD, McBride SM. Identification of functional Spo0A residues critical for sporulation in *Clostridioides difficile* [Internet]. Microbiology; 2022 Feb [cited 2022 Feb 9]. Available from: http://biorxiv.org/lookup/doi/10.1101/2022.02.07.479450

11. Edwards AN, Wetzel D, DiCandia MA, McBride SM. Three orphan histidine kinases inhibit *Clostridioides difficile* sporulation [Internet]. Microbiology; 2021 Nov [cited 2021 Dec 1]. Available from: http://biorxiv.org/lookup/doi/10.1101/2021.11.18.469199

12. Worner K, Szurmant H, Chiang C, Hoch JA. Phosphorylation and functional analysis of the sporulation initiation factor Spo0A from Clostridium botulinum. Mol Microbiol. 2006 Feb;59(3):1000–12.

13. Mearls EB, Lynd LR. The identification of four histidine kinases that influence sporulation in Clostridium thermocellum. Anaerobe. 2014 Aug;28:109–19.

14. Steiner E, Dago AE, Young DI, Heap JT, Minton NP, Hoch JA, et al. Multiple orphan histidine kinases interact directly with Spo0A to control the initiation of endospore formation in Clostridium acetobutylicum. Mol Microbiol. 2011 May;80(3):641–54.

15. Freedman JC, Li J, Mi E, McClane BA. Identification of an Important Orphan Histidine Kinase for the Initiation of Sporulation and Enterotoxin Production by Clostridium perfringens Type F Strain SM101. MBio. 2019 Jan 22;10(1).

16. Rosenbusch KE, Bakker D, Kuijper EJ, Smits WK. *C. difficile* 630Delta*erm* Spo0A regulates sporulation, but does not contribute to toxin production, by direct high-affinity binding to target DNA. PLoS One. 2012;7(10):e48608.

17. Strauch MA, Hoch JA. Signal transduction in Bacillus subtilis sporulation. Curr Opin Genet Dev. 1993 Apr;3(2):203–12.

18. Reizer J, Reizer A, Perego M, Saier MH. Characterization of a family of bacterial response regulator aspartyl-phosphate (RAP) phosphatases. Microb Comp Genomics. 1997;2(2):103–11.

19. Ohlsen KL, Grimsley JK, Hoch JA. Deactivation of the sporulation transcription factor Spo0A by the Spo0E protein phosphatase. Proc Natl Acad Sci. 1994 Mar 1;91(5):1756–60.

20. Perego M. A new family of aspartyl phosphate phosphatases targeting the sporulation transcription factor Spo0A of Bacillus subtilis. Mol Microbiol. 2001 Oct;42(1):133–43.

21. Stephenson SJ, Perego M. Interaction surface of the Spo0A response regulator with the Spo0E phosphatase: Spo0A interaction surface with Spo0E. Mol Microbiol. 2002 Jun 18;44(6):1455–67.

22. Bongiorni C, Stoessel R, Perego M. Negative Regulation of Bacillus anthracis Sporulation by the Spo0E Family of Phosphatases. J Bacteriol. 2007 Apr 1;189(7):2637–45.

23. Grenha R, Rzechorzek NJ, Brannigan JA, de Jong RN, Ab E, Diercks T, et al. Structural characterization of Spo0E-like protein-aspartic acid phosphatases that regulate sporulation in bacilli. J Biol Chem. 2006 Dec 8;281(49):37993–8003.

24. Dubey GP, Narayan A, Mattoo AR, Singh GP, Kurupati RK, Zaman MohdS, et al. Comparative genomic study of spo0E family genes and elucidation of the role of Spo0E in Bacillus anthracis. Arch Microbiol. 2009 Mar;191(3):241–53.

25. Perego M, Hoch JA. Isolation and sequence of the spoOE gene: its role in initiation of sporulation in Bacillus subtills. Mol Microbiol. 1987 Nov;1(3):125–32.

26. McKee RW, Mangalea MR, Purcell EB, Borchardt EK, Tamayo R. The second messenger cyclic Di-GMP regulates Clostridium difficile toxin production by controlling expression of sigD. J Bacteriol. 2013 Nov;195(22):5174–85.

27. El Meouche I, Peltier J, Monot M, Soutourina O, Pestel-Caron M, Dupuy B, et al. Characterization of the SigD regulon of C. difficile and its positive control of toxin production through the regulation of tcdR. PLoS One. 2013;8(12):e83748.

28. Dhungel BA, Govind R. Spo0A Suppresses *sin* Locus Expression in Clostridioides difficile. Ellermeier CD, editor. mSphere. 2020 Dec 23;5(6):e00963-20.

29. Stephenson K, Hoch JA. Evolution of signalling in the sporulation phosphorelay. Mol Microbiol. 2002 Oct;46(2):297–304.

30. Edwards AN, Anjuwon-Foster BR, McBride SM. RstA Is a Major Regulator of Clostridioides difficile Toxin Production and Motility. MBio. 2019 Mar 12;10(2).

31. Edwards AN, Krall EG, McBride SM. Strain-Dependent RstA Regulation of Clostridioides difficile Toxin Production and Sporulation. Federle MJ, editor. J Bacteriol [Internet]. 2020 Jan 2 [cited 2021 Sep 18];202(2). Available from: https://journals.asm.org/doi/10.1128/JB.00586-19

32. Altschul S. Gapped BLAST and PSI-BLAST: a new generation of protein database search programs. Nucleic Acids Res. 1997 Sep 1;25(17):3389–402.

33. Jumper J, Evans R, Pritzel A, Green T, Figurnov M, Ronneberger O, et al. Highly accurate protein structure prediction with AlphaFold. Nature. 2021 Aug 26;596(7873):583–9.

34. Verdugo-Fuentes A, Gastélum G, Rocha J, de la Torre M. Multiple and Overlapping Functions of Quorum Sensing Proteins for Cell Specialization in *Bacillus* Species. Margolin W, editor. J Bacteriol [Internet]. 2020 Apr 27 [cited 2022 Oct 27];202(10). Available from: https://journals.asm.org/doi/10.1128/JB.00721-19

35. Rocha J, Flores V, Cabrera R, Soto-Guzmán A, Granados G, Juaristi E, et al. Evolution and some functions of the NprR–NprRB quorum-sensing system in the Bacillus cereus group. Appl Microbiol Biotechnol. 2012 May;94(4):1069–78.

36. Perchat S, Talagas A, Poncet S, Lazar N, Li de la Sierra-Gallay I, Gohar M, et al. How Quorum Sensing Connects Sporulation to Necrotrophism in Bacillus thuringiensis. PLoS Pathog. 2016 Aug;12(8):e1005779.

37. Neiditch MB, Capodagli GC, Prehna G, Federle MJ. Genetic and Structural Analyses of RRNPP Intercellular Peptide Signaling of Gram-Positive Bacteria. Annu Rev Genet. 2017 Nov 27;51(1):311–33.

38. Declerck N, Bouillaut L, Chaix D, Rugani N, Slamti L, Hoh F, et al. Structure of PlcR: Insights into virulence regulation and evolution of quorum sensing in Gram-positive bacteria. Proc Natl Acad Sci U A. 2007 Nov 20;104(47):18490–5.

39. Feng J, Zong W, Wang P, Zhang ZT, Gu Y, Dougherty M, et al. RRNPP-type quorum-sensing systems regulate solvent formation, sporulation and cell motility in Clostridium saccharoperbutylacetonicum. Biotechnol Biofuels. 2020 Dec;13(1):84.

40. Sorg JA, Dineen SS. Laboratory maintenance of Clostridium difficile. Curr Protoc Microbiol. 2009 Feb;Chapter 9:Unit9A 1.

41. Putnam EE, Nock AM, Lawley TD, Shen A. SpoIVA and SipL are Clostridium difficile spore morphogenetic proteins. J Bacteriol. 2013 Jan 4;195(6):1214–25.

42. Edwards AN, Suarez JM, McBride SM. Culturing and maintaining *Clostridium difficile* in an anaerobic environment. J Vis Exp. 2013;(79):e50787.

43. Luria SE, Burrous JW. Hybridization between *Escherichia coli* and *Shigella*. J Bacteriol. 1957;74:461–76.

44. Purcell EB, McKee RW, McBride SM, Waters CM, Tamayo R. Cyclic diguanylate inversely regulates motility and aggregation in Clostridium difficile. J Bacteriol. 2012 Jul;194(13):3307–16.

45. Edwards AN, McBride SM. Determination of the in vitro Sporulation Frequency of Clostridium difficile. Bio-Protoc. 2017 Feb 5;7(3).

46. Childress KO, Edwards AN, Nawrocki KL, Woods EC, Anderson SE, McBride SM. The Phosphotransfer Protein CD1492 Represses Sporulation Initiation in Clostridium difficile. Infect Immun. 2016 Sep 19;

47. Edwards AN, Nawrocki KL, McBride SM. Conserved oligopeptide permeases modulate sporulation initiation in *Clostridium difficile*. Infect Immun. 2014 Oct;82(10):4276–91.

48. Edwards AN, McBride SM. Isolating and Purifying Clostridium difficile Spores. Methods Mol Biol. 2016;1476:117–28.

49. Woods EC, Nawrocki KL, Suarez JM, McBride SM. The Clostridium difficile Dlt pathway is controlled by the ECF sigma factor, sigmaV, in response to lysozyme. Infect Immun. 2016 Apr 11;

50. George WL, Sutter VL, Citron D, Finegold SM. Selective and differential medium for isolation of Clostridium difficile. J Clin Microbiol. 1979 Feb;9(2):214–9.

51. Wilson KH, Kennedy MJ, Fekety FR. Use of sodium taurocholate to enhance spore recovery on a medium selective for Clostridium difficile. J Clin Microbiol. 1982 Mar;15(3):443–6.

52. Soucek S, Zeng Y, Bellur DL, Bergkessel M, Morris KJ, Deng Q, et al. Evolutionarily Conserved Polyadenosine RNA Binding Protein Nab2 Cooperates with Splicing Machinery To Regulate the Fate of Pre-mRNA. Mol Cell Biol. 2016 Nov;36(21):2697–714.

53. Seyfried NT, Dammer EB, Swarup V, Nandakumar D, Duong DM, Yin L, et al. A Multi-network Approach Identifies Protein-Specific Co-expression in Asymptomatic and Symptomatic Alzheimer's Disease. Cell Syst. 2017 Jan;4(1):60-72.e4.

54. Tyanova S, Temu T, Sinitcyn P, Carlson A, Hein MY, Geiger T, et al. The Perseus computational platform for comprehensive analysis of (prote)omics data. Nat Methods. 2016 Sep;13(9):731–40.

55. Harju S, Fedosyuk H, Peterson KR. Rapid isolation of yeast genomic DNA: Bust n' Grab. BMC Biotechnol. 2004 Apr 21;4:8.

56. Langmead B, Salzberg SL. Fast gapped-read alignment with Bowtie 2. Nat Methods. 2012 Apr;9(4):357–9.

57. Wick RR, Judd LM, Gorrie CL, Holt KE. Unicycler: Resolving bacterial genome assemblies from short and long sequencing reads. Phillippy AM, editor. PLOS Comput Biol. 2017 Jun 8;13(6):e1005595.

58. Wattam AR, Davis JJ, Assaf R, Boisvert S, Brettin T, Bun C, et al. Improvements to PATRIC, the all-bacterial Bioinformatics Database and Analysis Resource Center. Nucleic Acids Res. 2017 Jan 4;45(D1):D535–42.

59. Krzywinski M, Schein J, Birol İ, Connors J, Gascoyne R, Horsman D, et al. Circos: An information aesthetic for comparative genomics. Genome Res. 2009 Sep;19(9):1639–45.

60. Thompson JD, Higgins DG, Gibson TJ. CLUSTAL W: improving the sensitivity of progressive multiple sequence alignment through sequence weighting, position-specific gap penalties and weight matrix choice. Nucleic Acids Res. 1994;22(22):4673–80.

61. Tamura K, Stecher G, Kumar S. MEGA11: Molecular Evolutionary Genetics Analysis Version 11. Battistuzzi FU, editor. Mol Biol Evol. 2021 Jun 25;38(7):3022–7.

62. Kelley LA, Mezulis S, Yates CM, Wass MN, Sternberg MJ. The Phyre2 web portal for protein modeling, prediction and analysis. Nat Protoc. 2015 Jun;10(6):845–58.

63. Hussain HA, Roberts AP, Mullany P. Generation of an erythromycin-sensitive derivative of Clostridium difficile strain 630 (630Δerm) and demonstration that the conjugative transposon Tn916ΔE enters the genome of this strain at multiple sites. J Med Microbiol. 2005;54(2):137–41.

64. Bordeleau E, Purcell EB, Lafontaine DA, Fortier LC, Tamayo R, Burrus V. Cyclic di-GMP riboswitch-regulated type IV pili contribute to aggregation of Clostridium difficile. J Bacteriol. 2015 Mar;197(5):819–32.

65. Koo BM, Kritikos G, Farelli JD, Todor H, Tong K, Kimsey H, et al. Construction and Analysis of Two Genome-Scale Deletion Libraries for Bacillus subtilis. Cell Syst. 2017 Mar;4(3):291-305.e7.

66. McBride SM, Sonenshein AL. Identification of a genetic locus responsible for antimicrobial peptide resistance in Clostridium difficile. Infect Immun. 2011 Jan;79(1):167–76.

Chapter 4: Discussion

C. difficile infections pose a significant and urgent threat to public health (1). The ability of *C. difficile* to form recalcitrant spores is critical for the dissemination of CDI, particularly in nosocomial settings in which patients may be immunocompromised and/or on antibiotics (2–4). Understanding the molecular mechanisms by which *C. difficile* initiates sporulation is essential for devising rational therapeutic intervention to combat spore formation and limit spread of CDI. By deciphering the molecular events that lead to and facilitate sporulation in *C. difficile*, we can better decipher how sporulation is controlled in this important pathogen.

I. **Spo0A**

Sporulation initiation and the regulatory mechanisms that control Spo0A activity have been extensively studied in the aerobic Bacilli (5–9,9–16). Comparatively less is known about the molecular pathways that regulate sporulation initiation in the anaerobic Clostridia (17–22). In this study, we identified Spo0A residues that are critical for sporulation and dimerization in *C. difficile* and confirmed that Spo0A is phosphorylated at a conserved aspartate residue.

Our results indicated that many residues that are important for Spo0A activity in *B. subtilis* are also important for *C. difficile* Spo0A function (**Chap. 2, Fig. 2, 3**). However, the sporulation phenotypes of known *B. subtilis* Spo0A mutants generally differed or had opposite sporulation phenotypes for the corresponding *C. difficile* Spo0A site-directed mutants that we created and tested (**Chap. 2, Table 1**). These findings are not entirely surprising considering the differences in factors known to regulate Spo0A activity in *B. subtilis* and *C. difficile* (**Chap. 2, Fig 1**). We also identified growth and morphology phenotypes for a subset of the *C. difficile* Spo0A site-directed mutants that were not previously described in *Bacillus* (**Chap. 2, Table 2**). It is unclear if these phenotypes are unique to the *C. difficile* Spo0A regulon, or if changes in growth

or morphology were simply not reported in earlier *B. subtilis* Spo0A characterization of functional residues. It would be valuable to investigate if similar Spo0A sporulation, growth, and morphology phenotypes are also present in other Clostridial Spo0A mutants to better understand Clostridial Spo0A regulation.

There remains much that is unknown about Spo0A regulation in *C. difficile*, namely the factors that are directly acting upon Spo0A to regulate its activity. The results from this study showed that Spo0A must be phosphorylated at the conserved active site to function, suggesting that there is at least one factor that phosphorylates Spo0A (**Chap. 2, Fig 4**). Identifying and verifying the protein(s) that activate Spo0A will be essential for completely understanding how *C. difficile* makes the decision to initiate sporulation. Interestingly, the sporulation-associated kinase PtpC was identified as a potential binding partner in a Spo0A pulldown experiment (**Chap. 3, Table 1; Table S2**). While we have found that PtpC negatively regulates sporulation, this phenotype is variable and not fully understood. Further investigation is required to verify that Spo0A directly interacts with PtpC, and to further determine how PtpC impacts sporulation. No additional histidine kinases were identified in the Spo0A pulldowns, though it is possible that direct interaction with Spo0A is transient, and some binding partners were not represented in our dataset. Additional biochemical experiments exploring interactions between Spo0A and its predicted binding partners would be highly beneficial to help establish a molecular mechanism for Spo0A regulation.

We were able to confirm that Spo0A forms a dimer, and that residues previously described as important for *Bacillus* Spo0A dimerization are functionally conserved in *C. difficile* (**Chap. 2, Fig 5**). *Bacillus* Spo0A undergoes a conformational change upon phosphorylation that facilitates dimerization, allowing Spo0A to become activated and able to bind to DNA (5). It is

therefore very likely that *C. difficile* likely retains the same mechanism of activation in order to induce gene expression that leads to the initiation of sporulation.

Regulation of Spo0A activity is tightly regulated and many of the findings in earlier *Bacillus* studies pertaining to sporulation initiation cannot be assumed to directly apply to the Clostridia, especially for gut pathogens like *C. difficile* that exist in a unique and niche environment. It is very likely that *C. difficile* has evolved unique mechanisms to regulate sporulation *in vivo* in response to an ever-fluctuating host environment. However, Spo0A is a response regulator that must be phosphorylated in order for sporulation to occur, so at a minimum, the fundamental requirement for interaction with a phosphotransfer protein is likely retained in *C. difficile*. Alternatively, Spo0A may become phosphorylated from non-specific interactions with a phosphate donor such as acetyl-phosphate in the absence of an activating partner. We have provided a framework for the regions of *C. difficile* Spo0A that are important for sporulation. Future studies could utilize this knowledge to identify the Spo0A residues that make direct contact with regulatory proteins to control sporulation initiation. Further, Spo0A residues with altered sporulation frequencies could be used in suppressor screens to identify additional regulators of sporulation. Defining the *C. difficile* sporulation initiation pathway is crucial for understanding this important facet of *C. difficile* physiology and pathogenesis.

II. Spo0E

We hypothesized that multiple regulatory factors interact with Spo0A to control sporulation initiation in *C. difficile*. We identified a putative ortholog to the *Bacillus* phosphatase Spo0E as a potential Spo0A binding partner. We also performed co-immunoprecipitation and LC-MS/MS to identify direct Spo0A binding partners to better define the *C. difficile* Spo0A interactome (**Chap. 3, Table 1**). In this work, we confirmed Spo0E interacts with Spo0A, and found that Spo0E similarly represses sporulation in *C. difficile*. We unexpectedly found that

Spo0E also represses virulence and motility, demonstrating broad regulation of different and important facets of *C. difficile* pathogenesis. We identified novel and conserved Spo0E function, and determined that Spo0E is more than a negative regulator of Spo0A, as was previously described for *Bacillus*.

We disrupted the gene encoding the putative ortholog to Spo0E (*CD630_32710*) and examined the effects on *C. difficile* physiology (**Chap 3, Fig. S1**). As found in *Bacillus*, we demonstrated that Spo0E represses sporulation in *C. difficile* (**Chap. 3, Fig. 1; Chap. 3 Fig. S2**). Unexpectedly, we noticed that the *spo0E* mutant traversed solid agar more rapidly than the wildtype strain. As Spo0E has only been described as a Spo0A phosphatase, and Spo0A does not regulate motility in *C. difficile*, we then hypothesized that Spo0E may regulate processes independent of Spo0A (23). We found that the *C. difficile spo0E* mutant is more motile than the wildtype and produces more toxin, demonstrating that Spo0E also represses toxin and motility in *C. difficile* (**Chap. 3, Fig. 1**). Toxin production and motility share similar mechanisms of regulation and are both regulated by the sigma factor SigD in *C. difficile*, which is not regulated by Spo0A (24,25). Therefore, we found that Spo0E regulates toxin and motility independently of Spo0A, indicating an entirely novel Spo0E function. In accordance with increased toxin production *in vitro*, we found that the *spo0E* mutant was more virulent in hamsters *in vivo* (**Chap. 3, Fig. 2**). We also established that hamsters infected with spores from the *spo0E* mutant experienced more rapid accumulation of toxin, but that the maximum threshold of toxin accumulation was not different from wildtype at time of death (**Chap. 3, Fig. 2**). Interestingly, we found that similar amounts of *C. difficile* CFU were recovered from moribund hamsters infected with either *spo0E* or wildtype spores (**Chap. 3, Fig. 2**). There was clearly a temporal dysregulation of toxin production in the *spo0E* mutant, suggesting that Spo0E also regulates the timing of toxin formation and release *in vivo*.

The finding that Spo0E repressed toxin and motility in addition to sporulation was unexpected. Spo0E is a small protein (53 amino acids in *C. difficile*) and has only been investigated for its role in sporulation in other systems. Further, there is no published data to our knowledge that indicate Spo0E has additional binding partners or multiple regulatory functions. However, the experimental studies investigating Spo0E function have been performed in *Bacillus*, which have different lifestyles and growth requirements than Clostridia. Additionally, we consider that the Spo0E motility and toxin phenotypes may have simply gone unnoticed in the initial characterization of Spo0E.

To better understand the Spo0E interactome and decipher how Spo0E impacts multiple facets of *C. difficile* pathogenesis, we performed co-immunoprecipitation and LC-MS/MS of Spo0E. As expected, we identified Spo0A in the pulldown data (**Chap. 3, Table 1; Table S1**). In accordance with identifying Spo0A-Spo0E interaction, we identified Spo0E in a separate Spo0A pulldown experiment, providing further support that Spo0A interacts with Spo0E in *C. difficile* (**Chap. 3, Table 1**). We also found that RstA co-purifies with Spo0E, but not with Spo0A (**Chap. 3, Table 1**). RstA directly represses transcription of toxin and motility genes and promotes sporulation in *C. difficile* (26). While we established the mechanism by which RstA directly represses toxin and motility gene expression, we previously did not understand how RstA positively influences sporulation (27). We therefore propose a new mechanism demonstrating how Spo0E influences sporulation, toxin and motility in *C. difficile* (**Chap. 3, Fig. S4**). In our model, Spo0E represses Spo0A activity during logarithmic growth to prevent inappropriate entry into sporulation, while RstA preferentially binds to DNA, repressing toxin and motility. As the cell transitions to post-exponential growth, we predict that RstA interacts with its cognate quorum sensing peptide and undergoes a confirmational change that preferentially favors interaction

with Spo0E. RstA would then interact with Spo0E, relieving the repressive effect of Spo0E on Spo0A, and promoting entry into sporulation.

In light of identifying novel Spo0E function, we wondered if Spo0E had conserved multifunctionality in other organisms. Since most of the information on Spo0E comes from experiments in *B. subtilis*, we decided to investigate if motility phenotypes would be recapitulated in this system. We found that Spo0E similarly represses motility in *B. subtilis*, demonstrating a conserved, previously unknown Spo0E function (**Chap. 3, Fig. 3**). It would be valuable to determine the interactions and mechanisms through which Spo0E regulates motility in *Bacillus* and further characterize Spo0E function. Identifying Spo0E binding partners in *B. subtilis* and other species could provide great insight into how Spo0E regulates important physiological processes in distantly related species.

In addition to identifying conserved Spo0E multifunctionality between *C. difficile* and *B. subtilis*, we identified putative Spo0E orthologs in a diverse distribution of Gram-positive and Gram-negative bacteria, as well as in Archaea (**Chap. 3, Fig. 4**). This finding was surprising since Spo0E has only been described as a Spo0A phosphatase in the Firmicutes, and many of the predicted orthologs were encoded in species that do not form spores (**Chap. 3, Fig. 4**). Spo0E orthologs were identified in pathogenic and non-pathogenic species, as well as motile and non-motile species. It is tempting to speculate that Spo0E regulates more than sporulation, toxin, and motility, particularly in species that do not include any of these processes in their physiology. Further investigation is required to characterize the full range of Spo0E function in different species. Spo0E may regulate processes simply by allosterically interacting with other regulatory proteins, and different bacteria could have evolved Spo0E interactions to influence niche-specific functions. Future studies could identify a range of *spo0E* mutant phenotypes in different bacteria that may help decipher the range of Spo0E functionality. Further, Spo0E may

also influence virulence in other pathogens or opportunistic species in which orthologs were identified, such as *M. tuberculosis*, *V. vulnificus*, *S. pneumoniae*, or *B. anthracis*, and may contribute to toxin production in species such as *C. perfringens* or *C. botulinum*. Further assessment of Spo0E could lead to the development of targeted therapeutics in clinically relevant pathogens in which Spo0E is present.

Due to the broad scope of the *C. difficile* Spo0E regulon , it is likely that Spo0E influences additional processes that were not addressed here. In particular, it would be valuable to pursue interaction studies with additional proteins that were identified in the Spo0E pulldown experiments. However, we provide evidence that Spo0E is important for *C. difficile* pathogenesis and identified conserved multifunctionality in different species. Additional studies will need to be performed to fully understand the broad impact Spo0E may have on physiology and pathogenesis in other bacteria.

III. Final Summary

In this work, we have examined regulation of Spo0A activity and elucidated a mechanism by which *C. difficile* regulates sporulation initiation. In doing so, we also discovered a link between the regulation of sporulation and toxin production, which are both critical aspects of *C. difficile* pathogenesis. By deciphering the Spo0A residues that are important for sporulation, we have identified regions that can be further investigated to better understand how and where different regulatory proteins recognize and bind to Spo0A. In addition, we found that Spo0E is important for regulating *C. difficile* pathogenesis through interactions with Spo0A and RstA. The apparent conservation of Spo0E in diverse species suggests that Spo0E is a widely conserved regulatory protein that has evolved to control multiple, niche functions.

Ultimately, this work broadens our understanding on the biology of a pathogen that is an urgent threat to public health. As sporulation is critical for the spread of CDI, defining the mechanisms that lead to sporulation is critical for combatting the spread of CDI. In addition, Spo0E orthologs are conserved in a diversity of species, including other pathogens. Our work could guide future studies on the potential role Spo0E may have in regulating virulence in bacteria that cause infection and disease.

REFERENCES

1. Lessa FC, Mu Y, Bamberg WM, Beldavs ZG, Dumyati GK, Dunn JR, et al. Burden of Clostridium difficile infection in the United States. N Engl J Med. 2015;372(9):825–34.

2. McDonald LC, Gerding DN, Johnson S, Bakken JS, Carroll KC, Coffin SE, et al. Clinical Practice Guidelines for Clostridium difficile Infection in Adults and Children: 2017 Update by the Infectious Diseases Society of America (IDSA) and Society for Healthcare Epidemiology of America (SHEA). Clin Infect Dis. 2018 Mar 19;66(7):e1–48.

3. Barbut F, Petit JC. [Epidemiology, risk factors and prevention of Clostridium difficile nosocomial infections]. Pathol Biol Paris. 2000 Oct;48(8):745–55.

4. McFarland LV, Mulligan ME, Kwok RY, Stamm WE. Nosocomial acquisition of Clostridium difficile infection. N Engl J Med. 1989 Jan 26;320(4):204–10.

5. Baldus JM, Green BD, Youngman P, Moran CP. Phosphorylation of Bacillus subtilis transcription factor Spo0A stimulates transcription from the spoIIG promoter by enhancing binding to weak 0A boxes. J Bacteriol. 1994 Jan;176(2):296–306.

6. Perego M, Cole SP, Burbulys D, Trach K, Hoch JA. Characterization of the gene for a protein kinase which phosphorylates the sporulation-regulatory proteins Spo0A and Spo0F of *Bacillus subtilis*. J Bacteriol. 1989 Nov;171(11):6187–96.

7. Tzeng YL, Hoch JA. Molecular recognition in signal transduction: the interaction surfaces of the Spo0F response regulator with its cognate phosphorelay proteins revealed by alanine scanning mutagenesis. J Mol Biol. 1997 Sep 19;272(2):200–12.

8. Jiang M, Tzeng YL, Feher VA, Perego M, Hoch JA. Alanine mutants of the Spo0F response regulator modifying specificity for sensor kinases in sporulation initiation. Mol Microbiol. 1999 Jul;33(2):389–95.

9. Diaz AR, Core LJ, Jiang M, Morelli M, Chiang CH, Szurmant H, et al. Bacillus subtilis RapA phosphatase domain interaction with its substrate, phosphorylated Spo0F, and its inhibitor, the PhrA peptide. J Bacteriol. 2012 Mar;194(6):1378–88.

10. Zuber P, Losick R. Role of AbrB in Spo0A- and Spo0B-dependent utilization of a sporulation promoter in Bacillus subtilis. J Bacteriol. 1987 May;169(5):2223–30.

11. Bongiorni C, Stoessel R, Perego M. Negative Regulation of Bacillus anthracis Sporulation by the Spo0E Family of Phosphatases. J Bacteriol. 2007 Apr 1;189(7):2637–45.

12. Ohlsen KL, Grimsley JK, Hoch JA. Deactivation of the sporulation transcription factor Spo0A by the Spo0E protein phosphatase. Proc Natl Acad Sci. 1994 Mar 1;91(5):1756–60.

13. Perego M, Hoch JA. Negative regulation of Bacillus subtilis sporulation by the spo0E gene product. J Bacteriol. 1991 Apr;173(8):2514–20.

14. Burbulys D, Trach KA, Hoch JA. Initiation of sporulation in *B. subtilis* is controlled by a multicomponent phosphorelay. Cell. 1991 Feb 8;64(3):545–52.

15. Hoch JA. Two-component and phosphorelay signal transduction. Curr Opin Microbiol. 2000 Apr;3(2):165–70.

16. Perego M, Hoch JA. Two-Component Systems, Phosphorelays, and Regulation of Their Activities by Phosphatases. In: Sonenshein AL, Hoch JA, Losick R, editors. Bacillus subtilis and Its Closest Relatives [Internet]. Washington, DC, USA: ASM Press; 2014 [cited 2022 Oct 28]. p. 473–81. Available from: http://doi.wiley.com/10.1128/9781555817992.ch33

17. Mearls EB, Lynd LR. The identification of four histidine kinases that influence sporulation in Clostridium thermocellum. Anaerobe. 2014 Aug;28:109–19.

18. Worner K, Szurmant H, Chiang C, Hoch JA. Phosphorylation and functional analysis of the sporulation initiation factor Spo0A from Clostridium botulinum. Mol Microbiol. 2006 Feb;59(3):1000–12.

19. Freedman JC, Li J, Mi E, McClane BA. Identification of an Important Orphan Histidine Kinase for the Initiation of Sporulation and Enterotoxin Production by Clostridium perfringens Type F Strain SM101. MBio. 2019 Jan 22;10(1).

20. Steiner E, Dago AE, Young DI, Heap JT, Minton NP, Hoch JA, et al. Multiple orphan histidine kinases interact directly with Spo0A to control the initiation of endospore formation in Clostridium acetobutylicum. Mol Microbiol. 2011 May;80(3):641–54.

21. Edwards AN, Wetzel D, DiCandia MA, McBride SM. Three orphan histidine kinases inhibit *Clostridioides difficile* sporulation [Internet]. Microbiology; 2021 Nov [cited 2021 Dec 1]. Available from: http://biorxiv.org/lookup/doi/10.1101/2021.11.18.469199

22. DiCandia MA, Edwards AN, Jones JB, Swaim GL, Mills BD, McBride SM. Identification of Functional Spo0A Residues Critical for Sporulation in Clostridioides difficile. J Mol Biol. 2022 Jul;434(13):167641.

23. Dhungel BA, Govind R. Spo0A Suppresses *sin* Locus Expression in Clostridioides difficile. Ellermeier CD, editor. mSphere. 2020 Dec 23;5(6):e00963-20.

24. McKee RW, Mangalea MR, Purcell EB, Borchardt EK, Tamayo R. The second messenger cyclic Di-GMP regulates Clostridium difficile toxin production by controlling expression of sigD. J Bacteriol. 2013 Nov;195(22):5174–85.

25. El Meouche I, Peltier J, Monot M, Soutourina O, Pestel-Caron M, Dupuy B, et al. Characterization of the SigD regulon of C. difficile and its positive control of toxin production through the regulation of tcdR. PLoS One. 2013;8(12):e83748.

26. Edwards AN, Tamayo R, McBride SM. A novel regulator controls Clostridium difficile sporulation, motility and toxin production. Mol Microbiol. 2016 Jun;100(6):954–71.

27. Edwards AN, Anjuwon-Foster BR, McBride SM. RstA Is a Major Regulator of Clostridioides difficile Toxin Production and Motility. MBio. 2019 Mar 12;10(2).